

**EFFECT OF FLYASH AND EGGHELL POWDER ON THE SHEAR STRENGTH OF
CLAYEY SOIL**

BY

AGBO CHIKAMSO STEPHEN

REG. NO: 2017224029

**A RESEARCH WORK SUBMITTED IN PARTIAL FULFILLMENT OF THE
REQUIREMENT FOR THE AWARD OF BACHELOR DEGREE IN CIVIL
ENGINEERING (B. ENG.)**

TO THE

DEPARTMENT OF CIVIL ENGINEERING

FACULTY OF ENGINEERING

NNAMDI AZIKIWE UNIVERSITY,

AWKA

MAY, 2023

CERTIFICATION PAGE

This is to certify that this project titled **“Effect of flyash and eggshell on the shear strength of clayey soil”** was carried out by AGBO CHIKAMSO STEPHEN, with Registration Number 2017224029 in the department of Civil Engineering, Nnamdi Azikiwe University, Awka.

Agbo Chikamsso Stephen

Date

(Student Name)

APPROVAL PAGE

This is to certify that this project on the effect of fly-ash and eggshell powder on the shear strength of clayey soil was carried out by Agbo Chikamso Stephen. NAU/201724029 and approved as meeting requirements of the department of civil engineering, Nnamdi Azikiwe university, Awka, Anambra state, Nigeria for the award of (B. ENG.) in Civil Engineering.

Engr. Mrs. N. M. Ezema
(Project supervisor)

Date

Engr. Prof. C. A. Ezeagu
(Head of Department)

Date

Engr. Prof. D. O. Onwuka
(External supervisor)

Date

DEDICATION

This project work is dedicated to God almighty for his love, mercies and kindness towards me. I equally dedicate this work to my beloved parents, Mr. and Mrs. A. Agbo for all the love, care and dedication towards my educational pursuit.

ACKNOWLEDGEMENT

I appreciate God for his profound mercy, strength, grace and wisdom that he gave to me which enabled me to complete this work and also for his guidance and protection throughout my stay in Nnamdi Azikiwe University, Awka.

I will also like to appreciate my ever loving parent (Mr. and Mrs. A. A. Agbo) for their love, kindness, support both financially and otherwise. I pray that the good lord will continue to keep them to enjoy the fruits of their labour.

I will like to use this opportunity to appreciate my project supervisor, Engr. Mrs. Nkechi Ezema for her patience, support, encouragement towards me into making this project work a reality.

I will like to appreciate the HOD (Engr. Prof. C.A Ezeagu) and all the lecturers of the department of Civil Engineering, Nnamdi Azikiwe University, Awka for the wisdom and knowledge they imparted on me throughout my study years. May God continue to give them strength to continue the work that they do.

I will like to also appreciate my Aunt and my elder sister for their support towards me.

I will also like to thank Mr. Etus Livinus and Mr. Ndukaife Christian for their financial support especially during the course of this work.

ABSTRACT

This study investigated the feasibility of using agricultural wastes: Eggshell powder and fly-ash powder for clay soil stabilization.

The samples were mixed using seven trial mixes: 0%FA:18%ESP, 3%FA:15%ESP, 6%FA:12%ESP, 9%FA :9%ESP, 12%FA:6%PLA, 15%FA:3%ESP, 18%FA:0%ESP and a control mix. Specific gravity, sieve analysis, Atterberg limits, compaction and Triaxial tests were carried out.

The clay soils were described as lean clay (UCSC). From the liquid limit results, on addition of 3%FA :15%ESP, a visible reduction in the liquid limit values were observed, also on addition of 6%FA:12%ESP, a reduction in values of the plastic index was documented in both soils respectively. Also, the addition of Eggshell powder alone significantly decreases atterberg limit values, while the addition of Fly-ash powder alone increases the values. The peak values for LL, PL and PI was obtained at 9%FA:9%ESP, 15%FA:3%ESP and 3%FA:15%ESP respectively. For compaction, 3%FA:15%ESP recorded the least MDD value with peak value at 15%FA: 3%ESP in both samples. 15%FA:3%ESP yeilded the best shear strength in both EE1 and EE2. In terms of regressional analysis, EE2 yeilded the best P-value while EE1 yielded the least t-stat. From the R-square value and the Adjusted R-square value, it shows that the work follows an almost linear pattern or sequence and can be predicted perfectly with a linear with a linear equation.

These findings reveal significant improvements in strength and index properties of the clay soil. In conclusion, eggshell powder and flyash produce an eco-friendly stabilizer that can be utilized as subbase material in the stabilization of clay soils.

TABLE OF CONTENTS

CERTIFICATION.....	i
APPROVAL PAGE.....	ii
DEDICATION.....	iii
ACKNOWLEDGEMENT.....	iv
ABSTRACT.....	v
TABLE OF CONTENTS.....	vi
TABLE OF FIGURES.....	viii
TABLE OF TABLES.....	ix
LIST OF SIGNS/SYMBOLS.....	x
LIST OF APPENDICES.....	xi
CHAPTER 1: INTRODUCTION.....	1
1.1 Background of study.....	1
1.2. Problem statement.....	3
1.3. Aims and objective.....	3
1.4. Scope of work.....	3
1.5. Significance of study	4
CHAPTER 2: LITERATURE REVIEW.....	5
2.1 Introduction.....	5
2.2. Clayey soils.....	5
2.3. Soil properties.....	5
2.4. Soil stablization.....	12
2.5. Fly ash.....	15
2.6. Egg shell powder.....	23
2.7. Review of previous work.....	24

CHAPTER 3: MATERIALS AND METHODS.....	33
3.1. Introduction.....	33
3.2 Collection and Preparation of Materials.....	33
3.3 Laboratory Investigations.....	35
CHAPTER 4:RESULTS AND ANALYSIS.....	54
4.1 Natural soil.....	54
4.2 Atterberg limit test.....	55
4.3 Compaction.....	59
4.4 Triaxial test.....	61
4.5. Regressional analysis.....	64
CHAPTER 5: CONCLUSIONS AND RECCOMENDATION.....	67
5.1 Conclusions.....	67
5.2 Recommendation.....	68
REFRENCE.....	69
APPENDIX 1.....	78
APPENDIX 2.....	138
OPERATING THE TRIAXIAL MACHINE.....	195

TABLE OF FIGURES

Figure 4.1: PARTICLE SIZE DISTRIBUTION FOR EE1 & 2	53
Figure 4.2: ATTERBERG LIMIT GRAPH FOR EE1	54
Figure 4.3: ATTERBERG LIMIT GRAPH FOR EE2	55
Figure 4.4: VARIATION IN THE LIQUID LIMIT WITH EACH ADDITION OF PERCENTAGE COMBINATIONS	56
Figure 4.5: VARIATION IN THE PLASTIC LIMIT WITH EACH ADDITION OF PERCENTAGE COMBINATIONS	56
Figure 4.6: COMPACTION GRAPH FOR EE1	58
Figure 4.7: COMPACTION GRAPH FOR EE2	59
Figure 4.8: SHEAR STRENGTH PARAMETERS IN BAR CHART FOR EE1	61
Figure 4.9: SHEAR STRENGTH PARAMETERS IN BAR CHART FOR EE2	62

TABLE OF TABLES

Table 3.1: COORDINATES OF SAMPLE MATERIAL	33
Table 3.2: DETAILS OF COMPACTION MOULD	45
Table 3.3: DETAILS OF COMPACTION PROCEDURE	46
Table 4.1: PHYSICAL PROPERTIES OF THE NATURAL SOIL	52
Table 4.3: ATTERBERG LIMIT FOR EE1	53
Table 4.4: ATTERBERG LIMIT FOR EE2	54
Table 4.5: COMPACTION FOR EE1	56
Table 4.6: COMPACTION FOR EE2	57
Table 4.7: SHEAR STRENGTH PARAMETERS FOR EE1	58
Table 4.8: SHEAR STRENGTH PARAMETERS FOR EE2	59
Table 4.9: SUMMARY OUTPUT OF THE REGRESSIONAL ANALYSIS FOR EE1	61
Table 4.10: SUMMARY OUTPUT OF THE REGRESSIONAL ANALYSIS FOR EE2	62

LIST OF SIGNS/SYMBOLS

Cc - Coefficient of curvature

Cu - Coefficient of uniformity

Kn/m^2 - Kilo-Newton per meter square

Kn/m^3 - Kilo-Newton per meter cube

$^\circ$ - Degrees

Kg – Kilogram

Kg/m^2 – Kilogram per meter square

Kg/m^3 – Kilogram per meter cube

% - Percentage

Wt – Weight

C – Cohesion

Phi – Angle of internal friction

LIST OF APPENDICES

APPENDIX 1	77
APPENDIX 2	135

CHAPTER 1

INTRODUCTION

1.1 BACKGROUND OF STUDY

Shear strength of a soil is perhaps the most important of its engineering properties. This is because all stability analysis in the field of geotechnical engineering, whether they relate to foundations, slopes of cuts or earth dams, earth retaining structures etc. Soil fills involve a basic knowledge of this engineering property of soil. Shearing strength of soil is the most difficult to comprehend in view of the multitude of factors known to affect it. A lot of maturity and skill may be required on the part of the engineer in interpreting the results of the laboratory tests for application to the conditions in the field. Moreover, in many occasion the collection of soil sample and laboratory tests may involve significant cost as compared to the volume of project. Geotechnical engineers have been addressing these problems evolving simple field tests and correlating the results to shear strength of soil (KHO JOO TIONG, 2005).

It is a well-established fact that resistance due to interlocking, frictional resistance and adhesion (cohesion) between the soil particles are the principal sources in deriving the shear strength of a soil. Granular soil or sands may derive their strength from the first two sources, while cohesive soils or clays may derive their shear strength from the second and third sources. Highly plastic clays, however, may exhibit the third source alone for their shearing strength (Venkatramaiah, 2005).

Shear strength of a soil mass is the internal resistance per unit area that the soil mass can offer to resist failure and sliding along any place inside it. One must understand the nature of shearing resistance in order to analyze soil stability problems such as bearing capacity, slope stability, and lateral pressure on earth retaining structures.

Clayey soil generally possesses volumetric changes when subjected to changes in moisture content because of the seasonal water fluctuations. Also, low strength and high compressibility behavior of most clay can cause severe damage to civil engineering structures. Therefore, these type of soil must be treated before commencing the construction operation. Various methods are

available to improve the engineering properties of these soils such as densification, reinforcement, chemical stabilization and techniques of pore water pressure reduction.(Tinku Kalita, Anita Saikia, Bhaskarjyoti Das,2017).

Disposal of waste materials is becoming a predominant issue for most countries in the world. The accumulation of these waste materials in huge quantities is causing both environment and financial problems. According to (Awuchi, 2019), the average waste generation is estimated at 15.4 billion pieces per day. The most prevalent waste materials are agricultural waste materials. These materials are the most usable material types in our daily life.

Many researchers have carried out studies to find effective methods to reduce the pollution of these materials including recycling and reusing these materials in civil engineering applications as a solution to preserve the environment from the pollution of agricultural waste materials. An effective method to utilise these materials is to be used as a soil stabiliser for road construction (Tatone et al. 2018). Traditional soil stabilisers such as cement and lime are widely used for improving the geotechnical properties of weak soils (Sherwood 2003; Yadav et al. 2018 and Yadav and Tiwari 2016). The effectiveness of these materials on improving the properties of soils is confirmed by various researchers (Bell 2006; Little 2005; Rout et al. 2012; Rasul et al. 2015; Rasul et al. 2016; Yadav and Tiwari 2017; Rasul et al. 2018). However, the high usage of these materials makes them non-cost-effective (Obo and Ytom 2014). Therefore, many researchers attempt to find alternative cost-effective soil stabilizers such as plastic, tyre chips, egg shells, fly-ash and rice husk.

Using agricultural wastes for soil stabilization can improve the foundation layers of pavement (Khattab et al. 2011). Thus, this can solve the problem of wastes by reducing the quantities and recycling these materials for enhancing the properties of soils. Several researches have been conducted to investigate the effectiveness of agricultural waste materials in the form of discrete fibres on properties of soils (Ziegler et al. 2008; Babu and Chouksey 2011; Mondal 2012; Ahmadinia et al. 2012; Modarres and Hamedi 2014; Fauzi et al. 2015; Changizi and Haddad 2015; Rawat and Kumar 2016; Peddaiah et al. 2018; Salimi and Ghzavi 2019). These researchers found that using agricultural waste materials for soil stabilization will improve the properties of weak soils such as an increase in UCS, CBR, and Mr and a decrease in the soil plasticity.

In this thesis, the effects of fly ash and granulated egg shell on the shear strength property of clayey soil sample around Awka North (Amansea) will be examined.

1.2 PROBLEM STATEMENT

Clayey soils exhibit low shear strength and high compressibility behaviors and this can negatively impact the stability of any civil engineering structure built on it.

With the increased generation of wastes in our environment and the heightened need to reduce the CO₂ emissions released into the atmosphere, the need for good sustainable alternatives has become paramount.

The shear strength of these clay soils can be improved by using some of the generated wastes in stabilizing them e.g. waste from coal plants, agricultural wastes, etc.

In this study, the engineering impact of the fly ash and crushed egg shells on the shear strength properties of problematic clay soils will be investigated

1.3 AIMS AND OBJECTIVE

The aim of this study is to investigate the effect of fly-ash and crushed egg shell on the shear strength of clayey soils.

The objectives of this study are:

1. To characterize the clay samples from its index properties.
2. To determine the influence of fly-ash and granulated egg shells on the clayey soil under triaxial and compaction.
3. To determine the optimum varied percentage that will yield the maximum shear strength value.

1.4 SCOPE OF WORK

The scope of this study is centered on investigating two samples of clay soils recovered at different point within Efab Estate, Awka and treating these recovered samples with fly ash and granulated egg shells. This experimental laboratory studies is limited to specific gravity,

atterberg, compaction and triaxial tests. These additives will be added to the clay soil at varied percentages.

1.5 SIGNIFICANCE OF STUDY

This research is a comprehensive study of some geotechnical properties of clayey soil when mixed with eggshell powder and fly ash. Through an experimental program, these behavioural characteristics will be examined. The innovation of this study by adding this sustainable material involves eliminating the pollution issues related to the disposal of eggshells and fly-ash. Due to the high percentage of calcium oxide in eggshell powder, it could be a reasonable supplement to lime stabilization of clayey soil by augmenting the pozzolanic reaction. Therefore, the benefits of adding the combination of eggshell powder and fly ash in the area of stabilization of expansive soil must be taken into account.

Moreover, the costs of maintenance and reconstruction of the building, particularly road embankments can be reduced. The amount of waste stockpiled in landfills can also gradually be reduced, and the carbon footprint resulting from the production of conventional stabilizers, such as lime and cement may decrease.

CHAPTER 2

LITERATURE REVIEW

2.1 INTRODUCTION

Soil behavior shows an important influence on the construction above it. Soil, as a material for construction, is applied as embankment material, which is collected from a borrow area, which is generally as clay cohesive soil. Clay behavior that is very sensitive to the water content addition and have a high shrink-swell characteristic as stated by (Munirwansyah, R. P. Munirwan, M. Sungkar, F. Fachrurrazi, 2019). Soil conditions that experience shrinkage can also affect the bearing capacity of the soil. Soil improvement efforts to increase soil bearing capacity by adding chemicals, industrial waste, and fiber materials have been carried out so far. (Munirwansyah, R. P. Munirwan, 2016) conducted a study on the addition of lime on clay so as to reduce the effect of soil shrinkage.(J. S. Yadav, S. K. Tiwari, 2017) studied the addition of rubber fibers on clay which is then stabilized with cement.

2.2 CLAYEY SOILS

Clayey soils are particles with the diameters of which are less than 0.005 millimeter; also a rock that is composed essentially of clay particles. Rock in this sense includes soils, ceramic clays, clay shale, mudstones, glacial clays (including great volumes of detrital and transported clays), and deep-sea clays (red clay, blue clay, and blue mud). These are all characterized by the presence of one or more clay minerals, together with varying amounts of organic and detrital materials, among which quartz is predominant (Sherwood, 2003). Clay materials are plastic when wet, and coherent when dry. Most clay results from weathering.

2.3 . SOIL PROPERTIES

2.3.1 Review of Geotechnical Properties of Clayey Soils

2.3.1.1 Particle Size Distribution

Clay has the smallest particle size of any soil type, with individual particles being so small that they can only be viewed by an electron microscope. This allows a large quantity of clay particles

to exist in a relatively small space, without the gaps that would normally be present between larger soil particles. This feature plays a large part in clay's smooth texture, because the individual particles are too small to create a rough surface in the clay.

Consequently great importance has also been accorded to particle-size distribution in dealing with clayey soils. Recent studies have revealed that clayey soils are strikingly different from temperate zone soils in terms of genesis and structure. Their concretionary structure as compared to the dispersed temperate zone soils has necessitated modifications to mechanical or grading tests (Remillion, 2007). Consistent reports of variations in the particle-size distribution with methods of pretreatment and testing have been widely reported on clayey soils. (Schofield 2007) found out that wet sieving increased the silt and clay fraction from 7 to 20% as compared to the dry sieving. It has been found that sodium hexametaphosphate generally gives better dispersion of the fine fractions. It was also found, for example, that using sodium oxalate on a halloysitic clay from Kenya gave between 20 and 30% clay fraction, while the sodium hexametaphosphate gave as high as between 40 to 50% clay fraction for the same soil (Quinones, 2003).

2.3.1.2 Plasticity

Textural clayey soils are very variable and may contain all fractions sizes; boulders, cobbles, gravel, sand, silt, and clay as well as concretionary rocks. The interaction of the soil particles at the micro scale is reflected in the atterberg limits of the soil at micro scale level. Knowledge of the atterberg limits may provide the following information:-

1. A basis for identification and classification of a given soil texture.
2. Strength and compressibility characteristics swell potential of the soil or the water holding capacity.

Atterberg limit depends on:

- 1 The clay content: plasticity increases with increase in clay content (Piaskowski, 2003).

- 2 Nature of soil minerals: only minerals with sheet-like or plate-like structures exhibit plasticity. This is attributed to the high specific surface areas and hence the increased contact in the shaped particles.
- 3 Chemical composition of the soil environment: the absorptive capacity of the colloidal surface of the actions and water molecules decrease as the ratio of silica to sesquioxides decreases (Baver, 2000).
- 4 Nature of exchangeable actions: this has a considerable influence upon the soil plasticity (Hough, 2009).

Pre-test preparation, degree of molding and time of mixing, dry and re-wetting, and irreversible changes may affect the plasticity of soil. Drying drives off absorbed water, which is not completely regained, on re-wetting (Fookes, 2007). Studies on the relationship between the natural moisture content, liquid limits and plastic limits of clay have shown that generally the natural moisture contents is less than the plastic limit in normal clayey soils (Vargas, 2003). However, the clay soil from high rain fall areas may have moisture contents as high as the liquid limit (Hirashima, 2009).

2.3.1.3 Compaction Characteristics

The compaction characteristics of clayey soils are determined by their grading characteristics and plasticity of fines (Firoozi and Baghini, 2016). Most clayey soils contain a mixture of quartz and concretionary coarse particles, which may vary from very hard to very soft (Firoozi and Baghini, 2016). The strength of these particles has major implications in terms of field and laboratory compaction results and their subsequent performance in civil engineering construction projects (Firoozi and Baghini, 2016). Placement variables (moisture content, amount of compaction, and type of compaction efforts) also influence the compaction characteristics. Varying each of these placement variables has an effect on permeability, compressibility, strength and stress-strain characteristics of the soil.

2.3.1.4 Shear Strength Characteristics`

Shear strength is a term used in soil mechanics to describe the magnitude of the shear stress that a soil can sustain. The shear strength of a lateritic soil is a function of the friction and interlocking of particles (soil angle of internal friction) and possibly cementation or bonding at particle contact relative to total and effective stress. Due to cohesion, particulate materials may expand or contract in volume as it is subject to shear strains. If soil expands in volume, the density of particles will decrease and the strength will decrease likewise the shear strength. The cohesion is attributable to the resultant of inter particle forces which are mainly associated with the clay-size particle of soils and will vary with the particle size and the distance separating them. The angle of internal friction included the effect of interlocking. The interlocking effect is affected to some degree by the shape of particles and the grain–size distribution. The two parameters cohesion (c) and angle of friction (ϕ) depends on the grading, particle shape and void ratio factors of the soil. Cohesion also depends on degree of saturation, while angle of internal friction does not (Gidigasu, 2006).

The shear strength characteristics of lateritic soils have been found to depend significantly on the parent materials, and the degree of weathering which in turn depends on the position of the sample in the soil profile and compositional factors as well as the pretest preparation of the samples (Lohnes, 2008).

2.3.1.5 Consolidation and Compaction

When a soil mass is subjected to a compressive force, its volume decreases. The property of the soil due to which it decrease in volume occurs under compressive force is known as the compressibility of soil. The compression of soil can occur due to;

1. Compression of solid particles and water in the void
2. Compression and expulsion of air in the void
3. Expulsion of water in the voids

The compression of saturated soil under a steady static pressure is known as consolidation. It is entirely due to expulsion of water from the voids. The consolidation characteristics of lateritic

soils are generally moderate with the modulus of compressibility ranging between 1×10^{-3} to 1×10^{-2} sq. ft. /ton.

2.3.1.6 Specific Gravity

The available data indicate that specific gravities vary not only with the textural soil groups but also within different fractions. In the first place lateritic soils have been found to have very high specific gravities of between 2.6 to 3.4 (De Graft-Johnson and Bhatia, 2009). For the same soil, gravel fractions were found to have higher specific gravities than fine fractions due to the concentration of iron oxide in the gravel fraction. While alumina is concentrated in the silt and clay fractions (Nascimento et al., 2009; Novais-Ferreira and Correia, 2005). It is common to find specific gravities reported for the gravel and fines separately. The average of the two values can be assumed to be more representative of the specific gravity for the whole soil.

2.3.1.7 Permeability Characteristics

One of the problems with clay soil is its slow permeability resulting in a very large waterholding capacity. Because the soil particles are small and close together, it takes water much longer to move through clay soil than it does with other soil types (Sherwood, 2003). Clay particles then absorb this water, expanding as they do so and further slowing the flow of water through the soil. This not only prevents water from penetrating deep into the soil but can also damage plant roots as the soil particles expand.

2.3.2 Review of Chemical Properties of Clayey Soils

2.3.2.1 Ion Exchange

Depending on deficiency in the positive or negative charge balance (locally or overall) of mineral structures, clay minerals are able to absorb certain cations and anions and retain them around the outside of the structural unit in an exchangeable state, generally without affecting the basic silicate structure (Firoozi and Baghini, 2016). These adsorbed ions are easily exchanged by other ions. The exchange reaction differs from simple sorption because it has a quantitative relationship between reacting ions (Firoozi and Baghini, 2016). Exchange capacities vary with

particle size, perfection of crystallinity, and nature of the adsorbed ion; hence, a range of values exists for a given mineral rather than a single specific capacity. With certain clay minerals—such as imogolite, allophane, and to some extent kaolinite—that have hydroxyls at the surfaces of their structures, exchange capacities also vary with the pH (index of acidity or alkalinity) of the medium, which greatly affects dissociation of the hydroxyls.

Under a given set of conditions, the various cations are not equally replaceable and do not have the same replacing power. Calcium, for example, will replace sodium more easily than sodium will replace calcium. Sizes of potassium and ammonium ions are similar, and the ions are fitted in the hexagonal cavities of the silicate layer (Firoozi and Baghini, 2016). Vermiculite and vermiculitic minerals preferably and irreversibly adsorb these cations and fix them between the layers. Heavy metal ions such as copper, zinc, and lead are strongly attracted to the negatively charged sites on the surfaces of the 1:1 layer minerals, allophane and imogolite, which are caused by the dissociation of surface hydroxyls of these minerals. The ion-exchange properties of the clay minerals are extremely important because they determine the physical characteristics and economic use of the minerals (Firoozi and Baghini, 2016).

2.3.2.2 Clay Mineral – Water Interactions

Clay materials contain water in several forms. The water may be held in pores and may be removed by drying under ambient conditions (Sherwood, 1993). Water also may be adsorbed on the surface of clay mineral structures and in smectites, vermiculites, hydrated halloysite, sepiolite, and palygorskite; this water may occur in interlayer positions or within structural channels. Finally, the clay mineral structures contain hydroxyls that are lost as water at elevated temperatures.

The water adsorbed between layers or in structural channels may further be divided into zeolitic and bound waters. The latter is bound to exchangeable cations or directly to the clay mineral surfaces. Both forms of water may be removed by heating to temperatures on the order of 100°–200° C and in most cases, except for hydrated halloysite, are regained readily at ordinary temperatures. It is generally agreed that the bound water has a structure other than that of liquid water; its structure is most likely that of ice (Firoozi and Baghini, 2016). As the thickness of the

adsorbed water increases outward from the surface and extends beyond the bound water, the nature of the water changes either abruptly or gradually to that of liquid water (Sherwood, 1993). Ions and molecules adsorbed on the clay mineral surface exert a major influence on the thickness of the adsorbed water layers and on the nature of this water (Firoozi and Baghini, 2016). The non-liquid water may extend out from the clay mineral surfaces as much as 60–100 Å.

Hydroxyl ions are driven off by heating clay minerals to temperatures of 400°–700° C. The rate of loss of the hydroxyls and the energy required for their removal are specific properties characteristic of the various clay minerals. This dehydroxylation process results in the oxidation of Fe^{2+} to Fe^{3+} in ferrous-iron-bearing clay minerals.

The water-retention capacity of clay minerals is generally proportional to their surface area. As the water content increases, clays become plastic and then change to a near-liquid state (Firoozi and Baghini, 2016). The amounts of water required for the two states are defined by the plastic and liquid limits, which vary with the kind of exchangeable cations and the salt concentration in the adsorbed water. The plasticity index (PI), the difference between the two limits, gives a measure for the rheological (flowage) properties of clays. A good example is a comparison of the PI of montmorillonite with that of allophane or palygorskite. The former is considerably greater than either of the latter, indicating that montmorillonite has a prominent plastic nature. Such rheological properties of clay minerals have great impact on building foundations, highway construction, chemical engineering, and soil structure in agricultural practices.

2.3.2.3 Hydraulic Conductivity

Hydraulic conductivity is directly affected by bulk density and swelling pressure and swelling pressure. High density and low electrolyte content of the clay mineral give rise to a very low conductivity for Na^+ -smectite (Sherwood, 2013). On the other hand, the conductivity of Ca^{2+} -smectite is slightly higher because of its low densities. Hydraulic conductivity is depended on density at fluid saturation for different clay minerals. If the hydraulic gradient is high, the particles can also move and this affects the hydraulic conductivity. Thus, particle sand aggregates, that are set free, can be transported by flowing pore water to narrow parts of the pore spaces and cause clogging (Hicks, 2002).

2.3.2.4 Organic Contents

Clay contains very little organic material; you often need to add amendments when plants are to be grown on clayey soil. Without added organic material, clay-heavy soil typically lacks the nutrients and micronutrients essential for plant growth and photosynthesis (Firoozi and Baghini, 2016). Mineral-heavy clay soils may be alkaline in nature, resulting in the need for additional amendments to balance the soil's pH before planting anything that prefers a neutral pH (Firoozi and Baghini, 2016). It's important to test clay-heavy soil before planting to determine both the soil's pH and whether it lacks important nutrients such as nitrogen, phosphorus and potassium.

2.4. SOIL STABILIZATION

2.4.1. Soil stabilization

Soil Stabilization is the biological, chemical or mechanical modification of soil engineering properties. In civil engineering, soil stabilization is a technique to refine and improve the engineering properties of soils. These properties include mechanical strength, permeability, compressibility, durability and plasticity. Physical or mechanical improvement is common but some schools of thought prefer to use the term “stabilization” in reference to chemical improvements in the soil properties by adding chemical admixtures.

For any construction project, whether it is a building, a road or an airfield, the base soil acts as the foundation. Additionally, soil is one of the crucial construction raw materials. As such, the soil should possess properties that create a strong foundation.

The practice of stabilizing or modifying soils dates back to the age of the Romans. Other nations such as the United States and China among many others adopted it in the latter half of the 20th century. (Behnood, A, 2018)

2.4.2 Materials used in soil stabilization

The materials used in soil stabilization depend on what technique is being employed. The following list includes everything from biological, chemical and mechanical soil stabilization techniques:

- a) Different grades of soil.
- b) Different grades of aggregates.
- c) Seedlings
- d) Seeds
- e) Hydromulch mixtures
- f) Hydroseeding mixtures
- g) Geomaterials – geogrids, geoblankets
- h) Polymers -synthetic and natural
- i) Synthetic resins
- j) Emulsions
- k) Cement
- l) Lime
- m) Fly ash
- n) Bitumen
- o) Recycled and waste products – solid municipal, mining and industrial wastes.

2.4.3. Soil stabilization methods

Mechanical stabilization – its objective is to achieve dense, well graded material by mixing and compacting two or more soils and/or aggregates.

Chemical stabilization – refers to the alteration of soil properties by changing its chemical make-up with different additives like lime, cement, fly ash or by the addition of chemicals such as polymers, resins and enzymes.

Biological stabilization – refers to the planting of vegetative cover to prevent wind, water and soil erosion. The roots hold and aggregate soil particles together although in the beginning, other methods of stabilization should be used to support the growth of seeds and seedlings.

The method of stabilizing soils is a commonly undertaken procedure in the construction of airfields, parking lots, landfills, embankments, roads and foundations, waterway management, agriculture and mining sites. The type of stabilization that might be used depends on the site; it may use a single method or a combination of the two.

2.4.4. Purpose of soil stabilization

There are several reasons for it and some of the reasons include:

- a) Substituting poor grade soils with aggregates possessing more favourable engineering properties.
- b) Enhancement of the strength and therefore bearing capacity of the soil.
- c) Dust control for a good working environment.
- d) Waterproofing for conservation of natural or manmade structures.
- e) To promote the use of waste geo-materials in constructions.
- f) Finally, enhancing the properties of soil on site.

Not all sites offer favourable construction conditions. At such sites, a contractor usually has six main reasons why soil stabilization is needed as described above. Reasons 1, 2, 3 and 4 are more chemical and mechanical soil stabilization, whereas reason 5 is biological and mechanical stabilization. Today, with better research and more effective equipment and materials, soil stabilization for reason 6 involves choosing the best suitable technique which achieves the deliverables of the soil stabilization project according to prior cost-benefit analysis. Some

definitions of soil stabilization also refer to the process as soil modification of steady or weak soil.

2.5 . FLY ASH

Fly ash or coal fly ash (CFA) is a spherical, glass-like, heterogeneous particle produced as a by-product from the combustion of pulverized coal during electricity production in thermal power plants (TPPs). Morphologically, fly ash particles are spherical in shape, with sizes varying from 200 nm to several microns, and structurally have ferrospheres, cenospheres, aluminosilicate spheres, or plerospheres, and irregular-shaped carbonaceous particles (Choudhary, N., 2020). Fly ash has almost all the elements present in geological samples—that is, metals, heavy metals, and organic contents. Though the major composition of fly ash almost remains same throughout the world, the composition still varies based on the source of coal, their geographical origin, furnace temperature, and the operating conditions of the boiler (Ohenoja, K., 2020). As fly ash is derived from coal, which is rich in minerals, fly ash is also rich in silica, alumina, and ferrous (Fuller, A., 2018), which are the three major contents of fly ash. Besides this, CFA also has minor oxides, such as rutile, K_2O , CaO , Na_2O , and phosphorous oxides, as well as traces of Cu, Cr, Zn, Ni, and Mo oxides (Wei, Q., 2020). In addition to this, fly ash is also loaded with several toxic heavy metals, such as Al, Ni, Co, Cr, Cd, Zn, Mo, As, and Hg, which categorizes fly ash into —hazardous materials (Rodrigues, P.; Silvestre, J.D.; Flores-Colen, I.; Viegas, C.; Ahmed, H.H.; Kurda, R.; de Brito, J., 2020) and poses a potential threat to the flora, fauna, and the environment.

Every year, a million tonnes (MTs) of fly ash are produced around the globe, especially in the USA, China, France, and India (Alam, J.; Akhtar, M., 2011). Fly ash is not a serious concern for developed countries, but it poses a potential threat for developing countries (Yadav, 2019). This is because the fly ash utilization rate of some of developed countries is more than 90%; for instance, France utilizes almost 100% of fly ash, which indicates complete recycling of the fly ash (Ohenoja, K., 2020). At the same time, for a developing country, such as India, the fly ash utilization rate is 50–60%, whereas for other developing countries, it is below 40%. The more aggravating situation is the production of millions of tonnes of fly ash every year around the

world. Even in the 20th century, 50% of global fly ash is dumped in the vicinity of TPPs. The dumping of fly ash on fertile agricultural land as landfills deteriorates hundreds of acres of land every year (Nisham, K, 2016), which will ultimately lead to a negative impact on the environment. Moreover, the rainfall on piles of heavy metal-loaded fly ash leads to the leaching of heavy metals into the soil, groundwater, and ultimately rivers and other water bodies (Yadav, 2019). This will further lead to water pollution and also poses a potential threat to the aquatic flora and fauna, owing to the increased concentration of heavy metals.

The pollution arising from fly ash might be a negative side, but the presence of valuable minerals (silica, alumina, and ferrous) in higher compositions is the positive side of fly ash (Zhao, Y, 2018) (Valentim, B, 2018). As fly ash is derived from coal, which has a high amount of silica, alumina, and ferrous, these elements are also common in the fly ash after combustion (Fuller, A, 2018). Today, with the continuous advancement of technology and research and development, these fly ashes have found applications in the fields of ceramics and construction, adsorbents, fertilizers, landfills, geopolymers, and metallurgy (Yadav, 2019). In ceramics and construction alone, they are used for making fly ash amended cement, tiles, pavement blocks, dike preparation, and embankments, among others. Here, however, we are concerned with the recovery and synthesis of alumina, silica, and ferrous nanoparticles from fly ash. In the last decade, there has been a tremendous revolution in the field of nanotechnology and nanoparticles, which has helped it to find applications in the field of catalysis, drug delivery, medicine, and environmental clean-up (Li, S.; Qin, S, 2017). However, as nanotechnology is still in its infancy stage, the synthesis of nanoparticles involves expensive precursor materials and sophisticated instruments, which makes the final nanoparticles very costly. Therefore, the nanotechnology replaces the expensive precursor material with waste materials such as agricultural waste (sugarcane bagasse, rice husk ash, citrus waste) and industrial waste, such as gypsum waste, eggshell waste (Habte, L, 2019), red mud, and fly ash. If nanoparticles are synthesized from any of the above-mentioned waste, then the final product will be not only cost-effective, but also ecofriendly thanks to the minimization of the solid waste as pollution.

One such precursor material for the synthesis of silica, alumina, and ferrous nanoparticles is fly ash. Fly ash is a rich source of ferrous (5–15%), silica (40–60%), alumina (20–40%), and calcium (0.5–15%), based on the types of coal used, geographical origin, and operating

conditions for the combustion of coal in the thermal power plant(Zhao, Y, 2018). Generally, class F fly ashes are rich sources of ferrous, alumina, and silica, as they are derived from the higher grades of coal—that is, anthracite and bituminous—whereas class C fly ashes have a lower content of ferro-alumino-silicate (FAS), as they are derived from the lower grades of coal—that is, sub-bituminous, lignite, and peat. As silica is present in the highest concentration in all of the fly ashes, most attempts have been made for the synthesis of silica nanoparticles (SiNPs) from various parts of the globe. The most preferred method for the synthesis of SiNPs from fly ash is the alkali dissolution method(Peng, X, 2019), where the fly ash is treated with 4–16 molarity of sodium hydroxides or potassium hydroxides at a temperature in the range of 90–100°C for 1–3 h. Another method for silica nanoparticle synthesis is the alkali fusion method (Purnomo, C., 2019), where the fly ash is mixed with 4–16 M NaOH or KOH and fusion is done at higher temperatures of 600–1200 °C for 3–8 h in a muffle furnace. The high calcination temperature transforms the inert and crystalline minerals of fly ash into the reactive phase of Al and Si after reacting with sodium and potassium hydroxides(Guo, C., 2019). The advantages of such a method is that the new products formed after calcination have high reactivity with acids and bases, which drastically increases the yield of silica. Further, as Al is amphoteric in nature, it can react with both acids and bases, and thus it can be extracted by treating the fly ash with concentrated mineral acids, such as sulphuric acid (H₂SO₄), hydrochloric acid (HCl), and nitric acid (HNO₃), by keeping 4–16 molarity of acids, at temperatures of 100– 130 °C for 1–3 h along with continuous stirring. Besides this, alumina can be extracted from fly ash by treating it with 4–16 M NaOH (keeping the solid-to-liquid ratio 1:5) at 90–100 °C for 1–3 h along with continuous stirring. These procedures do not involve any pretreatment for the elimination of impurities in the form of Fe, Al, Na, Ca, etc., which may contribute, to some extent, to the final synthesized nanoparticles and make them undesirable.

2.5.2 Properties and Applications of Fly Ash

2.5.2.1 Morphological Properties of Fly Ash

Fly ash is a sphere-shaped, micron-sized (0.01–100 μ) heterogeneous material, having depositions of mainly Al, Si, Fe and C in variable compositions on its surface, and closely resembles the volcanic ashes(Langmann, B., 2013). The fly ash particles can be either rough or

smooth surfaced based on the type of depositions on their surface. Figure 1 show a typical fly ash particle, which is spherical in shape, whose sizes vary from 0.2 microns to several microns (6μ). Morphologically, fly ash particles may have differently shaped particles, which also vary in their elemental composition viz. ferrospheres (ferrous rich spherical particles)(Sunjidmaa, D., 2019), cenospheres or alumino-silicate spheres (Al- and Si-rich particles), plerospheres (larger spherical particles encapsulate smaller particles), plerospheres, and carbon nanomaterial—i.e., soots, buck balls, fullereness(Silva, L., 2010)(Fu, B., 2018) and unburned carbon, including both organic and inorganic(Ohenoja, K., 2020). Plate 2.1a,b show fly ash plerospheres, which are thick- and thin-walled. Both the plerospheres have trapped numerous smaller sized spherical particles, along with gases and minerals. While Plate 2.1c depicts cenospheres which are spherical in shape, having mainly Al and Si, along with carbon, on their surface, plate 2.1d shows ferrospheres, which have depositions of ferrous on their surface, due to which they have magnetic properties. The ferrospheres have rough surfaced and dendritic shape on their surface. In comparison to ferrospheres, cenospheres are lighter in weight (Yoriya, S., 2019) and have high mechanical strength, thermal resistance and have fireproof property. The globular shape of such microspheres is due to the precipitation of crystalline phases during the cooling of iron aluminosilicate melt drops of complex composition (Hower, J., 2017). The crystallite size and the composition of the iron-containing phases, that governs the magnetic properties of the microspheres, depend on both the melt composition and the thermal conditions of microsphere formation. Cenospheres are more dominant structures in the fly ash (Yoriya, S., 2019), followed by the ferrospheres, which are spherical-shaped ferrous-rich particles, whose sizes fall in the micron range. The ferrospheres have high depositions of ferrous or Fe, which could be either rough, smooth, elliptical or molten drop-shaped. Besides cenospheres and ferrospheres there is the third type of micron-sized spherical-shaped particles, called plerospheres, which are less frequent in fly ash in comparison to the other two forms. These plerospheres encapsulate several small fly ash particles, minerals and gases inside them during the formation from the molten slag at high temperature in the furnace(Wang, P., 2013)(Krishnamoorthy, V., 2015). Additionally, there are a large number of carbonaceous nanomaterials, such as fullerenes, graphene, soots and unburned irregular-shaped carbon particles in fly ash, formed due to the combustion of organic and inorganic carbon minerals present in the coal. Such irregular or angular-shaped carbon-rich

particles are shown in plate 2.2, taken through Scanning Electron Micrograph (SEM), while the bright colored particles are electron-rich Fe, Al and Si rich region(Liu, H., 2016).

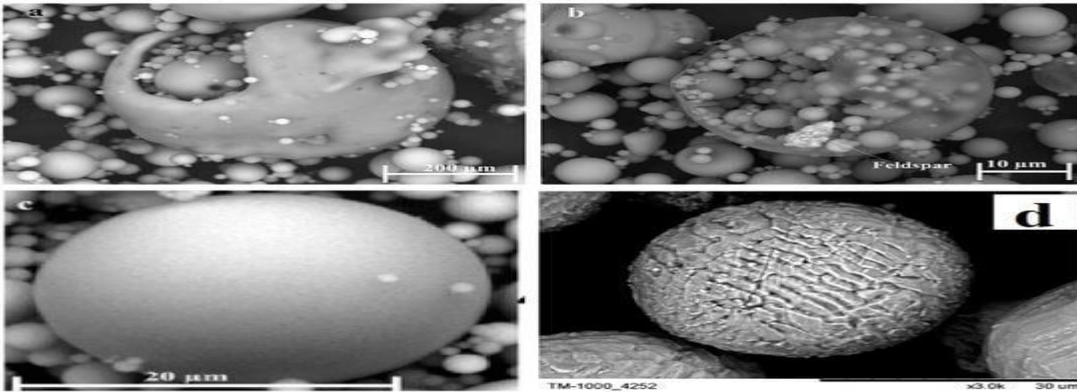


Plate 2.1. SEM micrograph of fly ash, plerospheres (a,b) cenospheres (c) ferrospheres (d) adapted from Goodzari and Sanei(Sharonova, O., 2015)and Olga Sharonova et al.(Sharonova, O., 2015).

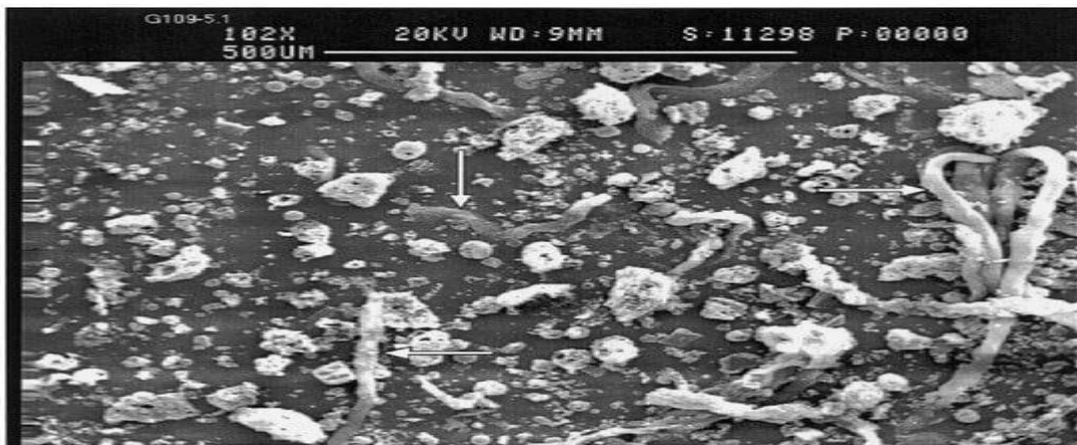


Plate 2.2. SEM micrograph of fly ash carbon rich particles adapted from Veranth et al.(Veranth, J.M., 2000).

2.5.2.2. Elemental Properties of Fly Ash

The mineralogy and composition of fly ash is not constant, rather it varies from place to place, parent coal source, operating parameters and temperature of TPPs(Vassilev, S., 2004), the extent of coal preparation and cleaning, furnace design, usual climate storage and handling. The

mineralogical properties determine the crystalline phases of the fly ash, and their composition varies from 15–45% in the fly ash. Generally, fly ash has silica 40–60%, alumina 20–40% and ferrous 5–15% by weight fractions. Almost all the fly ash has mullite, quartz, magnetite, hematite and calcite as the common crystalline minerals (Šešljija, M., 2016). Based on mineral composition and sources of coal, fly ash is categorized into two classes—class F and class C. The major differences between these two classes of fly ash are described here. The source of class F fly ash is anthracite and bituminous coal, whereas for class C it is younger lignite and sub-bituminous coal. The lime content in class F is less than 20%, while class C has more than 20% of it. Ca in class F is mainly present in the form of $\text{Ca}(\text{OH})_2$, CaSO_4 and glassy components, which is 1–12%, and in class C it is 30–40%. Class C has larger amount of crystalline content—i.e., 25–45%—than the class F, which has only 15–45% of the carbon (Eisele, T.C., 2004) (Vassilev, S., 2003). The class F fly ash has a higher amount of alkali and sulfate than the class C fly ash. While, for cementing agent, class F requires Portland cement, hydrated lime and quicklime, whereas class C has self-cementing properties. Class F generally requires an addition of air entrainer, which is not required by the class C fly ash. When it comes to the application, class F is used in high SO_4^{3-} exposure conditions, has high fly ash content concrete mixes and is explored for the structural and HP concretes. Whereas class C fly ash is not suitable for high sulfate conditions, limited to low fly ash content concrete mixes are mainly used for the residential construction.

2.5.2.3. Chemical Properties of Fly Ash

The pH of the fly ash tends to vary from acidic to alkaline (4.5 to 12.0), depending on the source of coal and the number of trace elements in them (Basu, M., 2009). Fly ash produced from bituminous coal, is mostly acidic even though it has higher sulfur content, while alkaline fly ash is produced from the sub-bituminous coal, which has lower sulfur content, and has higher Ca and Mg content than that derived from bituminous coal. Similarly the electrical conductivity (EC) of fly ash varies between 0.177 to 14 S/m, which directly corresponds to the quantitative concentration of soluble cations and anions in the fly ash (Fulekar, M.H., 2017). Likewise, mineralogy and chemical composition too depend on the various parameters of coal combustion. Chemically, about 90–99% of the fly ash fraction constitutes oxides of silicon, aluminum, iron, calcium and titanium, (~0.5% to 3.5%), which are made up of oxides of sodium, potassium,

phosphorus, manganese and sulfur(Papatzani, S., 2020), and the remaining fractions are the trace elements, including rare earth and radioactive elements. As per the universal rule, smaller particles with higher surface areas than the larger ones are also applicable to the fly ash particles—hence, smaller fly ash particles tend to accumulate a higher concentration of elements (As, Cd, Cu, Ga, Mo, Pb, S, Sb, Se, Ti and Zn) on their surface in comparison to the larger fly ash particles. Fly ash particles have both crystalline and glassy amorphous materials. Silicates are present in crystalline form—i.e., sillimanite and mullite, while most of the silicates are present in the glass form. The average glass content in U.S. fly ash is 90%, while in Indian fly ash it varies from 49–69% by weight. This indicates that Indian fly ash has more crystalline content than the U.S. fly ash.

The chemical composition of the core or interior part of the fly ash is almost masked by the depositions of elements on the surface layer of fly ash particles. Moreover, these surface layers get depositions of various elements during volatilization and condensation of molten slag in the furnace. It has been reported that the concentration of some of the elements on the surface layer has many more folds than that of parent coal (Wuana, R.A., 2011). All fly ashes derived from different coal types, have oxides of Fe, Al, Si and varying carbon content.

2..5.2.4. Physical Properties of Fly Ash

Based on the percentage of unburned carbon, fly ash color may vary from tan to grey or black. The darker the colour of fly ash, the higher the carbon content. Based on the above fact, it is obvious that lower grades of coal (lignite, sub-bituminous) having a lesser amount of carbon, will produce light —i.e., tan to buff-colored fly ash(Chou, M.-I.M., 2012) while the higher grades of coal (anthracite and bituminous), being rich in carbon, will produce dark colored fly ash—i.e., grey to black. Moreover, calcium oxide content too contributes in the color of fly ash, as lower grades of coal have higher calcium content than the higher grades of coal, and provide white shade to the fly ash. The specific surface area and the specific gravity of fly ash tend to vary in the range of 2000 to 6800 cm² per gram and 2.1 to 3.0 g/cm³, respectively. Regarding the particle sizes of fly ash, their composition varies from one geographical area to other, and for instance, the size of sandy particles is 2–0.5 mm and 4.75–0.075 mm in the U.S. and Indian fly ash, respectively, while the size of silt particles in U. S. fly ash vary from 0.05–0.002 mm and

0.075–0.002 mm in Indian fly ashes. However, the size of clay particles in both U.S. and Indian fly ashes are less than 0.002 mm. Sandy particles in U.S. fly ash are sub-divided into very coarse, coarse, medium, fine and very fine, and their total composition in fly ash is 32.4%, whereas in Indian, fly ash total composition of sandy particles is 35.69%, which indicates that the Indian fly ashes have 2–4% more sandy particles than the U.S. fly ashes. The percentage of silty particles in both U.S. fly and Indian fly ash are more than 60%; however, the U.S. fly ash have marginally higher content of silty particles than the Indian fly ash. The average silty content in U.S. Fly ash is 63.2%, whereas in Indian fly ash it is 62.39%. Clay particles in U.S. fly ash are 4.3% in comparison to Indian fly ash having 1.91% of the clay. Hence, the U.S. fly ash has a 2–3% higher amount of clay particles than the Indian fly ash. Variation in fly ash is also seen due to the different structural properties of the particles i.e., cenospheres (Żyrkowski, M., 2016), plerospheres, ferrospheres and irregular- or angular-shaped carbon particles (Ibeto, C.N., 2020), which are already briefly described in the introduction section. Cenospheres have a bulk density in the range of 0.4–0.6 ton/m³ and constitute up to 5% of the total weight of fly ash (Yoriya, S., 2019).

2.5.3. Applications of Fly Ash

Fly ash has great importance and numerous advantages either in the bulk form or in their separate natural nanostructured particles, which is depicted in the Figure 3. Besides, the fly ash also has a higher amount of Si, Al, and Fe that can be used in hydrometallurgy using the environmentally-friendly approach for the recovery of minerals at an economical cost (Meer, I., 2017) (Zhang, W., 2020). The bulk form of fly ash can be potentially used as a bio-fertilizer, as it contains a rich source of plant nutrients such as, Na, Ca, K, P, Zn, Mg, Mn, Mo, etc. Moreover, the zeolites synthesized from fly ash can also be used for the sustained and controlled release of the N, P, K and other minerals to the plants (Miricioiu, M.G., 2020) (Kunecki, P., 2020). In the field of agriculture, the bulk fly ash can be used for resource conservation, reclamation of the contaminated sites and restoration of industrial sites (Behera, A., 2018). Besides agriculture, the fly ash also finds application in civil engineering (Attarde, S., 2014) (bricks, tiles, cements, blocks), tiles (Luo, Y., 2017) (Fİ Gen, A., 2017), brick making, cements, geopolymer (Zhuang, X.Y., 2016), landfills (Nordin, N., 2016), mining, agriculture river embankments, fillers (Baykal, G., 2004) (Dasgupta, M., 2013), panels and composite materials (Gaikwad, A., 2017) and in

metallurgy for the recovery of value-added minerals. The natural nanostructured form of fly ash i.e., cenospheres, ferrospheres, carbonaceous particles and plerospheres, finds applications in nano-ceramics, mechanical engineering, construction of lightweight materials (Nadesan, M.S., 2017) and wastewater treatment. Besides, individual microspheres are also used for making thermoset plastics, concrete materials, nylon, material for coating (Rudić, O., 2019), high-density polyethylene (HDPE), and others. In hydrometallurgy, the high content of ferrous, alumina and silica in the fly ash, which is a waste, can possibly be considered as one of the most reliable materials for the recovery of ferrous, alumina and silica and their derivatives (Rudić, O., 2019). The recovery of such value-added minerals opens new horizons, as it not only reduces the global pollution in the form of solid waste but also acts as an alternative material for Si, aluminum and ferrous (Brännvall, E., 2016).

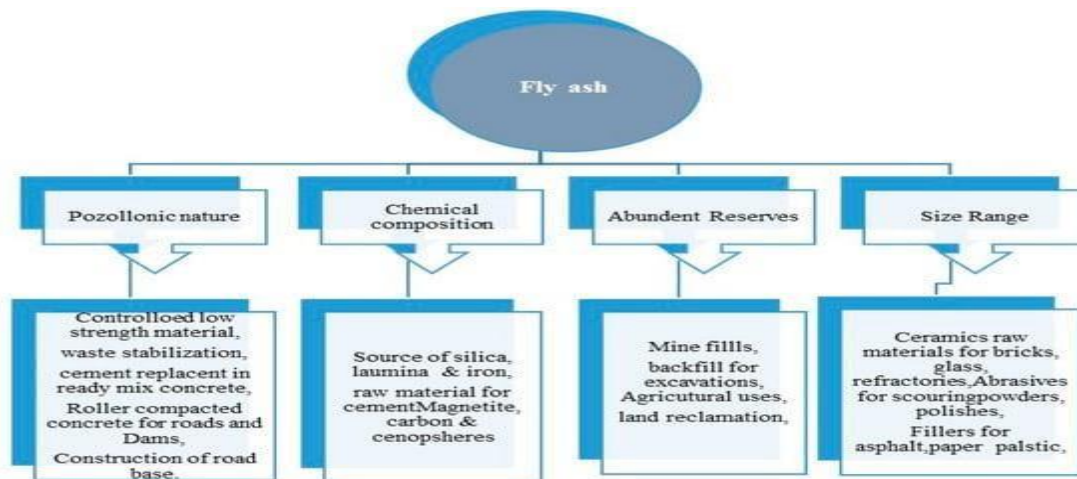


Plate 2.3. Broad areas of fly ash applications.

2.6. EGG SHELL POWDER (ESP)

Eggshell consists of several mutually growing layers of CaCO₃, the innermost layer-maxillary layer (100µm) grows on the outermost egg membrane and creates the base on which palisade layer constitutes the thickest part (200µm) of the eggshell. The top layer is a vertical layer (5.8µm) covered by the organic cuticle, Frontng and Bergquist (2009).

Tocan (2009), stated that eggshell primarily contains calcium, magnesium carbonate (lime) and protein. He however evaluated the quantity of the lime in eggshell waste to be as almost the same as ground chalk or limestone tonne for tonne. Eggshell waste does have a theoretical value either as an animal feed or as a fertilizer or lime substitute. In many other countries, it is the accepted practice for eggshell to be dried and use as a source of calcium in animal feeds. The quality of lime in eggshell waste is influenced greatly by the extent of exposure to sunlight, raw water and harsh weather conditions. Froning and Bergquist (2009) specified that eggshell waste should be ground not more than 2 days after recovery from source to prevent depletion of lime content.

The physical nature of the shell waste and the foul rotten egg odours produced when the material degrades, reduce the lime value and renders the waste difficult to recycle to land. Ideally, the waste should be dried at source, transported to a site where it would be finely ground immediately and used as source of lime to agriculture and for other applications. In order to maximize the recycling opportunities for eggshells, Froning and Bergquist (2009), recommended that eggshell waste should be incinerated independently of other wastes so that the calcium/magnesium content of the shell will be converted into calcium/magnesium oxide (quicklime) and the resultant burnt lime could be used as a liming agent.

2.7 REVIEW OF PREVIOUS WORK

Birundha P., et.al (2017). In this journal paper, Egg Shell Powder and Quarry Dust were used to study the effect on the properties of clayey soil. An improvement in the engineering properties of soil by addition of ESP and QD will help to find an application for waste materials to improve the properties of clayey soil. Addition of various percentages of ESP and QD into the soil decreases optimum moisture and increases maximum dry density.

Alzaidy M.N.J. (2019) In this paper, the effect of the combination of Egg Shell Powder and Plastic Waste Strips in some engineering properties of clayey soil represented by compaction characteristics, unconfined compressive strength, swelling potential, California bearing ratio test and finally shear strength parameters have been studied. The aim of this paper is to investigate the influence of plastic wastes, eggshell powder contents and the curing duration in the strength

behavior of clayey soil. An increase in ESP content causes to an increase in unconfined compressive strength. A significant net positive change has been noticed in the engineering characteristics of the clayey soil after adding both of ESP and PWS. These beneficial changes depend on ESP, PWS contents and the curing duration.

Erdal Cokca (2001) Conducted a research on the effect of fly ash on expansive soil was studied by Erdal Cokca. Fly ash consists of often hollow spheres of silicon, aluminum and iron oxides and unoxidized carbon. There are two major classes of fly ash, Class C and class F. The fly ash can provide an array of divalent and trivalent cations under ionized conditions that can promote flocculation of dispersed clay particles. Thus expansive can be potentially stabilized effectively by cation exchange using fly ash. He carried out investigations using some fly ash and added it to expansive soil at 0-25%. And his experimental findings confirmed that the plasticity index, activity and swelling potential of the sample decreased with increasing percent and curing time and optimum percent was found to be 20%.

Mujtaba, et al.(2019). Investigated the effect of Different ratios from (0% to 55%) of slag on lean clay and fat clay. At 50% of slag, the maximum dry density was increased by 10%. At 50% of slag, the CBR value increased from (3.2% to 11.5%) for fat clay, and for lean clay the result was from (2.4% to 10.7%). At 20% of slag, the swelling potential reduced from (5% to 2%) for lean clay. At 30% of slag, the swelling potential reduced from (8% to 2%) for fat clay. At 30% of slag, the shear strength increased up to 35% with 28 days of curing.

Hasan(2012).Conducted a research on the effect of different ratios of fly ash on expansive soil. 20% of fly ash decreased all the following properties of the soil: Liquid limits (74% to 56), Plastic limits from (31% to 25%), Plasticity index (44%-31%), Maximum dry density (1.697 to 1.275) g/cm³. 20% of fly ash increased the optimum moisture content from (19.2 to 29.3)%.

Bose, (2012). Conducted a research on different ratios of fly ash on expansive soil. Adding fly ash reduced the plasticity, linear shrinkage, moisture content free swell -index, and swelling pressure while shrinkage limit increased. 20% of fly ash achieved the maximum value of maximum dry density and UCS. Beyond 20% of fly ash, the strength decreases.

Gopala Krishna, et al., (2013). Investigated the effect of different ratios of (class-f) fly ash and zycosil on Black cotton soil. 3% fly ash and 2% of zycosil achieved the highest value of unsoaked CBR. 4% fly ash and 2% zycosil achieved the highest value of the soaked CBR.

Senol et al. (2006) investigated different proportions of fly-ash (0%, 10%, 18%, and 30%) and water contents in soil stabilisation process and concluded that fly-ash enhanced the CBR value of soil with a range of 15% to 31%.

Hatipoglu et al., (2008) stated that stabilisation of road surface gravel in Minnesota with fly-ash increased the CBR value by 2 times.

Prabakar et al. (2004) determined that fly-ash decreased the dry density by 15% to 20%, and increased the void ratio and porosity in soil. For example, the void ratio was increased by 25% with the addition of up to 46% fly-ash in soil.

Paul et al. (2014) investigated that ESP increased the optimum moisture content (OMC) and decreased the maximum dry density (MDD).

Mn and Fo (2018) argued that eggshell could be a potential replacement of cement stabilised soil after observing the increase in soil strength with different proportion of eggshell powder mixed with cement stabilised soil.

Ahmed et al. (2016) found that the optimum soil stabilisation with ESP could increase the CBR value by 11%.

The improvement behavior of soil by geo-textile technique conducted by Krishnaswamy et al (1988) concluded with the increase in reinforcement aspect the soil strength ratio increases.

Ramanatha Ayyar et al. (1989) performed tests on coir fiber reinforced clay and it was observed that the discrete fibre of small diameter offer greater resistance to swelling than the larger diameter fibre placed similarly.

Kolay et al. (2010) explained the soil stabilization of locally available peat soil from Sarawak, using fly ash and gypsum. The unconfined compressive strength test results showed that the peat soil got strengthened due to the addition of different proportions of gypsum and fly ash and it was also observed that the strength of peat soil increases with the increase in curing period.

Ramlakhan et al. (2013) observed that with the increase in lime and fly ash content in the soil the optimum moisture content and California bearing ratio of soil increases.

R. Chavali and R. K. Sharma (2014) carried out a study on influence of sand and fly ash on clayey soil stabilization. The results show significant improvement in California bearing ratio of composite containing clay, sand and fly ash as (70: 30: 10).

Gyanen et al. (2013) considered the effect of both coarse and fine fly ash in unconfined compressive strength of black cotton soil. It was observed that the peak strength is attained by fine fly ash composite was 1.25 times the strength obtained with coarse fly ash composite.

Jirathanathworn and Chantawarangul (2003) found that by using fly ash mixed with small amount of lime, the engineering properties of clayey soil such as strength and hydraulic conductivity improved.

Kaushik and Ramasamy (2006) investigate the different properties of coal ash to be used as construction material. It was found that the fly ash exhibits high strength at optimum moisture content but poor shear strength at saturated conditions.

Alqaisi.R.O (2020) He conducted the study on the effect of ESP as a supplementary additive to lime stabilization in expansive soil. The addition of Egg Shell Powder alone to soil had a marginal effect on the geotechnical properties of stabilized expansive soils. The unconfined compressive strength (UCS) of treated soils increased.

Aneesh P.C,et.al (2020) It is an experimental study focused on stabilization of cochin clay with Egg Shell Powder(ESP) and Shredded LPDE. 3 various proportions of ESP (2%, 5%, 8%) plastic wastes (0.25%, 0.5%, 0.75%, 1%) were added to obtain optimum percentage of each additive. The collected sample comes under silt clay (53.3%) and from the plasticity index, according to Unified soil classification system (USCS) our clay sample is grouped under CH category. The combination of 5% ESP and 0.5% plastic we obtain the maximum compressive strength of 86.24kN/m² and thereafter the value goes on decreasing.

Sharmila.S.M.R,et.al(2019)This literature deals about the experimental study on the stabilization of soil using organic waste and coir fibres of varying lengths. Basic properties of virgin soil like Atterberg's limits, unconfined compressive strength, compaction characteristics, California

bearing ratio, were determined. The soil was then treated with an optimum percentage of eggshell powder and varying percentages of coir fibres of different lengths (L=1cm, 1.5cm). Addition of 10% ESP gives an increment of about 39.5 % in UCC values. It can be observed that as the length increases, the fibre-fibre interaction dominates over the fibre-soil interaction and reduces the effect of interlocking. The CBR and UCC value for the virgin soil sample was found to be 5.71% and 124 kN/m² respectively. Addition of 10% ESP gives an increment of about 54.6 % and 39.5 % in CBR and UCC values. The CBR and UCC values showed an increment of 107% and 182 % when the soil was treated with 10% ESP and 1.25% of coir fibre, when the length of the fibre was limited to 1 cm.

Soundara.B and Vilasini.P.P (2015) In this paper, the suitability of Egg Shell Powder (ESP) as a possible stabilizing agent to improve the strength of soils is studied by various laboratory tests. The maximum dry density slightly increases and after then decreases for increasing percentage of ESP. The OMC values are constantly decreasing upon increasing percentage of ESP. There is an increasing trend of UCS upon increasing percentage of ESP is observed.

Dr.Mathada.V.S (2019) It is an experimental study on black cotton soil is stabilized by using admixture which is easily available and waste material. The admixture used is Chicken Fur (CF) is a waste from poultry farming. Here, tests are carried out such as, Compaction Test and Unconfined Compressive Strength Test for the Soil and also for the soil replaced with CF in Percentage variation of 1%, 2% and 3%. The Compressive strength value increased by 857.07% when compared with the original Soil sample and the Soil replaced with 2% CF by the weight of soil mass.

Elias.T (2016) This research paper is conducted to stabilize clayey soil using human hair fiber and lime. The optimum percentage of lime and human hair that should be added in Kuttanad Clay is 9%, 1.5% respectively. The compressive strength increase of 90.4% is observed. Human Hair Fibres can be added to soil as a stabilizing agent. Hair as a cheap reinforcing agent is abundantly available as a waste product from saloons and is facing a major disposal issue. In the present study lime is added to clay in its natural water content. Lime content was varied from 3%, 6%, 9% and 12% by weight of soil. In case of hair stabilization, human hair was added by hand to achieve a homogeneous soil-hair mix. The hair used in the present study were of length 4-40mm and it was added to the mix in varying percentages of 0.5%, 1.0%, 1.5%, 2.0% and 2.5% by

weight. The optimum percentage of lime and human hair that should be added in Kuttanad Clay so as to make it properly stabilized is 9%, 1.5% respectively.

Krishnakumari.B,et.al (2019) In this study discussed about the stabilization of clayey soil using various additives. Egg shell primarily consists of magnesium carbonate, protein, calcium and the quantity of lime. The increase is because of the addition of ESP, that decreases the quantity of free silt, clay fraction and coarser materials with larger surface areas.

Manoj.N,et.al (2017) This study focused on stabilization of soft soil using chicken feathers as biopolymer. We know that, biopolymer means a polymeric material created by living life forms, e.g. protein, starch, cellulose. The compressive strength of soft soil increases with the increase in biopolymer up to 5% and after that eventually the compressive strength of the soil decreases. Generally, these chicken feathers are the dumped wastes of poultry farms. Chicken feathers are used as an animal feeder, melted and made into plastic. The usage of chicken feathers in any field is very less and they become debris to over this problem, they are for stabilization of soft soils which are very weak in nature and contain many voids.

The aim of Abhijith (2015) study was to research the effect of coir textiles on CBR strength of soil subgrade and to determine the ideal position to place the coir geotextiles. Coir fibres with various lengths and proportions, 5-30mm, 28% of the total weight of soil were added. The optimum fibre length and proportion were 15mm, 5% of the total weight of soil respectively. At this value, the CBR strength was enhanced. It was observed that the best position for placing the coir geotextiles at the top position of the subgrade while the least value obtained was at the lowest position.

The effectiveness of adding coal ash and coconut coir fibre in local soil (silty sand) was explored by Singh & Arif (2014). Different proportions of coal ash, 20, 30, 40 and 50% were added to the soil. The maximum values of UCS and CBR were noticed to be at 20% coal ash content. The mixture of coal ash and soil 20% and 80%, respectively, was mixed with randomly coconut coir fibre. The optimum percentages of soil, coal ash and coir fibre mix were reached at 80:20:0.25 by dry weight of soil. At these values, all of the properties of the soil were greatly improved.

Anggraini et al. (2015) investigated the effect of coir fibre content and curing time on the tensile and compressive strength of soft soil treated by lime. The test results indicated that compressive strength was less sensitive to lime and coir fibre stabilization compared to tensile strength.

Kumar et al. (2007) investigated the effect of fly ash, lime and polyester fibers on compaction and strength properties of expansive soils. They reported that cured 7 day, 14 day and 28 day specimens of clay-lime-fly ash mixture showed higher unconfined compressive strength than specimens without fly ash mixture. They also found that polyester fibers significantly increased the strength of soil lime fly ash mixture. Research has shown that eggshell is a rich source of lime, calcium and protein SO that it may be used as an alternative to such soil stabilizers as lime because it contains lime-like ingredients. Used as source of lime in agriculture, eggshell proved to contain a Considerable amount of lime. In the present study, eggshell powder was used as an alternative to stabilize expansive soils. To this end, various laboratory experiments were carried out on soil specimens mixed with different percentages of additives.

Okonkwo et al. (2012) concludes that the increase in the eggshell ash content will increase the strength of properties of the cement stabilized matrix up about 35% averagely. That show the usage of eggshell ash as an additive will increase the strength of the concrete.

According to Mtalib et al. (2009), he said that the addition of eggshell ash to the Ordinary Portland Cement decrease the setting time of the cement. So they conclude that the eggshells ash as an accelerator in a concrete because the higher content of the faster rate of setting. But it is different to the effect of eggshell on the soil.

Amu et. A! (2005) investigated that the eggshell powder could be good replacement in industrial lime because they have similarity in chemical composition.

Brook (2009) conducted a study on soil stabilization with fly ash and Rice Husk Ash, it was shown that the stress –strain behaviour of UCS showed that failure stress and strains increased by 106% and 50% respectively when fly ash content was increased from 0 to 25%. When the RHA content was increased from 0 to 12 %, UCS increased by 97% while CBR improved by 47%. It was therefore concluded that RHA content of 12% and fly ash content of 25% are recommended for blending into RHA for forming a swell reduction layer because of its satisfactory performance in Laboratory tests.

Anil and Sudhanshu (2014) performed a study on laboratory study on soil stabilization using fly ash and rice husk ash ,they treated black cotton soil with fly ash at (5%, 10%, 15%, 20% and 25%) while Rice husk ash was treated with (10%, 15%, 20%,25% and 30%) and examined after 28 days of curing. It was observed that Liquid limit was reduced to 55% for (20% fly ash and 25% RHA mixed with soil sample. Plasticity index was reduced to 86% for 20% Fly ash and 25% RHA mixed with soil, differential free swell reduced to 75% for 15% fly ash and 20% RHA mixed with soil, specific gravity reduced significantly as well.

Agbede et al (2016) did a study on production of concrete roofing tiles using rice husk ash (RHA) in partial replacement of cement, The work was based on an experimental study of roof tiles produced with ordinary Portland cement (OPC) and 5 %,10 %, 15 % , 20 % and 25 % (OPC) replaced by RHA. The result showed that addition of RHA show better results at 10 % replacement level than OPC at 28 days. Sudipta and Koyel (2016) made a study on potentials of Rice –Husk Ash as a soil stabilizer with virgin soil. RHA was added in 5%, 10%, 15% and 20% by weight of dry virgin soil. They conducted UCS, CBR, Atterberg’s Limit, and Standard Proctor tests, maximum dry density (MDD), optimum Moisture content (OMC) .It thus concluded that RHA is good material to be used in soil stabilization for special fine grained soil. Considering the fact that it is very cheap in terms of its availability and financial aspects as well.

Akshaya et al. (2012) made a study on effect of Polypropylene fibre on engineering characteristics of RHA-Lime stabilized expansive soil.0.5 -2% of polypropylene fibre was added at an increment of 0.5 %. The optimum proportion of soil: RHA: Lime fibre was found to be 84.5: 10: 4:1.5. Muntohar and Hantoro (2000) made a laboratory study on effects of Rice Husk and Lime on engineering characteristics of black cotton soil also known as expansive soil and noticed a significant improvement in engineering properties such as CBR , plasticity Index, Shear strength parameters etc.

Rao et al (2011) studied effect of Rice Husk Ash, Lime and gypsum on engineering properties of expansive soil and found an increase in Unconfined compression strength by 548% at 28 days of curing and CBR increased by 1350 %at 14 days curing at RHA- 20%, Lime -5% and gypsum - 3%.

Basha et al (2003) made a study on effects of RHA and cement on plasticity and compaction properties of expansive soil (bentonite) and had recommended 10-15% of RHA and 6-8% of cement as optimum percentages for expansive soil stabilization.

Sabat (2013) on effect of Lime sludge on compaction, CBR, shear strength, Compressive Coefficient and durability of an expansive soil stabilized with optimum Percentages of RHA after 7days of curing. The optimum proportion soil: RHA: Lime sludge was found to be 75:10:15.

Ashango and Patra (2014) made a study on both static and cyclic properties of RHA and Portland slag cement stabilized clay subgrade. They obtained optimum percentage of RHA to be 10% while Portland slag cement as 7.5% for expansive soil stabilization.

Sharma et al. (2008) in their study on the characteristics of expansive clay stabilized using lime, Rice husk Ash and calcium chloride. The optimum percentage for calcium chloride and was obtained to be 1% and 4% respectively in stabilization of expansive soil without addition of RHA. From UCS and CBR point of view when the soil was mixed with lime or calcium chloride, RHA content of 12% was found to be the optimum. In expansive soil – RHA mixes, 4% lime and 1% calcium chloride were also found to be optimum.

CHAPTER 3

MATERIALS AND METHODS

3.1. INTRODUCTION

This chapter presents the materials and methods used to accomplish the research goal. Relevant standards were employed to ascertain how the materials collected be analyzed and also the various laboratory tests to be conducted. All Tests such as sieve analysis test specific gravity, atterberg limit test (liquid and plastic limit), compaction and triaxial test were carried out at Nnamdi Azikiwe University Civil Engineering Geotechnical Laboratory.

3.2 Collection and Preparation of Materials

3.2.1 Clayey Samples

Natural clayey samples used for the experimental study designated as EE was collected at Efab Estate located along Enugu-Onitsha expressway Awka, Anambra State as shown in figure 3.1. The clay sample collected was disturbed samples. The choice of sites for collection of the clay samples was justified by the significant deposit of clay samples located within the region. The clay samples collected was a representative of clayey soils in that, it was sticky, constitute of substantial amount of lumps and with the individual particles not visible to the naked eyes. This soil sample was collected in two empty cement bags, marked indicating the sampling depth, soil description, sampling date and conveyed to geotechnical laboratory of Department of Civil Engineering Nnamdi Azikiwe University. After conveyance, the natural moisture content of the clay sample was determined and was thereafter air-dried for one week to allow partial elimination of natural water which may affect analysis. After drying, the lumps in the samples were slightly pulverized with minimal pressure in order not to damage the individual particles, the samples were passed through sieve No 4 (4.75mm) and the materials passing through the sieve were stored in cement bags in a safe location preparatory for laboratory testing.

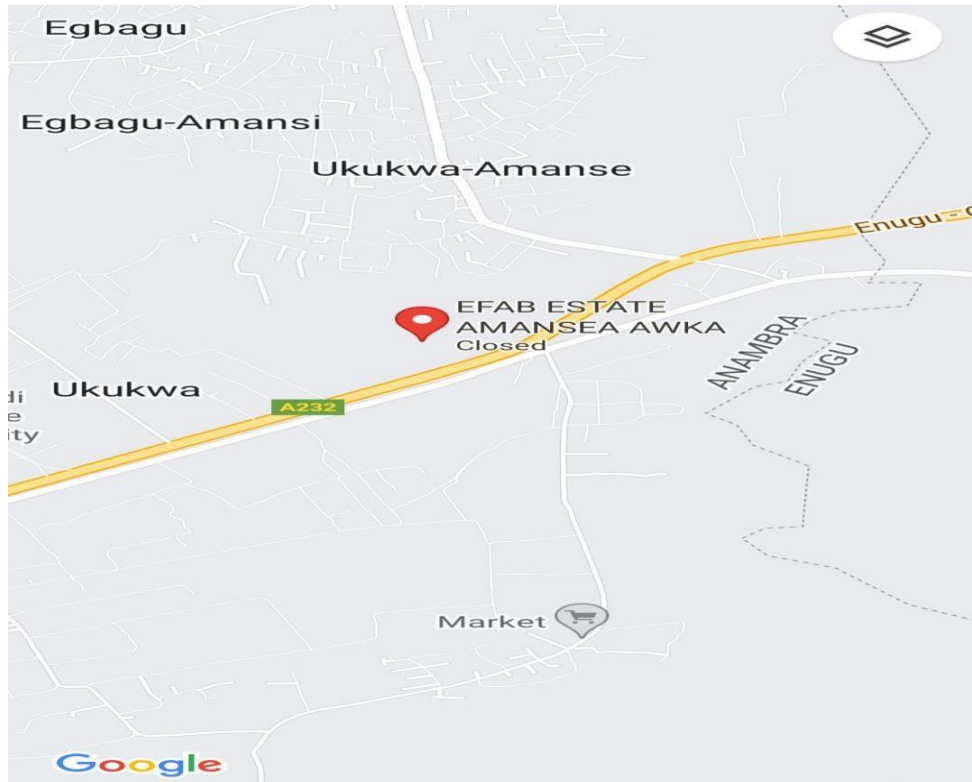


Plate 3.1: Map showing sample location (source: Goggle map)

Table Table 3.1: coordinates of sample materials

S/N	SAMPLES	LATITUDE	LONGITUDE
1	EE1	N6° 15' 0.2442	E7° 8' 23.3088
2	EE2	N6° 14' 59.0424	E7° 24.5184

3.2.2 Egg shells powder

Egg shell powder used in the experimental study was designated as ESP was collected from food vendors within ifite-Awka, transported to Enugu to be grounded and conveyed to Geotechnical laboratory. Upon arrival, the powder was passed through sieve 425 micrometer, the egg shell powder was thereafter stored in a safe location preparatory for various laboratory testing.

3.2.3 Fly-ash powder

Fly-ash powder was obtained from a vendor at Oji River, Enugu State. The fly-ash was conveyed to the Geotechnical laboratory. The ash was then passed through the BS No 200 sieve (75 μ m) before storing in a safe place

3.3 Laboratory Investigations

This section presents the experimental procedure and laboratory tests that were adopted for the project work. The tests was conducted for the natural clayey samples and clayey samples stabilized with Egg shell powder and fly-ash. The test includes: sieve analysis test, specific gravity, atterberg limit (liquid and plastic limit) and triaxial test. The aforementioned tests were carried out at Geotechnical Laboratory located inside the school campus. Below is a description of test procedures and apparatus:

3.3.1 Particle Size Distribution (Sieve Analysis)

Sieve analysis is a procedure used to assess the particle size distribution of a granular material (sand, gravel). The size distribution is often of critical importance to the behaviour of the material during use. Sieve analysis can performed on any type of non-organic or organic granular material including sand, crushed rock, clay, granite, feldspar and a wide range of manufactured powders, grains and seed down to minimum size depending on the exact method. The standard grain size analysis test determines the relative proportion of different grain sizes as they are distributed among certain size ranges.

Soil posses a number of physical characteristics which can be used as aid to identify it sizes in the field. A handful of soil rubbed through the finger can yield the following:

1. Sand and other coarser particle are visible to the naked eye.
2. Silt particle becomes dusty and are easily brushed off.
3. Clay particle are greasy and sticky when wet and hard when dry and have to be scrapped or washed off hand and boot

The apparatus needed for this experiment is listed below:

1. Stack of sieves including pan and cover.
2. Mechanical sieve shaker.
3. Weighing balance of 0.01g sensitivity.
4. Hand brush
5. Mortar and pestle (Used for crushing if the sample is conglomerated or lumped)
6. Thermostatically controlled Oven (With temperature of about 80°C-110°C).
7. Masking tape for identification of sample.
8. Exercise book and pen for recording of result.
9. The calculation for attaining Coefficient of uniformity and Coefficient of curvature are outlined below.

$$\text{Percentage retained (\%)} = \frac{\text{mass of soil retained in the sieve(g)}}{\text{total mass of soil sample(g)}} \times 100$$

$$\text{Cumulative percentage retained} = \sum \text{Percentage retained (\%)}$$

$$\text{Cumulative Percentage Finer (\%)} = 100 - \text{Cumulative percentage retained.}$$

$$\text{Coefficient of Curvature} = \frac{D_{60}}{D_{10}}$$

$$\text{Coefficient of Uniformity} = \frac{(D_{30})^2}{D_{10} \times D_{60}}$$

Where

D₁₀= particle size such that 10% of the soil is finer than the size

D₃₀= particle size such that 30% of the soil is finer than the size.

D₆₀= particle size such that 60% of the soil is finer than the size.



Plate 3.2: Apparatus for Particle Size Distribution Test (Sieve Analysis).

Test Procedure

1. Clean properly the stack of sieves to be used for the experiment using hand brush.
2. Weigh about 500g of air-dried soil sample on a weighing balance.
3. Pour the weighed soil sample into 75 μ m sieve and wash under a steady supply of water until clear water start coming out from the sieve after passing through the soil sample.
4. After washing pour the washed soil sample into a pre-weighed plate and dry it inside the thermostatically controlled oven at a controlled temperature of 80-110 $^{\circ}$ C for 16-24hrs.
5. Remove the sample from the oven and determine its weight (net weight) by deducting the weight of plate from the weight of plate and soil.
6. Arrange the stacks of sieve in the ascending order, place in a mechanical sieve shaker, and thereafter pour the sample and connect the shaker for about 10-15 minute.
7. Disconnect the sieve shaker and determine the mass retained on each of the sieve sizes.
8. Determine the percentage retained, Cumulative percentage retained and Cumulative percentage finer.

9. Plot the graph of sieve Cumulative percentage finer against sieve sizes.
10. Determine D10, D30 and D60 from the plotted graph.
11. Determine the Coefficient of Curvature and Coefficient of Uniformity and classify the soil using the American Association of State Highway and Transportation Official (AASHTO) and Unified Soil Classification System (USCS) respectively.

3.3.2 Specific Gravity Test

Specific gravity is the ratio of mass of unit volume of soil at a stated temperature to mass of equal volume of gas-free distilled water at the same temperature (Krishna, 2002). Also as defined by (Braja, 2006), Specific gravity can be defined as the ratio of unit weight of a material to unit weight of water. The specific gravity of soil solids is often needed for various calculations in soil mechanics. It can be determined accurately in the soil laboratory.

The apparatus employed for this experiment includes:

1. Density bottle of 50ml capacity and a stopper.
2. Desiccator containing anhydrous silica gel.
3. Thermostatically controlled oven with temperature of about 80-110°C.
4. Weighing balance of 0.01g sensitivity.
5. Mantle heater.
6. Plastic wash bottle.
7. Distilled water.
8. Funnel
9. Thin glass rod for stirring.
10. 425um Sieve.
11. Dry piece of cloth for cleaning.
12. Masking tape for identification of sample.
13. Exercise book and pen for recording of result.



Plate 3.3: Apparatus used for Specific Gravity Test

Test Procedure

1. Firstly clean the density bottle properly and rinse it with distilled water, oven- dry the clean density bottle with stopper, then cool it in a desiccator so as to remove any moisture present.
2. Weigh and record the weight of the empty clean and dry density bottle say (M_1)
3. Place 10-15g of soil passing through 425um sieve inside the density bottle, weigh and record the weight of density bottle +dry soil + stopper say (M_2).
4. Add distilled water to fill about half to three-fourth of the density bottle, soak the sample for 24hrs (The time stated is to enable complete settlement of the soil particle which is evident when clear water appears above the submerged soil).
5. Gently stir the density bottle using thin glass rod and thereafter connect to a mantle heater to de-air the sample, do not allow the sample to boil over.
6. After agitation, allow to cool at room temperature and fill it with distilled water up to the specified mark (at lower meniscus level), clean the exterior surface of the density bottle with a clean dry cloth and determine the weight of the density bottle + stopper +soil filled with water say (M_3).
7. Empty the density bottle clean and rinse with distilled water, then fill it with distilled water up to the same mark. Clean the exterior surface of the density bottle with a clean dry cloth and determine the weight of the density bottle filled with distilled water + stopper say (M_4).
8. Repeat the procedure for two more trials and take the average specific gravity value obtained from the total no of trial, the variation in the specific gravity result obtained for each trial must not exceed 2%, otherwise repeat the experiment.

The Procedure for Computation of result obtained is as follows:

$$\text{Specific gravity (G}_s\text{)} = \frac{(M_2 - M_1)}{(M_2 - M_1) - (M_3 - M_4)}$$

Where M_1 = weight of density bottle + stopper

M_2 = Weight of density bottle + air-dried soil + stopper.

M_3 = Weight of density bottle filled with water + wet soil + stopper.

M_4 = Weight of density bottle filled with water + stopper

3.3.3. ATTERBERG LIMIT TEST

The Atterberg limit refers to the liquid limit and plastic limit of soil. These two limits are used internationally for soil identification, classification, and strength correlations. When clay minerals are present in fine-grained soil, the soil can be remolded in the presence of some moisture without crumbling. This cohesiveness is caused by the adsorbed water surrounding the clay particles. At a very low moisture content, soil behaves more like a solid; at a very high moisture content, the soil and water may flow like a liquid. Hence on an arbitrary basis, depending on the moisture content, the behavior of soil can be divided into the four basic states, namely; solid, semisolid, plastic, and liquid.

Qualitative positions of Atterberg limits on a moisture content scale. Solid, semisolid, plastic and liquid state of soil depends on the shrinkage limit, plastic limit and liquid limit.

The percent of moisture content at which the transition from solid to semi-solid state takes place is defined as the shrinkage limit (SL). The moisture content at the point of transition from semisolid to plastic state is the plastic limit (PL), and from plastic to liquid state is the liquid limit (LL). These parameters are also known as Atterberg limits. The liquid and plastic limits of a soil and its water content can be used to express its relative consistency or liquidity index.

The plasticity index and the percentage finer than $2\mu\text{m}$ particle size can be used to determine its activity number.

The liquid limit of a soil containing substantial amounts of organic matter decreases dramatically when the soil is oven-dried before testing. A comparison of the liquid limit of a sample before and after oven-drying can therefore be used as a qualitative measure of the organic matter content of a soil.

3.3.3.1. PRACTICAL APPLICATION

This test method is used as an integral part of several engineering classification systems (USCS, AASHTO, etc.) to characterize the fine-grained fractions of soils and to specify the fine-grained fraction of construction materials.

The liquid limit, plastic limit, and plasticity index of soils are also used extensively, either individually or with other soil properties to correlate with engineering behavior such as compressibility, hydraulic conductivity (permeability), shrink-swell, and shear strength.

This method is sometimes used to evaluate the weathering characteristics of clay-shale materials. When subjected to repeated wetting and drying cycles, the liquid limits of these materials tend to increase. The amount of increase is considered to be a measure of the shale's susceptibility to weathering.

3.3.3.2.OBJECTIVE

The objective of this experiment is:

To determine the liquid limit (LL), plastic limit (PL), and the plasticity index (PI) of fine-grained cohesive soils.

EQUIPMENTT

1. Balance
2. Casagrande's liquid limit device
3. Grooving tool
4. Mixing dishes

5. Spatula
6. Oven

3.3.3.3. METHOD

3.3.3.3.1. LIQUID LIMIT TEST

1. Determine the mass of each of the three moisture cans (W1).
2. Calibrate the drop of the cup, using the end of the grooving tool not meant for cutting, so that there is consistency in the height of the drop.
3. Put about 250 g of air-dried soil through a # 40 sieve into an evaporating dish and with a plastic squeeze bottle, add enough water to form a uniform paste.
4. Mixing of soil with water



Plate 3.4: Preparation of soil slurry

5. Place the soil in the Casagrande's cup and use a spatula to smooth the surface so that the maximum depth is about 8mm



Plate 3.5: Placing the soil paste on the Casagrande apparatus

6. Placing the soil paste on the Casagrande apparatus
7. Using the grooving tool, cut a groove at the center line of the soil cup.
8. Cutting a groove at the middle of the soil paste with a standard grooving tool



Plate 3.6: Cutting a groove at the middle of the soil paste with a standard grooving tool

9. Crank the device at a rate of 2 revolutions per second until there is a clear visible closure of $\frac{1}{2}l$ or 12.7 mm in the soil pat placed in the cup. Count the number of blows (N) that caused the closure. (Make the paste so that N begins with a value higher than 35.)

10. The groove at the middle of the soil sample before the application of the blows



Plate 3.7: The groove at the middle of the soil sample before the application of the blows

11. The groove at the middle of the soil sample after the application of the blows. The blows need to be stopped as soon as the soil merges about half inches

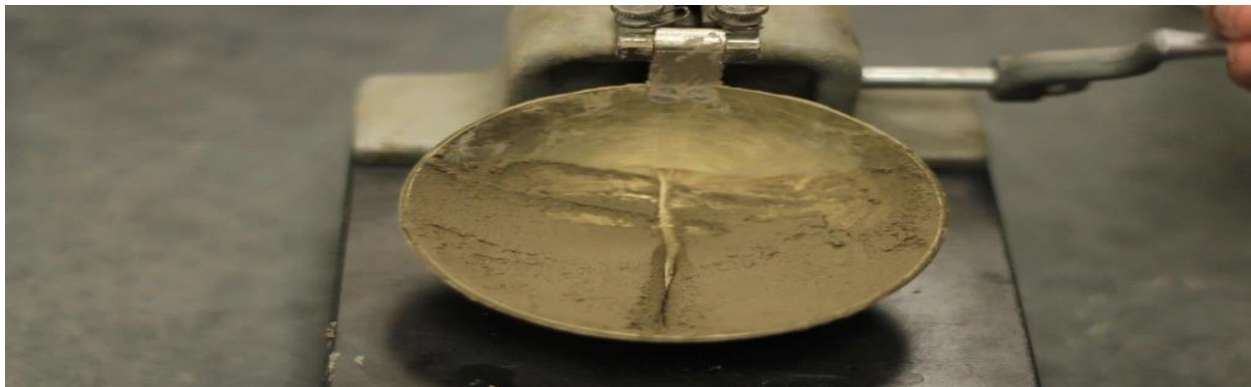


Plate 3.8: The groove at the middle of the soil sample after the application of the blows

12. If $N = 15$ to 40 , collect the sample from the closed part of the cup using a spatula and determine the water content weighing the can + moist soil (W_2). If the soil is too dry, N will be higher and will reduce as water is added.
13. Do not add soil to the sample to make it dry. Instead, expose the mix to a fan or dry it by continuously mixing it with the spatula.
14. Perform a minimum of three trials with values of $N = 15$ to 40 , cleaning the cap after each trial.
15. Determine the corresponding $w\%$ after 24 hours (W_3) and plot the N vs $w\%$, which is called the —flow curve.

3.3.3.2. PLASTIC LIMIT TEST

1. Mix approximately 20 g of dry soil with water from the plastic squeeze bottle.
2. Determine the weight of the empty moisture can, (W_1).
3. Prepare several small, ellipsoidal-shaped masses of soil and place them in the plastic limit device. Place two fresh sheets of filter paper on either face of the plates.
4. Sample preparation for plastic limit test. Preparing a soil ball with an arbitrary water content.



Plate 3.9: Sample preparation for the plastic limit test

5. Roll the upper half of the device which has a calibrated opening of 3.18 mm with the lower half plate.



Plate 3.10: A sample thread of 3mm in diameter

6. If the soil crumbles forming a thread approximately the size of the opening between the plates (around 3 mm diameter), collect the crumbled sample, and weigh it in the moisture can (W2) to determine the water content. Otherwise, repeat the test with the same soil, but dry it by rolling it between your palms.
7. Determine the weight of the dry soil + moisture can, (W3).
8. The water content obtained is the plastic limit.

3.3.4. Compaction Test

Compaction is the process of increasing the bulk density of the soil by driving out air. It involves the densification of soils by mechanical means thereby increasing the dry density of the soil. According to (Shruthi, 2017) Compaction of soil is the process by which the soil solid are packed more closely together by mechanical means, thus increasing its dry density. It could also be stated as the process of packing the soil particles more closely together usually by tamping, rolling or other mechanical means, thus increasing the dry density of the soil. It is achieved through the reduction of the volume of air void in the soil with little or no reduction in water content. The process must not be confused with consolidation in which water is squeezed out under the action of steady static load. Consolidation is a natural process and results in dense packing of the soil.

In civil engineering practice soil compaction is essential for the following reasons:

1. Increasing the bearing strength of foundation
2. Provide stability to slope and foundation.
3. Prevention of undesirable settlement of structures
4. Reduction of water seepage from structure

The compaction methods to be adopted for this research are:

1. British Standard Light for the natural samples of clay soil collected from Amansea.
2. British Standard Light for the specimen (fly ash and egg shell powder stabilized clay sample).

Table 3.2 Details of Compaction Mould

Type	Diameter (mm)	Height (mm)	Volume(cm ³)
British Standard	105	115.5	1000

Table 3.3 Details of Compaction Procedure.

Type of test	Mould (cm ³)	Rammer(kg)	Drop (mm)	No of layers	Blow per layer
BS light	1000	2.5	300	3	27
BS heavy	1000	4.5	450	5	27

The mechanical energy applied in each type of British Standard in term of work done is given as follows:

$$\text{British Standard Light Mechanical energy} = \frac{\text{Weight of rammer} \times \text{no of layers} \times \text{no of blows} \times \text{height of drop}}{\text{Volume of mould}}$$

$$\frac{2.5g \times 3 \text{ layers} \times 27 \text{ blows} \times 300 \text{ mm}}{1000} = 60.75 \text{ kgm} = 60.75 \times 9.81 \text{ Nm} = 596 \text{ kn}\backslash\text{m}$$

$$\text{Work done per unit volume of soil} = \frac{596}{1000} = 596 \text{ kn/m}^3$$

The apparatus used for the test are as follows:

1. Compaction mould with a detachable base plate and removable extension collar.
2. Metal rammer (either 2.5kg or 4.5kg)

3. Measuring Cylinder 200ml or 500ml
4. Large Metal tray (600mm×600mm ×600mm)
5. Balance up to 10kg readable to 1g
6. Small tools such as palette knife, steel straight edge about 300mm long.
7. Drying oven temperature of 105-110⁰C

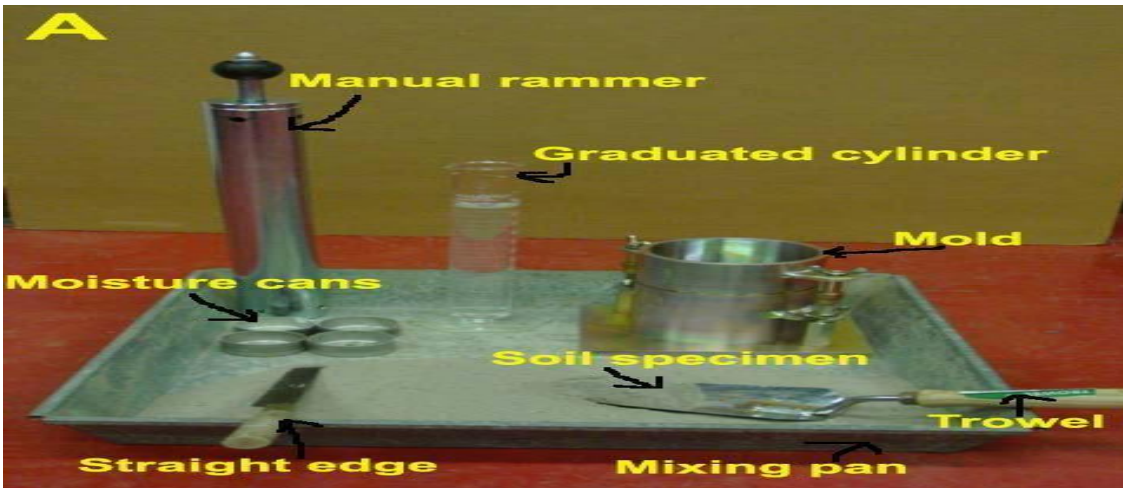


Plate 3.11: Compaction test apparatus

Test Procedure.

1. Check to see if the mould, extension collar and base plate are clean and dry. Measure the dimension and weigh to the nearest 1kg check if the rammer falls freely.
2. Grease the internal surface of the mould
3. Attach the extension collar to the mould.
4. Weigh about 3kg of the soil sample on a weighing balance
5. Add about 4% water to the soil sample, mixing it thoroughly and separating the soil into three layers for British Standard Light and five layers for British Standard Heavy.
6. Pour the wet soil into the mould and compact by applying the required no of blow using either a 2.5kg or 4.5kg rammer falling freely from a height of 300mm. The blow must be distributed uniformly over the surface of the mould.

7. After completion of the compaction operation remove the extension collar and level carefully the top of the mould by means of a straight edge.
8. Weigh the mould with the compacted soil to the nearest 1kg, record the weight as W_2 .
9. Determine the moisture content of the representative sample of the specimen; record the moisture content as M .
10. Repeat the procedure for 8%, 12%, 16% and 20% of water to be added and record the value obtained.
11. Plot the graph of dry density against moisture content and determine the maximum dry density (MDD) of the soil at the corresponding optimum moisture content (OMC).

The Computation of the result obtained is as follows:

Determination of Dry Density (P_d).

$$\text{Wt of mould (kg)} = W_1$$

$$\text{Wt of mould + wet soil (kg)} = W_2$$

$$\text{Wt of wet soil (kg)} = W_2 - W_1$$

$$\text{Volume of mould (M}^3\text{)} = W_4$$

$$\text{Bulk Density (kg/m}^3\text{)} = \frac{\text{Wt of wet soil (kg)}}{\text{Vol of mould (m}^3\text{)}} = \frac{W_2 - W_1}{W_4}$$

$$\text{Moisture Content (\%)} = \frac{\text{moisture content (top)} + \text{moisture content (bottom)}}{2}$$

$$\text{Dry Density (kg/m}^3\text{)} = \frac{\text{Bulk density}}{1 + \text{moisture content (\%)}} = \frac{P_b}{1 + w/100}$$

Determination of Moisture Content (w) for top and bottom respectively.

$$\text{Wt of tin (kg)} = W_1$$

$$\text{Wt of tin + wet soil} = W_2$$

$$\text{Wet of wet soil (kg)} = W_3 = W_2 - W_1$$

$$\text{Wt of tin + dry soil (kg)} = W_4$$

$$\text{Wt of dry soil (kg)} = W_5 = W_4 - W_1$$

$$\text{Wt of water (kg)} = W_6 = W_3 - W_5$$

$$\text{Moisture Content (\%)} = \frac{\text{Wt of water}}{\text{Wt of dry soil}} \times 100 = \frac{W_6}{W_5} \times 100$$

3.3.5. TRIAXIAL TEST

Triaxial testing is a type of shear test for solid materials performed while the specimen is under confining pressures on all sides. The confining pressures are generated in a fluid chamber to simulate stresses from surrounding soil materials. It then can give a clearer picture of the behavior of materials in place. This testing principle applies to rocks, powders, and construction materials, but this blog post will focus on the triaxial shear testing of soils.

3.3.5.1. OBJECTIVES

The aim of the various procedures is to measure the triaxial shear strengths of soil specimens subjected to different drainage conditions in the field. The results provide valuable information for the engineered design and construction of soil embankments, pavements, and structure foundations. Determining the mechanical behavior of soil materials through triaxial testing helps ensure that the soils supporting the structures are adequate for the proposed use – and its continued performance.

Triaxial shear testing for soils is not just one test. This blog post will discuss three different test methods, each one with variable requirements based on soil types and properties of individual specimens.

3.3.5.2. Triaxial Shear Test Apparatus

These are some significant components of the specialized equipment required for triaxial testing:

1. Triaxial Cells are chambers in a variety of sizes where the prepared specimens are mounted. A pressurized fluid, usually water, in the cell creates confining pressure around the sample. Brass or stainless-steel fittings on the cell control filling and draining while a low-friction piston applies compressive force to the specimen during testing. Triaxial Test Cell Accessories are required and are available as individual items or a kit. Kits contain porous stones, latex membranes, cap and pedestal, and O-Rings corresponding in size to the test specimen.
2. Load Frames apply axial loading forces at the correct strain rate to the specimen via the test cell. Load frames with 10,000lbf or 20,000lbf (44.5 or 89kN) capacities and fitted with the proper triaxial components provide analog or digital measurement of pressures and deformation during testing.
3. Triaxial Control Panels equipped with measuring burettes, connections, and controls regulate and monitor fluid and air pressures, and the filling and draining of test cells. The Master Panel provides all necessary functions for a single test cell, and an Auxiliary Panel can be added for each new test cell to perform simultaneous testing.
4. Pore Pressure Transducer is available to measure the pressure of fluids within the specimen during testing. This unit is available as a stand-alone instrument with an included digital readout.
5. Triaxial Data Acquisition Software works together with Gilson digital triaxial load and deformation instruments to log, calculate, graph, and report axial load and deformation data of triaxial soil tests.
6. The Vacuum Pump applies vacuum pressures for specimen saturation phases and deairing of water for triaxial and permeability testing. A laboratory Drierite Gas Drying Unit is a recommended accessory.
7. Deairing Tank works with a vacuum source to remove entrapped air from water supplies for triaxial and permeability tests.

3.3.5.3. Sample Preparation

Soil samples, either undisturbed and extruded from thin-walled tube (Shelby tube) samplers, or remolded or compacted in the laboratory, are formed and trimmed to size using specialized sample preparation equipment. A latex membrane to control fluid migration, porous stones at

each end, along with a cap and pedestal for mounting in the test cell, are fitted using A test cell kit and other tools and accessories.

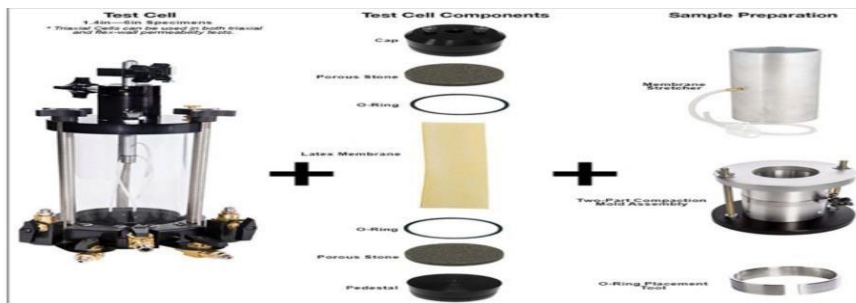


Plate 3.12: Triaxial test apparatus

3.3.5.4. Triaxial Shear Test Procedure

The assembled test cell containing the prepared specimen and water is mounted in the load frame. Air and water lines to the triaxial control panel are connected, and load and deformation measurement instruments are installed and zeroed. There are three phases for triaxial tests, and each step has variations unique to the particular test method. Successful testing depends on a thorough reading and understanding of the specific test method used.

1. Saturation is the process of filling all voids in the soil specimen, as well as the porous stones and drain lines, with water without undue disturbance of the sample. The different test methods vary slightly on the steps required, but most use deaired water produced in a deaeration device in conjunction with back pressure saturation. Backpressure, additional pressure applied to the pore-water of the specimen, compresses air in the sample and forces it into solution, thereby increasing saturation.
2. Consolidation occurs under confining pressures applied to the fluid in the test cell. In the UU test, where drainage is not permitted, a totally saturated specimen cannot consolidate as a result of confining pressures. Partially saturated samples can consolidate and may have different strengths if tested at different confining pressures. For CU and CD specimens drained during consolidation, a volume change of the sample will occur. Drainage continues until consolidation reaches equilibrium, and the values determine the strain rate used during axial loading.

3. Shear is the final phase of the test when the specimen is axially loaded. For the UU (or quick) test, the rate of loading is set between 0.3% and 1% per minute so that failure will occur within about 15 minutes. For CU and CD tests, strain rates must be calculated based on values from each consolidation phase and are much slower. Total test times may stretch into days or weeks for these methods.

CHAPTER 4

RESULTS AND ANALYSIS

The results analysis was carried out in this section to relate the properties of the soil tested and its relation to the aim of the project work. Tests results to be discussed include: compaction, atterberg limit and triaxial test.

4.1 Natural soil

The natural soil is fine grained, having reddish colour. The percentage passing at 0.075mm aperture sieve is 5.01% with D60, D30 and D10 values of 0.3, 0.15 and 0.075 respectively. It has C_u and C_c values of 2 and 1 respectively. The soil has liquid limit of 53.13%, plastic limit 34.11% and plasticity index of 19.02%.

Table 4.1. Physical properties of the natural soil

PROPERTIES	EE1	EE2
Specific gravity	2.23	2.59
Liquid limit (%)	52.10	53.44
Plastic limit (%)	33.62	34.11
Plasticity index (%)	18.48	19.33
Optimum moisture content (%)	11.60	12.87
Maximum dry density	18.02	18.25
Cohesion (kN/m^3)	30	17
Angle of internal friction ($^\circ$)	22	20
Shear strength (kN/m^3)	35.11	21.68

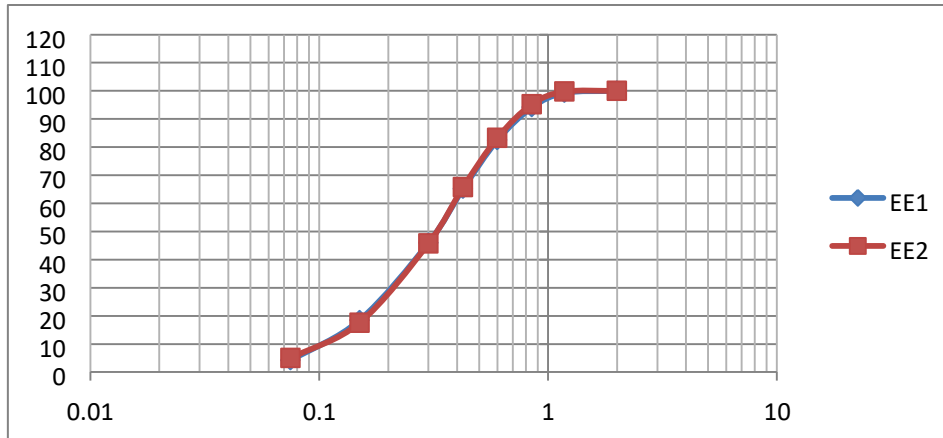


Figure 4.1: Particle size distribution for EE1 and EE2

4.2 ATTERBERG LIMIT TEST

The test done here include liquid limit (LL), plastic limit (PL) and plasticity index (PI), and there were carried out in accordance to BS 1377-2-1990. From the natural liquid limit result 52.00% and 53.13%, a decrease was noticed on addition of 0%FA:18%ESP as was also noticed by (Arash Barazesh et al,2012) showing that addition of Eggshell powder to Clay soil decreases the liquid limit. The liquid limit then began to increase as the amount of Eggshell powder reduced before getting to a peak value of 48.45% and 53.23% in both soils at 15%FA 3%ESP. The increase in the liquid limit with increase in fly-ash as also shown in Table 4.2 and Table 4.3 below indicates that the soil is less prone to swelling and shrinkage due to changes in moisture content. This is because fly-ash has pozzolanic properties that can react with calcium hydroxide in the soil to form a cementitious material that can fill the pores and voids in the soil. For the plastic limit, a decrease was noticed upon addition of eggshell powder which was followed by an increase, having a peak value at 15%FA 3%ESP.

Table 4.2 Atterberg's limit characteristics for EE1

PERCENTAGE COMBINATIONS	LL	PL	PI
SOIL 100%	52.10	33.62	18.48
0%FA 18%ESP	45.25	29.94	15.31

3%FA 15%ESP	46.14	31.06	15.08
6%FA 12%ESP	46.50	31.97	14.53
9%FA 9%ESP	47.15	34.27	12.88
12%FA 6%ESP	48.00	36.16	11.84
15%FA 3%ESP	49.45	38.53	10.92
18%FA 0%ESP	50.66	40.77	9.89

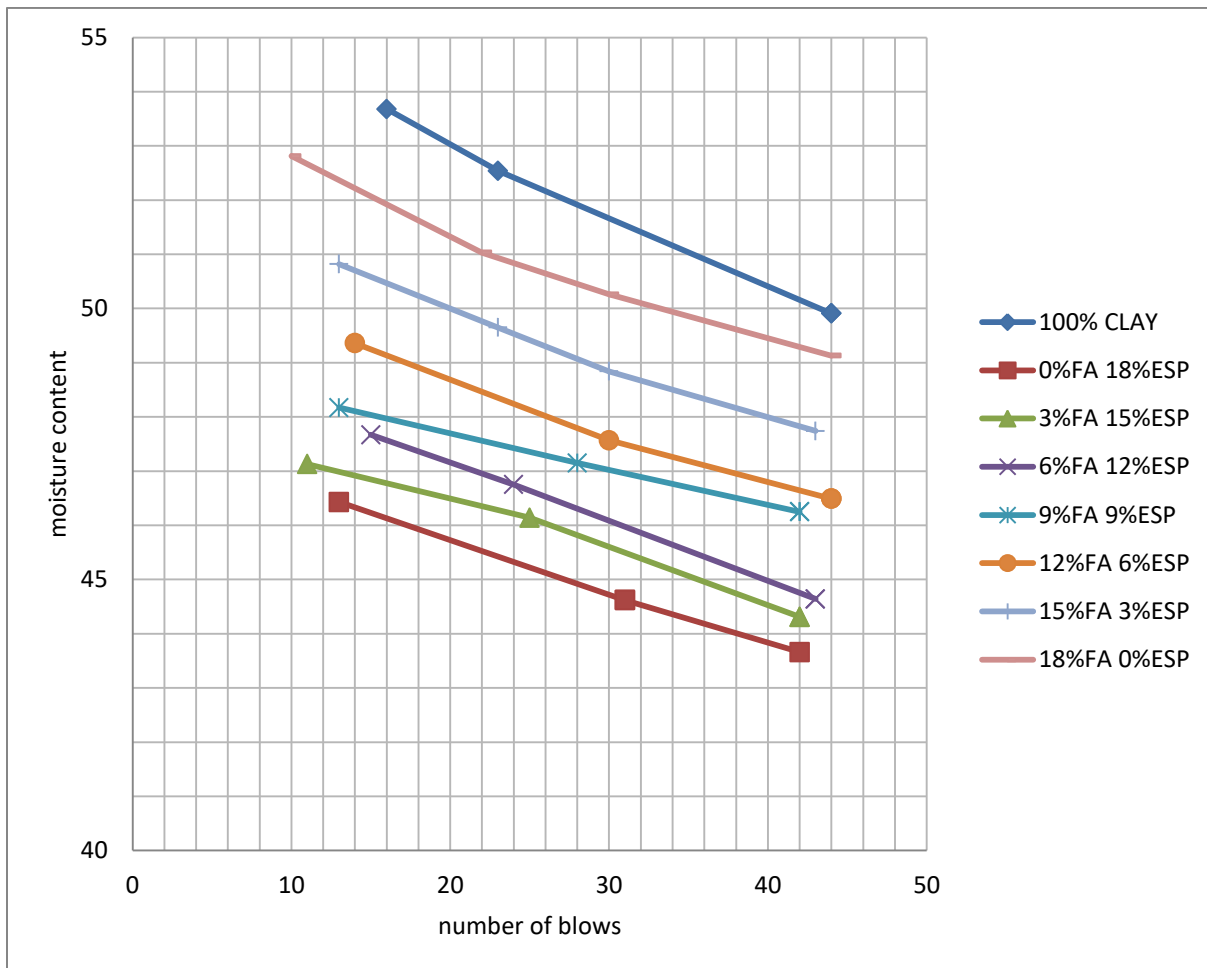


Figure 4.2: Atterberg's limit for EE1

Table 4.3: Atterberg's limits characteristics for EE2

PERCENTAGE COMBINATIONS	LL	PL	PI
SOIL 100%	53.44	34.11	19.33
0%FA 18%ESP	46.41	29.00	17.41
3%FA 15%ESP	47.66	31.00	16.66
6%FA 12%ESP	49.76	34.22	15.54
9%FA 9%ESP	50.71	36.12	14.59
12%FA 6%ESP	52.65	38.84	13.81
15%FA 3%ESP	53.91	41.39	12.52
18%FA 0%ESP	54.80	42.90	11.9

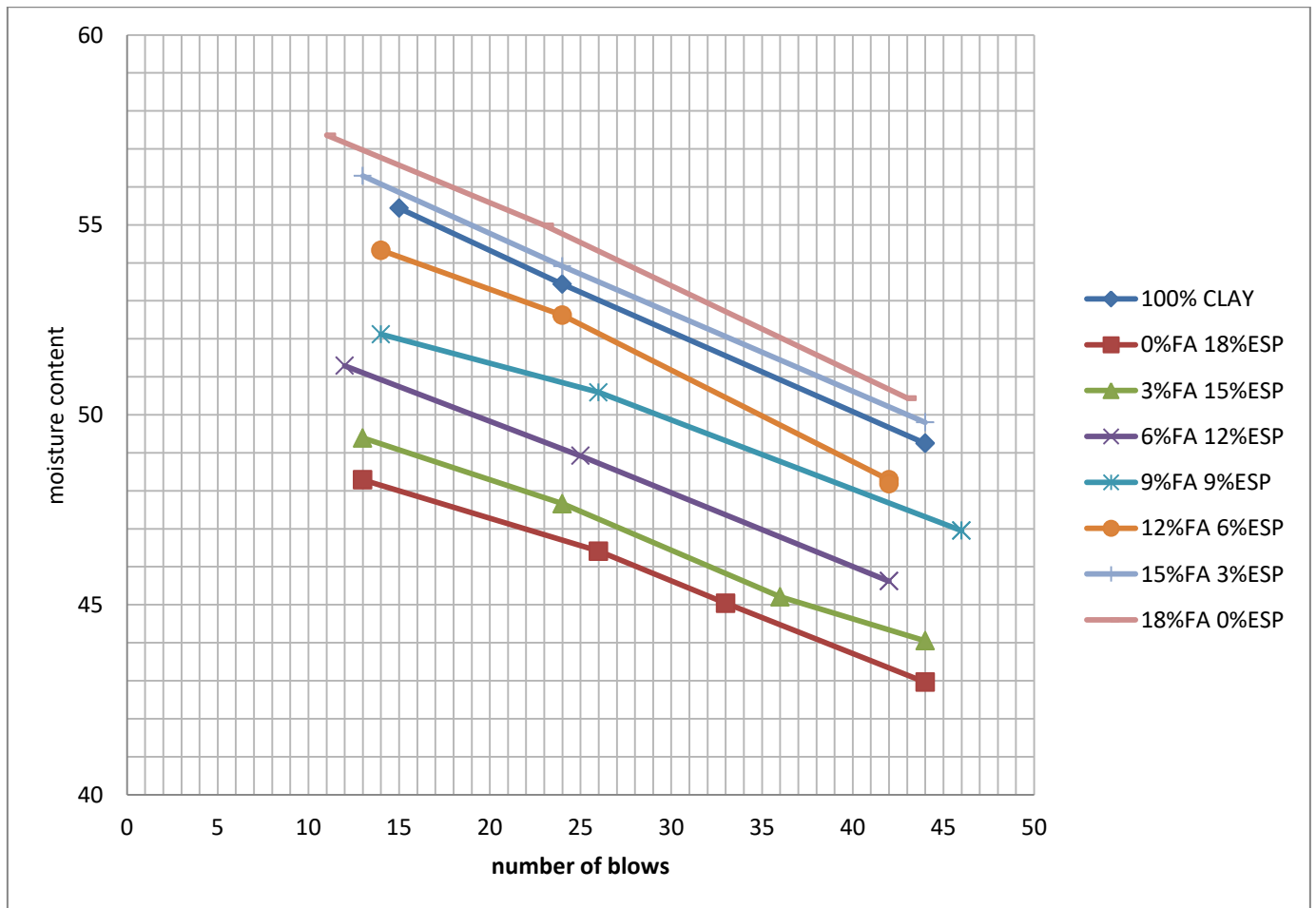


Figure 4.3: Atterberg limit for EE2

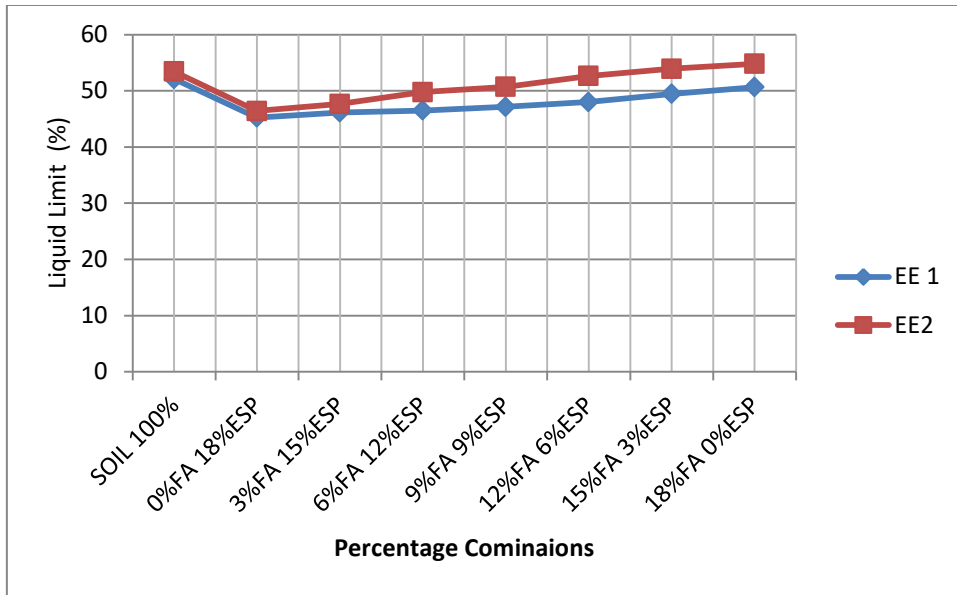


Figure 4.4: Variation in the liquid limit with each addition of percentage combinations

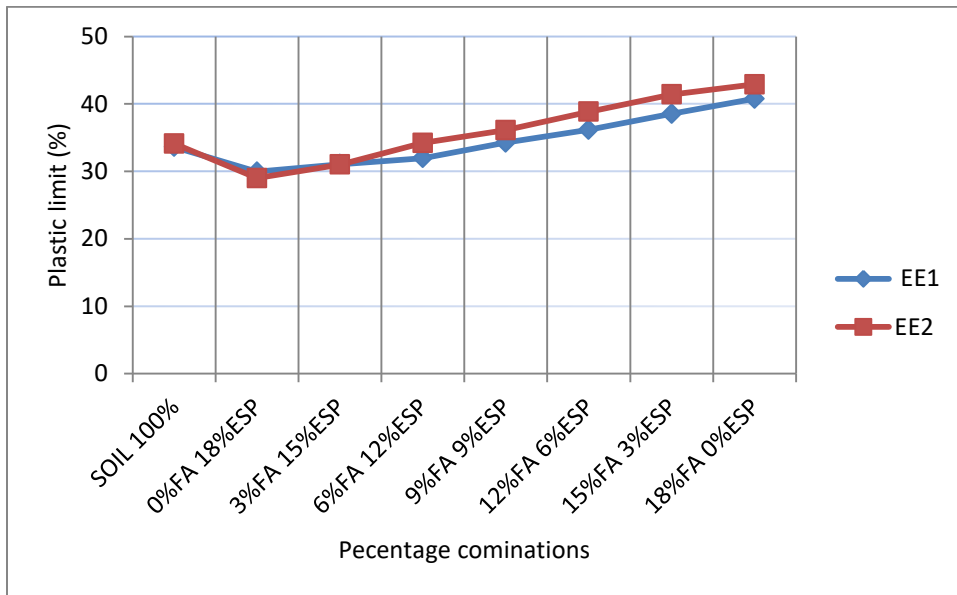


Figure 4.5: Variation in the plastic limit with each addition of percentage combinations

4.3 COMPACTION

Eggshell acting alone causes a reduction in both the OMC and MDD values. Further reduction was noticed in the OMC values but a noticeable increase was noticed in the MDD values. A sharp rise was noticed in the OMC value at 15%FA 3%ESP and in the MDD values at 12%FA 6%ESP. The increase in MDD values as the additives went on can be ascribed to the pozzolanic nature of the additives that can react with the clay minerals in the soil resulting in the formation of cementitious compounds that can improve the soil's strength. The combination of both additives has a peak value at 15%FA 3%ESP.

Table 4.4: Compaction characteristics for EE1

PERCENTAGE COMBINATIONS	OMC	MDD
SOIL 100%	11.6	18.02
0%FA 18%ESP	10.95	17.68
3%FA 15%ESP	10.89	18.13
6%FA 12%ESP	10.25	18.24
9%FA 9%ESP	10.02	18.24
12%FA 6%ESP	9.81	19.65
15%FA 3%ESP	17.15	19.67
18%FA 0%ESP	16.92	19.71

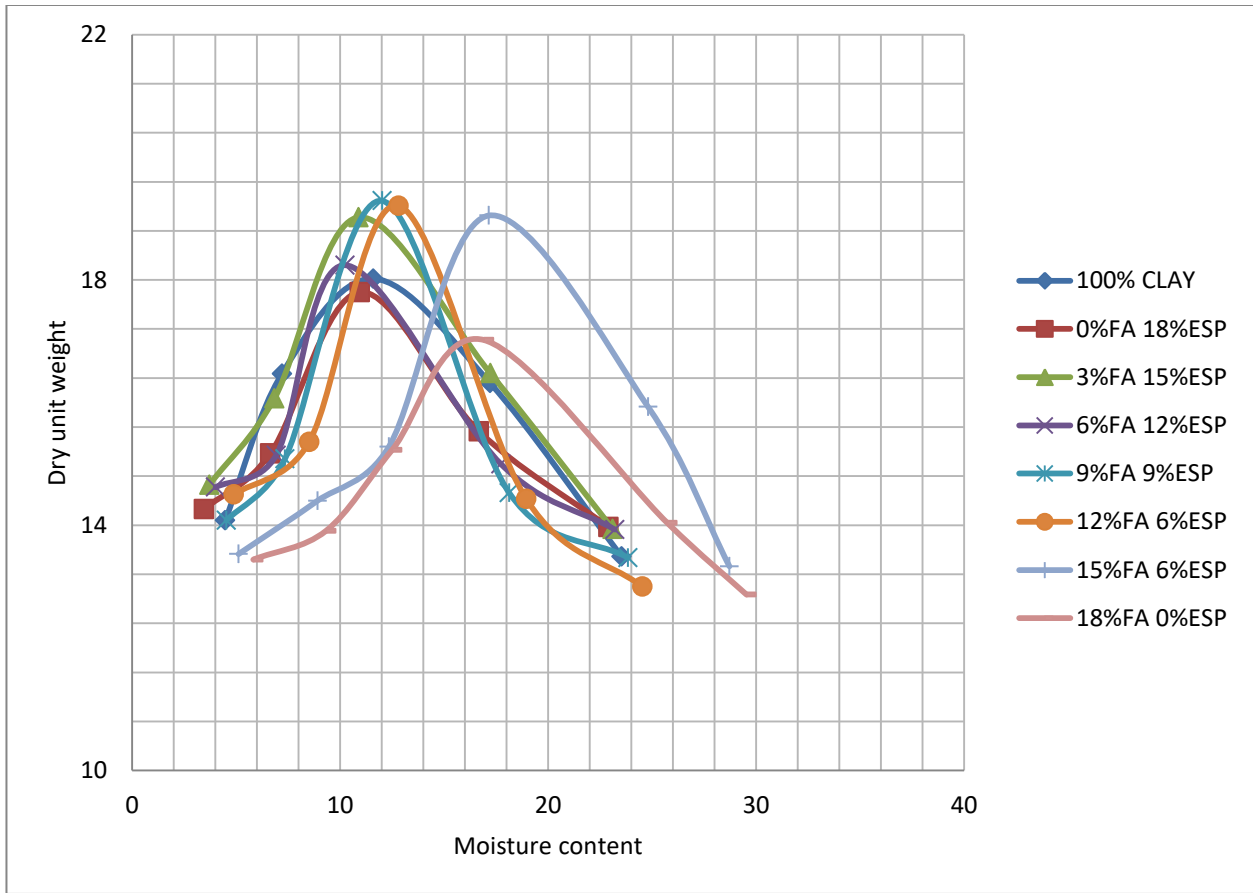


Figure 4.6: Compaction for EE1

Table 4.5: Compaction characteristics for EE2

PERCENTAGE COMBINATIONS	OMC	MDD
SOIL 100%	12.87	18.25
0%FA 18%ESP	11.74	17.16
3%FA 15%ESP	11.91	17.53
6%FA 12%ESP	11.71	18
9%FA 9%ESP	11.43	18.05
12%FA 6%ESP	11.61	18.49
15%FA 3%ESP	18.22	18.77
18%FA 0%ESP	17.22	18.83

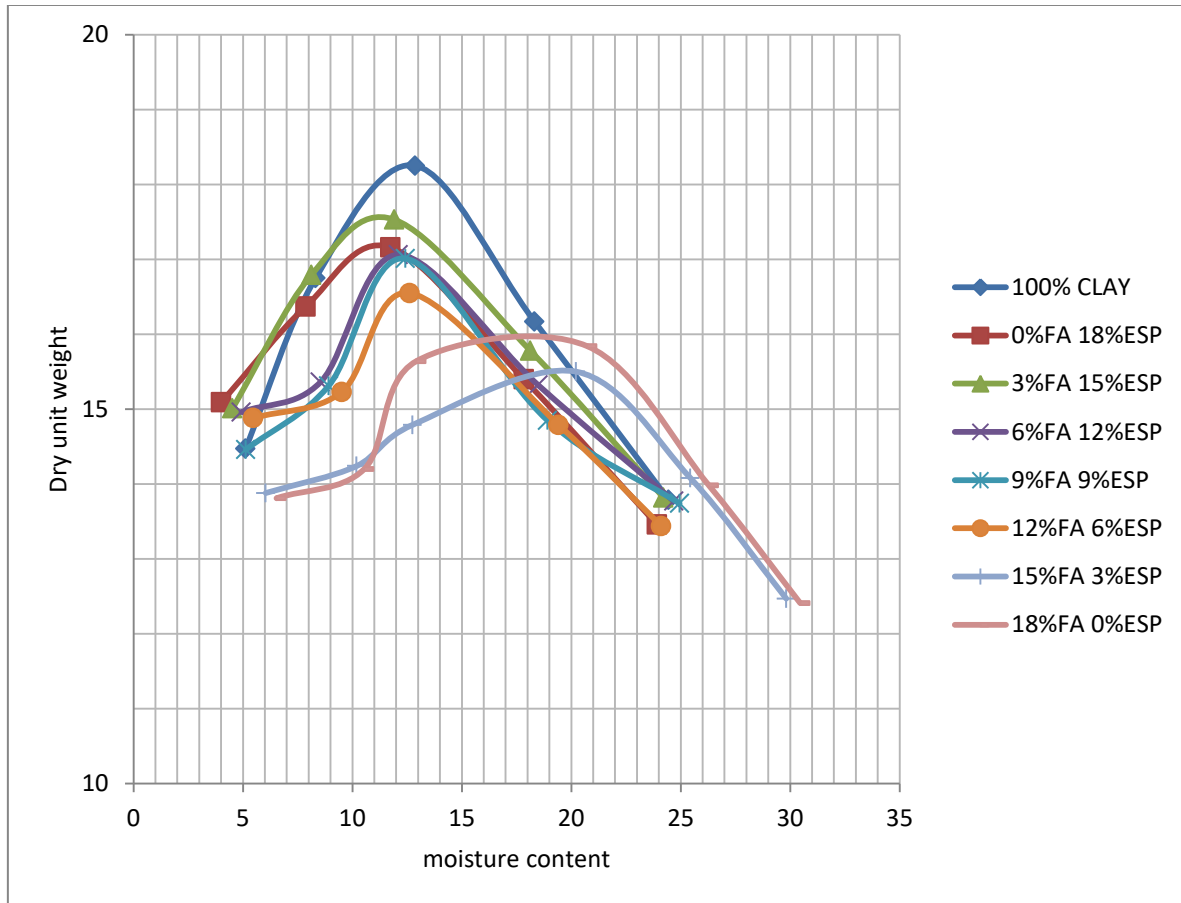


Figure 4.7: Compaction for EE2

4.4 TRIAXIAL TEST

The variation in the shear strength parameters, Phi and C with flyash and eggshell powder content is shown in the graphical plot presented in Figures 4.9 and 4.10. The results indicate a reduction in Phi from its natural value of 22° and an increase in its C value from its natural value of 30kN/m^3 to a peak value of 70kN/m^3 at 18%FA:0%ESP. The reduction in the phi value can be attributed to the FA, which may have introduced some fines which lead to the reduction in the friction angle of the clay. The increase in the C value can also be attributed to the flyash, which reacts with water and forms cementitious compounds that can contribute to the development of some cohesion in the soil, leading to the increase in cohesion of the clay soil. The shear strength value increased with reduction in ESP and had a great increase in value when the flyash percentage was higher. The combination of both additives has a shear strength peak value of 68.66kN/m^3 and 91.56kN/m^3 at 15%FA 3%ESP. The shear strength is gotten by;

$$\text{Shear strength} = C + \delta \times \text{Tan phi}$$

Where;

C = Cohesion

δ = Sigma1

Phi = Angle of internal friction

Table 4.6 Shear strength parameters for different mix for EE1

PERCENTAGE COMBINATIONS	Phi	C	Shear strength (kN\m ³)
SOIL 100%	22	30	35.11
0%FA 18%ESP	15	40	43.85
3%FA 15%ESP	13	45	49.61
6%FA 12%ESP	10	48	51.78
9%FA 9%ESP	10	50	53.81
12%FA 6%ESP	10	51	54.89
15%FA 3%ESP	9	65	68.66
18%FA 0%ESP	7	70	72.89

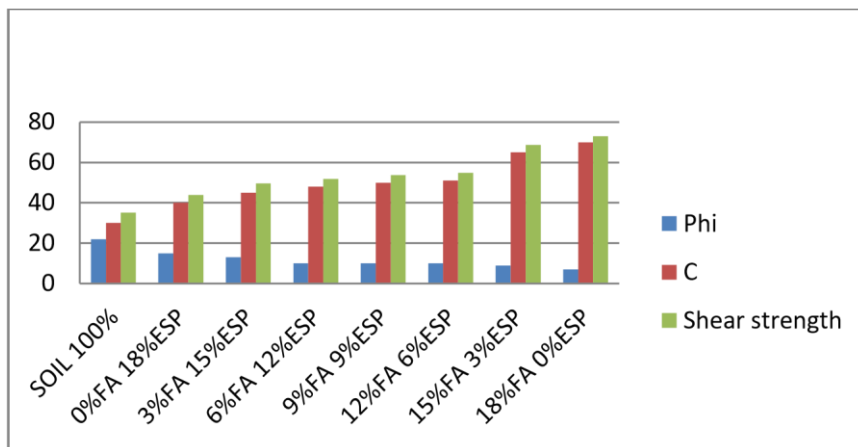


Figure 4.8: Shear strength parameters at different percentage mix for EE1

Table 4.7: Shear strength for different mix for EE2

PERCENTAGE COMBINATIONS	Phi	C	Shear strength (Kn\m ³)
SOIL 100%	20	17	21.68
0%FA 18%ESP	15	40	43.83
3%FA 15%ESP	11	51	54.83
6%FA 12%ESP	9	61	64.32
9%FA 9%ESP	9	61	64.46
12%FA 6%ESP	9	65	68.66
15%FA 3%ESP	6	89	91.56
18%FA 0%ESP	5	95	97.21

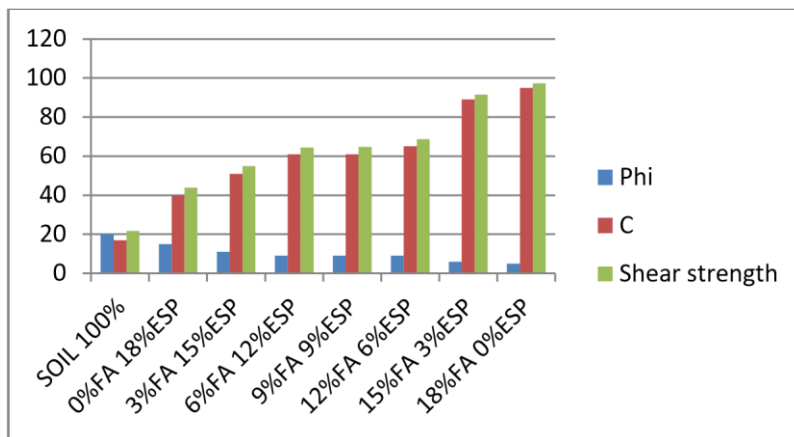


Figure 4.9: Shear strength parameters at different percentage mix for EE2

4.5. REGRESSIONAL ANALYSIS

4.5.1. ANALYSIS FOR EE1

The following results are the regressional analysis of the result of the Shear strength values of Clay-Flyash-Eggshell powder mixtures; the P-value for the Phi (0.076045) > 0.05, it shows that the Phi is less significant to the shear strength, the P-value for C (7.02E-06) < 0.05, it shows that the C is statically significant, the t-stat for Phi (0.034339) < 0.05, it shows that the Phi is statically significant, the t-stat for C (30.348280) > 0.05, it shows that the C is statically insignificant, the R-square for the regression statistics is (0.999008902) and the Adjusted R-square is (0.998513353), it shows that the work follows an almost linear pattern or sequence and can be predicted perfectly with a linear with a linear equation. The predicted and measured values are shown below:

Table 4.8: summary of the regressional output for EE1

SUMMARY OUTPUT

<i>Regression Statistics</i>	
Multiple R	0.999686677
R Square	0.999008902
Adjusted R Square	0.998513353
Standard Error	0.363833902
Observations	8

ANOVA					
	<i>df</i>	<i>SS</i>	<i>MS</i>	<i>F</i>	<i>Significance F</i>
Regression	2	1055.724124	527.8621	3987.623	9.82617E-09

Residual		5	0.661875541	0.132375		
Total		7	1056.386			
<hr/>						
			<i>Standard</i>			
	<i>Coefficients</i>		<i>Error</i>	<i>t Stat</i>	<i>P-value</i>	<i>Lower 95%</i>
<hr/>						
Intercept	4.165884471		1.895240157	2.198077	0.069286	0.705985451
Phi	0.069787433		0.064040261	0.034339	0.076045	0.094833297
C	0.978880528		0.023536826	30.348280	7.02E-06	0.91837719
<hr/>						

4.5.2. ANALYSIS FOR EE2

The following results are regressional analysis of the result of the Shear strength values of Clay-Fly-ash-Eggshell powder mixtures; the P-value for the Phi (0.049534) < 0.05, it shows that the Phi is statistically significant to the shear strength, the P-value for C (7.02E-06) < 0.05, it shows that the C is statically significant, the t-stat for Phi (0.049534) < 0.05, it shows that the Phi is statically significant, the t-stat for C (82.45608) > 0.05, it shows that the C is statically insignificant, the R-square for the regression statistics is (0.99995831) and the Adjusted Rsquare is (0.99994163), it shows that the work follows an almost linear pattern or sequence and can be predicted perfectly with a linear with a linear equation. The predicted and measured values are shown below:

Table 4.9: summary of the regressional analysis for EE2

SUMMARY OUTPUT

Regression Statistics

Multiple R	0.99997915
R Square	0.99995831
Adjusted R Square	0.99994163
Standard Error	0.1862645
Observations	8

ANOVA

				<i>Significance</i>	
	<i>df</i>	<i>SS</i>	<i>MS</i>	<i>F</i>	<i>F</i>
Regression	2	4160.554528	2080.277	59959.92	1.12241E-11
Residual	5	0.173472318	0.034694		
Total	7	4160.728			

	<i>Standard</i>				
	<i>Coefficients</i>	<i>Error</i>	<i>t Stat</i>	<i>P-value</i>	<i>Lower 95%</i>
Intercept	6.79146753	1.311473892	5.1785	0.00353	3.420216569
Phi	-0.0704905	0.059522967	-1.18426	0.049534	0.223499182
C	0.9565542	0.011600772	82.45608	4.97E-09	0.926733471

CHAPTER 5

CONCLUSIONS AND RECCOMENDATION

5.1 Conclusions

Based on the study, the following conclusion was made:

Natural soil was classified as lean clay (CL) according to the Unified standard classification system (USCS) and A-1-a according to AASHTO.

Significant improvement was noticed in the strength characteristics of the sample when stabilized with egg shell powder and fly-ash powder, compared to the natural strength characteristics of the natural clay.

The maximum dry unit weight (MDD) of the soil increased with increase in fly-ash ratio as compared with the control value. The peak value was recorded at 15%FA: 3%ESP for all samples. Also, appreciable changes were also observed for the optimum moisture content (OMC) with peak value at 15%FA:3%ESP

The addition of fly-ash alone for the stabilization caused a significant decrease in the Liquid limit and Plasticity limit values compared to the control values for all samples, with peak values at 9%FA:9%ESP and 15%FA:3%ESP. The plastic limit also has a peak value at 15%FA:3%ESP.

In terms of cohesion, when both additives work together, 15%FA:3%ESP gives the best result at 65Kn/m² and 89Kn/m² for both soils.

In terms of shear strength, combination of both additives gave a maximum shear strength value of 68.66Kn/m² and 91.56Kn/m² at 15%FA:3%ESP

From the regression analysis, it was noticed that EE2 is more statically significant in terms of the P-value than EE1, while in terms of t-stat, EE1 is more viable.

5.2 Recommendation

Based on the conclusions, the following recommendations can be made:

1. The engineering performance of the clay soil sample can be improved for use in foundations for soils with low load bearing capacity by modifying and stabilizing the sample with Fly-ash powder and Eggshell powder respectively.
2. The percentage mix ratios for Fly-ash powder and Eggshell powder can be increased for future research to observe its effect on natural clay soil.
3. Characterization of the stabilizing agents should be done in order to fully understand its chemical compositions and reactions.
4. More geotechnical laboratory tests can be done in investigating the effect of Fly-ash powder and Eggshell powder on clay like; CBR, Hydraulic conductivity, permeability test, etc.

REFERENCE

- Ahmed B, Rahman A, Das J (2016). Egg shell Powder utilization as CBR modifying agent to improve the subgrade soil. Proceedings of the 3rd International Conference on Civil Engineering for Sustainable Development; pp.12-14
- Attarde, S.; Marathe, S.; Sil, A. (2014). Utilization of fly-ash in construction industries for environment management. *Int. J. Environ. Sci.*, 3, pp.117–121
- Alam, J.; Akhtar, M. (2011). Fly ash utilization in different sectors in Indian scenario. *Int. J. Emerg. Trends Eng. Dev.*, 1, pp. 1–14.
- Alzaidy M.N.J (2019). Experimental Study for Stabilizing Clayey Soil with Eggshell Powder And Plastic Wastes, 2nd International Conference On Sustainable Engineering Techniques, DOI:10.1088/1757-899x/518/2/022008.
- Balba, A.M. (2012). *Management of Problem Soils in Arid Ecosystems*. CRC Press. Boca Raton, Florida. pp. 250
- Bose, B., (2012). Geo engineering properties of expansive soil stabilized with fly ash. *Electronic Journal of Geotechnical Engineering*, 17.1, pp. 1339-1353.
- Basu, M.; Pande, M.; Bhadoria, P.B.S.; Mahapatra, S.C. (2009). Potential fly-ash utilization in agriculture: A global review. *Prog. Nat. Sci.*, 19, pp. 1173–1186.
- Bayukov, O.A.; Anshits, N.N.; Balaev, A.D.; Sharonova, O.M.; Rabchevskii, E.V.; Petrov, M.I.; Anshits, A.G. Mössbauer (2005). Study of magnetic microspheres isolated from power plant fly ash. *Inorg. Mater.* 41, pp. 50–59.
- Behnood, A. (2018). Soil and clay stabilization with calcium and non-calcium-based additives: A state of the art review with challenges, approaches and techniques. *Transportation Geo-technics*. 17. Pp. 14-32.
- Birundha P., Suguna S., Prabudevan S. and Vignesh Kumar B.(2017). Stabilization Of Clay Soil Using Egg Shell Powder And Quarry Dust, *International Journal Of Chemtech Research*, 10(8), pp. 439-445.

- Brady, N. and R. Weil. (2012). *The Nature and Properties of Soils*, 13th Edition. Prentice Hall. Upper Saddle River, New Jersey. 960 p.
- Behera, A.; Mohapatra, S.S. (2018). Challenges in Recovery of Valuable and Hazardous Elements from Bulk Fly Ash and Options for Increasing Fly Ash Utilization. In *Coal Fly Ash Beneficiation—Treatment of Acid Mine Drainage with Coal Fly Ash*; Akinyemi, S., Gitari, M.W., Eds.; IntechOpen: London, UK,; pp. 19–39.
- Baykal, G.; Edinçliler, A.; Saygılı, A. (2004). Highway embankment construction using fly ash in cold regions. *Resources Conservation Recycle*, pp. 42, 209–222.
- Brännvall, E.; Kumpiene, J. (2016). Fly ash in landfill top covers—a review *Environ. Sci. Process. Impacts*, 18, pp. 11–21.
- Carter, M.R. (2012). Soil quality for sustainable land management: organic matter and aggregation interactions that maintain soil functions. *Agron. J.* pp. 94: 38-47.
- Cokca E., Yazici V. and Ozaydin V., (2009). Stabilization of expansive clays using granulated blast furnace slag (GBFS) and GBFS-cement. *Geotechnical and Geological Engineering*, 27(4), pp. 489-499.
- Choo, T.F.; Salleh, M.A.M.; Kok, K.Y.; Matori, K.A.; Rashid, S.A. (2020). Effect of Temperature on Morphology, Phase Transformations and Thermal Expansions of Coal Fly Ash Cenospheres. *Crystals*, 10, pp. 481.
- Chou, M.-I.M. (2012). Fly Ash. In *Encyclopedia of Sustainability Science and Technology*; Meyers, R.A., Ed.; Springer: New York, NY, USA,; pp. 3820–3843.
- Choudhary, N.; Yadav, V.K.; Malik, P.; Khan, S.H.; Inwati, G.K.; Suriyaprabha, R.; Singh, B.; Yadav, A.K.; Ravi, R.K.(2020). Recovery of Natural Nanostructured Minerals: Ferrospheres, Plerospheres, Cenospheres, and Carbonaceous Particles From Fly Ash. In *Handbook of Research on Emerging Developments and Environmental Impacts of Ecological Chemistry*; Gheorghe, D., Ashok, V., Eds.; IGI Global: Hershey, PA, USA, 2020; pp. 450–470.

- Dasgupta, M.; Kar, S.; Gupta, S.D.; Mukhopadhyay, R.; Bandyopadhyay, A. (2013). Effect of Fly Ash as Filler in Rubber—A Comprehensive Study of the Vulcanisate Properties of Styrene-Butadiene Rubber Compounds. *Prog. Rubber Plastic Recycle. Technol.*, 29, pp. 151–168.
- Eisele, T.C.; Kawatra, S.K.; Nofal, A. (2004). Comparison of class C and class F fly-ashes as foundry sand binders and the effectiveness of accelerators in reducing curing time. *Miner. Process. Extr. Metall. Rev.*, 25, pp. 269–278.
- Frey S.D., E.T. Elliot and K. Paustian. (2009). Bacterial and fungal abundance and biomass in conventional and no-tillage agroecosystems along two climatic gradients. *Soil Biol. Biochem.* 31 (4): pp. 573-585.
- Fuller, A.; Maier, J.; Karampinis, E.; Kalivodova, J.; Grammelis, P.; Kakaras, E.; Scheffknecht, G. (2018). Fly Ash Formation and Characteristics from (co-)Combustion of an Herbaceous Biomass and a Greek Lignite (Low-Rank Coal) in a Pulverized Fuel Pilot-Scale Test Facility. *Energies* 2018, 11, pp. 1581.
- Fu, B.; Hower, J.C.; Dai, S.; Mardon, S.M.; Liu, G. (2018). Determination of Chemical Speciation of Arsenic and Selenium in High-As Coal Combustion Ash by X-ray Photoelectron Spectroscopy: Examples from a Kentucky Stoker Ash. *ACS Omega* 3, pp. 17637–17645.
- FİGen, A.; ÖZÇAy, Ü.; Pişkin, S. (2017). Manufacturing and Characterization of Roof Tiles a Mixture of Tile Waste and Coal Fly Ash. *Süleyman Demirel Üniversitesi Fen Bilimleri Enstitüsü D erg.* 21, 10 p.
- Gaikwad, A.; Patel, B.K.; Verma, V.; Rai, A. (2017). Development of fly ash based new Bio-Composites Material as Wood Substitute. *Int. J. Mech. Prod. Eng. Res. Dev.*, 7, pp. 1–6.
- Gardiner, D. T. and R.W. Miller. (2004). *Soils in our environment*, 10th Edition. Pearson Education, Inc. Upper Saddle River, New Jersey. 641 p.
- Guo, C.; Zou, J.; Ma, S.; Yang, J.; Wang, K. (2019). Alumina Extraction from Coal Fly Ash via Low-Temperature Potassium Bisulfate Calcination. *Minerals* 2019, 9, 585 p.

- Gong, Y.; Sun, J.; Sun, S.-Y.; Lu, G.; Zhang, T.-A. (2019). Enhanced Desilication of High Alumina Fly Ash by Combining Physical and Chemical Activation. *Metals* 2019, 9, 411 p.
- Gupta, D.K.; Rai, U.N.; Tripathi, R.D.; Inouhe, M. (2002). Impacts of fly-ash on soil and plant responses. *J. Plant Res.* 2002, 115, pp. 401–409.
- Gopalakrishna, Y.S.S., Padmavathi, M. and Prashanth Kumar, K.S., (2013). Stabilization of black cotton soil treated with fly ash and zycosoil, *International Journal of Civil Engineering and Building Materials*, 3(3), pp., 133-44.
- Habte, L.; Shiferaw, N.; Mulatu, D.; Thenepalli, T.; Chilakala, R.; Ahn, J. (2019). Synthesis of Nano-Calcium Oxide from Waste Eggshell by Sol-Gel Method. *Sustainability*, 11, 3196 p.
- Hasan, H.A., (2012). Effect of fly ash on geotechnical properties of expansive soil. *Journal of Engineering and Sustainable Development*, 16(2), pp., 306-316.
- Hower, J.; Groppo, J.; Graham, U.; Ward, C.; Kostova, I.; Maroto-Valer, M.; Dai, S. (2017). Coal -derived unburned carbons in fly ash: A review. *Int. J. Coal Geol.* 2017, 179, pp. 11–27.
- Ibeto, C.N., Obiefuna, C.J., Ugwu, K.E. (2020). Environmental effects of concretes produced from partial replacement of cement and sand with coal ash. *Int. J. Environ. Sci. Technol.* 2020, 17, pp. 2967–2976.
- Krishnamoorthy, V., Pisupati S. A. (2015). Critical Review of Mineral Matter Related Issues during Gasification of Coal in Fixed, Fluidized, and Entrained Flow Gasifiers. *Energies* 2015, 8, pp. 10430–10463.
- Kishor, P., Ghosh, A., Kumar, D. (2010). Use of Flyash in Agriculture: A Way to Improve Soil Fertility and its Productivity. *Asian J. Agric. Res.* 2010, 4, pp. 1–14.
- Kleinhans, U.; Wieland, C.; Frandsen, F.J.; Spliethoff, H. (2018). Ash formation and deposition in coal and biomass fired combustion systems: Progress and challenges in the field of ash particle sticking and rebound behavior. *Prog. Energy Combust. Sci.* 2018, 68, pp. 65–168.

- Kodikara, J., Islam, T., and Sountharajah, A. (2018). Review of soil compaction: History and recent developments. *Transportation Geotechnics*. 17. Pp. 24-34.
- Luo, Y.; Zheng, S.; Ma, S.; Liu, C.; Wang, X.(2017). Ceramic tiles derived from coal fly ash: Preparation and mechanical characterization. *Ceram. Int.* 2017, 43, pp. 11953–11966.
- Liu, H.; Sun, Q.; Wang, B.; Wang, P.; Zou, J.(2016). Morphology and Composition of Microspheres in Fly Ash from the Luohuang Power Plant, Chongqing, Southwestern China., 30 p.
- Langmann, B.(2013). Volcanic Ash versus Mineral Dust: Atmospheric Processing and Environmental and Climate Impacts. *ISRN Atmos. Sci.*, 17 p.
- Li, S.; Qin, S.; Kang, L.; Liu, J.; Wang, J.; Li, Y.((2017). An Efficient Approach for Lithium and Aluminum Recovery from Coal Fly Ash by Pre-Desilication and Intensified Acid Leaching Processes. 272 p.
- Murugesan, S.; Ramaswamy, J.; Parshwanath, R.; Sundararaj, J.; Jose, R.(2019). Evaluation of Suitability of Alumino-Silicate Precursor for Geopolymerization through Advanced Analytical Techniques. *Asian J. Chem.* pp. 1771–1776.
- Meer, I.; Nazir, R.(2017). Removal techniques for heavy metals from fly ash. *J. Mater. Cycles Waste Management*, pp. 703–722.
- Miricioiu, M.G.; Niculescu, V.C.(2020). Fly Ash, from Recycling to Potential Raw Material for Mesoporous Silica Synthesis. *Nanomaterials (Basel)*, 474 p.
- Maduabuchi M, Obikara F.(2018). Effect of egg shell powder (ESP) on the strength properties of cement stabilization on olokoro lateritic soil. *J Waste Manage Xenobio*. 103 p.
- Mujtaba, H., Aziz, A., Farooq, K., Sivakugan, N., and Das, B., (2019). Improvement in engineering properties of expansive soils using ground granulated blast furnace slag. *Journal of the Geological Society of India*, 92(3), pp., 357–362.
- Nadesan, M.S.; Dinakar, P.(2017). Mix design and properties of fly ash waste lightweight aggregates in structural lightweight concrete. *Case Stud. Constr. Mater.*, pp. 336–347.

- Ngu, L.-N.; Wu, H.; Zhang, D.-k.(2007). Characterization of Ash Cenospheres in Fly Ash from Australian Power Stations. *Energy Fuels*, pp. 3437–3445.
- Nordin, N.; Abdullah, M.M.A.B.; Tahir, M.F.M.; Sandu, A.V.; Hussin, K. (2016). Utilization of fly ash waste as construction material. *Int. J. Conserv. Sci.*, pp. 161–166.
- Neva Elias (2015). Strength Development of Soft Soil Stabilize with Waste Paper Sludgel, *International Journal of Advanced Technology in Engineering and Science*, Vol. 3, pp 141-149.
- Nisham, K.; Sridhar, M.B.; Kumar, V. (2016). Experimental study on class F fly ash cement bricks using partial replacement of fly ash by metakaolin. *Int. J. Chem. Sci.* 2016, 14, pp. 227–234
- Olfert, O., G.D. Johnson, S. A. Brandt, and A.G. Thomas. (2002). Use of arthropod diversity and abundance to evaluate cropping systems. *Agron. J.* 94: pp. 210-216.
- Ohenoja, K.; Pesonen, J.; Yliniemi, J.; Illikainen, M. (2020). Utilization of Fly Ashes from Fluidized Bed Combustion: A Review. *Sustainability*. 2988 p.
- Papatzani, S.; Paine, K. (2020). A Step by Step Methodology for Building Sustainable Cementitious Matrices. *Appl. Sci.*, 2955 p.
- Prabakar J, Dendorkar N, Morchhale RK. (2004). Influence of fly ash on strength behavior of typical soils. *Constr Build Mater.* 2004; 18: pp. 263-267.
- Paul A, Anumol VS, Moideen F, Jose JK, Abraham A. (2014). Studies on improvement of clayey soil using egg shell powder and quarry dust. *Int J Eng Res Appl.* pp. 55-63.
- Rudić, O.; Ducman, V.; Malešev, M.; Radonjanin, V.; Draganić, S.; Šupić, S.; Radeka, M. (2019). Aggregates Obtained by Alkali Activation of Fly Ash: The Effect of Granulation, Pelletization Methods and Curing Regimes. *Materials*. 776 p.
- Rodrigues, P.; Silvestre, J.D.; Flores-Colen, I.; Viegas, C.A.; Ahmed, H.H.; Kurda, R.; de Brito, J. (2020). Evaluation of the Ecotoxicological Potential of Fly Ash and Recycled Concrete Aggregates Use in Concrete. *Appl. Sci.*, 351 p.

- Savin, M. C., J. H. Görres, and J.A. Amador. (2004). Microbial and microfaunal community dynamics in artificial and *Lumbricus terrestris* (L.) burrows. *Soil Sci. Soc. Am.* 68: pp. 116-124.
- Senol A, Edil TB, Bin-Shafique MS, Acosta HA, Benson CH. (2006). Soft subgrades' stabilization by using various fly ashes. *Resour Conserv Recycl.*:pp. 365-376.
- Singh, R.P.; Gupta, A.K.; Ibrahim, M.H.; Mittal, A.K. (2010). Coal fly ash utilization in agriculture: Its potential benefits and risks. *Rev. Environ. Sci. Bio/Technol.*, pp. 345–358.
- Šešlija, M.; Rosić, A.; Radović, N.; Vasić, M.; Đogo, M.; Jotić, M. (2016). Physi-properties of fly ash and slag from the power plants. *Geol. Croat.*, pp. 317–324.
- Singh, G.B.; Subramaniam, K.V. (2018). Characterization of Indian fly ashes using different Experimental Techniques. *Indian Concr. J.*, pp. 10–23.
- Sharonova, O.; Anshits, N.; Fedorchak, M.; Zhizhaev, A.; Anshits, A. (2015). Characterization of Ferrospheres Recovered from High-Calcium Fly Ash. *Energy Fuels*, pp. 5404–5414.
- Sunjidmaa, D.; Batdemberel, G.; Takibai, S. (2019). A Study of Ferrospheres in the Coal Fly Ash. *Open J. Appl. Sci.*, pp. 10–16.
- Valentim, B.; Flores, D.; Guedes, A.; Shreya, N.; Paul, B.; Ward, C.R.(2016). Notes on the occurrence of char plerospheres in fly ashes derived from Bokaro and Jharia coals (Jharkhand, India) and the influence of the combustion conditions on their genesis. *Int. J. Coal Geol.* pp. 29–43.
- Veranth, J.M.; Fletcher, T.H.; Pershing, D.W.; Sarofim, A.F. (2000). Measurement of soot and char in pulverized coal fly ash. *Fuel* 2000, 79, pp. 1067–1075.
- Vassilev, S.; Menendez, R.; Borrego, A.; Díaz-Somoano, M.; Martínez-Tarazona, M. (2004). Phase-mineral and chemical composition of coal fly ashes as a basis for their multicomponent utilization. 3. Characterization of magnetic and char concentrates. *Fuel*, pp. 1563–1583.

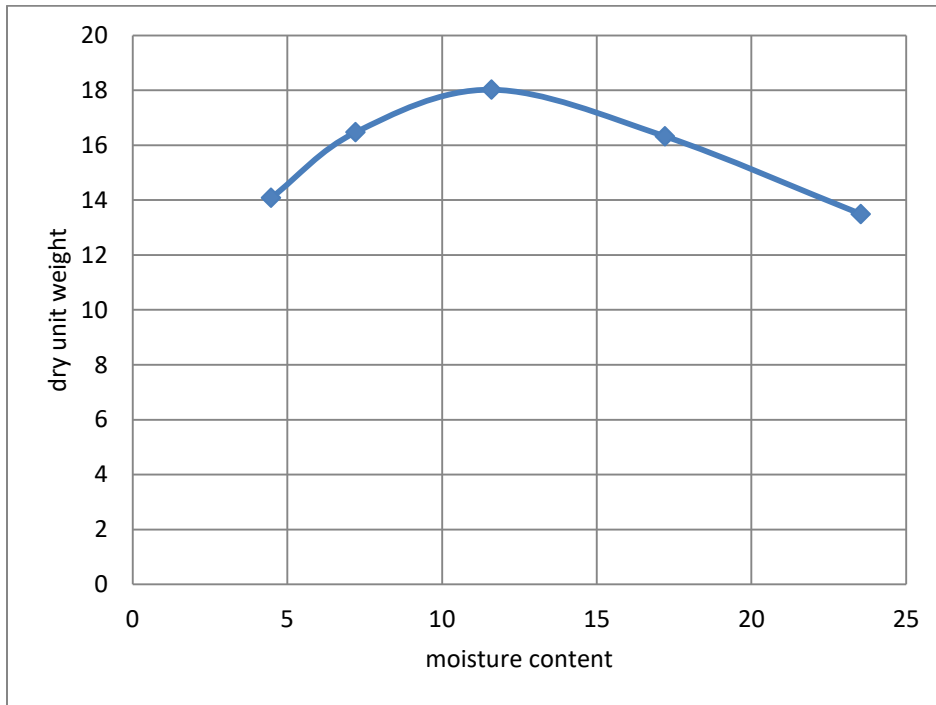
- Valeev, D.; Kunilova, I.; Alpatov, A.; Varnavskaya, A.; Ju, D. (2019). Magnetite and Carbon Extraction from Coal Fly Ash Using Magnetic Separation and Flotation Methods. *Minerals*, 320 p.
- Vassilev, S.; Menendez, R.; Alvarez, D.; Díaz-Somoano, M.; Martínez-Tarazona, M.(2003). Phase-Mineral and Chemical Composition of Coal Fly Ashes as a Basis for Their Multicomponent Utilization. 1. Characterization of Feed Coals and Fly Ashes. *Fuel*, pp. 1793–1811.
- Valentim, B.; Białocka, B.; Gonçalves, A.P.; Guedes, A.; Guimarães, R.; Cruceiro, M.; Całus-Moszko, J.; Popescu, G.L.; Predeanu, G.; Santos, C.A.(2018). Undifferentiated Inorganics in Coal Fly Ash and Bottom Ash: Calcispheres, Magnesiocalcispheres, and Magnesiaspheres. *Minerals*, p. 140.
- Wang, P.; Massoudi, M. Slag Behavior in Gasifiers.(2013). Part I: Influence of Coal Properties and Gasification Conditions. *Energies* 2013, 6, pp. 784–806.
- Wuana, R.A.; Okieimen, F.E.(2011). Heavy Metals in Contaminated Soils: A Review of Sources, Chemistry, Risks and Best Available Strategies for Remediation. *ISRN Ecol.* 2011. p. 20.
- Wang, Y.-S.; Alrefaei, Y.; Dai, J.-G. (2019). Silico-Aluminophosphate and Alkali-Aluminosilicate Geopolymers: A Comparative Review. *Front. Mater.* P. 106.
- Wei, Q.; Song, W. (2020). Mineralogical and Chemical Characteristics of Coal Ashes from Two High-Sulfur Coal-Fired Power Plants in Wuhai, Inner Mongolia, China. *Minerals*. P. 323.
- Yadav, V.K.; Fulekar, M.H.(2018). The current scenario of thermal power plants and fly ash.:Production and utilization with a focus in India. *Int. J. Adv. Eng. Res. Dev.* pp. 768–777.
- Yadav, V.K.; Pandita, P.R. (2019). Fly Ash Properties and Their Applications as a Soil Ameliorant. In *Amelioration Technology for Soil Sustainability*; Rathoure, A.K., Ed.; IGI Global: Hershey, PA, USA, 2019; pp. 59–89.

- Yadav, V.K.; Choudhary, N. (2019). An Introduction to Fly Ash: Natural Nanostructured Materials; Edu-creation: New Delhi, India, 2019; Volume 1, p. 162.
- Yoriya, S.; Intana, T.; Tepsri, P. (2019). Separation of Cenospheres from Lignite Fly Ash Using AcetoneWater Mixture. *Appl. Sci.* p. 3792.
- Yadu, Laxmikant and Tripathi, R. K. (2013). Stabilization of Soft Soil with Granulated Blast Furnace Slag and Fly ash, *International Journal of Research in Engineering and Technology*, vol. 2, pp. 115-119.
- Zhao, Y.; Soltani, A.; Taheri, A.; Karakus, M.; Deng, A. (2018). Application of Slag—Cement and Fly Ash for Strength Development in Cemented Paste Backfills. *Minerals* 2018, 9, p. 22
- Żyrkowski, M.; Neto, R.C.; Santos, L.; Witkowski, K. (2016). Characterization of fly-ash cenospheres from coal-fired power plant unit. *Fuel*. pp. 49–53.
- Zhao, Y.; Zhang, J.; Sun, J.; Bai, X.; Zheng, C. (2006). Mineralogy, Chemical Composition, and Microstructure of Ferrospheres in Fly Ashes from Coal Combustion. *Energy Fuels*. Pp. 1490–1497.
- Zhang, W.; Noble, A.; Yang, X.; Honaker, R. A. (2020). Comprehensive Review of Rare Earth Elements Recovery from Coal-Related Materials. *Minerals*, p. 451
- Zhuang, X.Y.; Chen, L.; Komarneni, S.; Zhou, C.H.; Tong, D.S.; Yang, H.M.; Yu, W.H.; Wang, H. (2016). Fly ash-based geopolymer: Clean production, properties and applications. *J. Clean. Prod.*, pp. 253 –267.

APPENDIX 1
CLAY EE1
COMPACTION

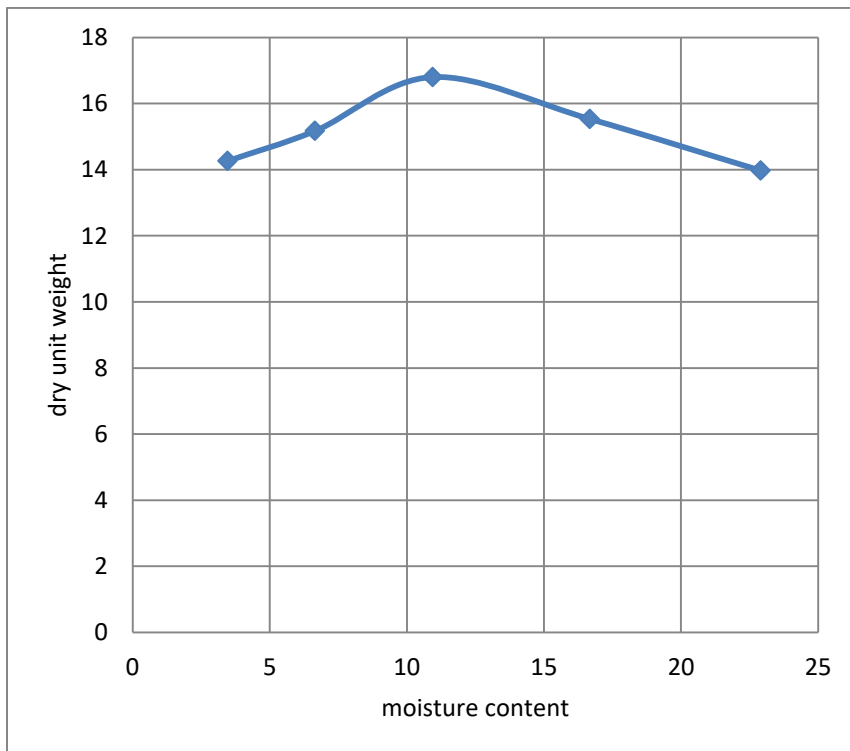
SOIL – 100%

%	VOLUME OF MOULD (M³)	MASS OF MOULD (KG)	MOULD + SAMPLE (KG)	MOISTURE CONTENT (%)	BULK DENSITY	DRY DENSITY
4	0.001	4.2	5.7	4.48	1500	14.08
8	0.001	4.2	6.0	7.21	1800	16.47
12	0.001	4.2	6.25	11.60	2050	18.02
16	0.001	4.2	6.15	17.21	1950	16.32
20	0.001	4.2	5.90	23.54	1700	13.49



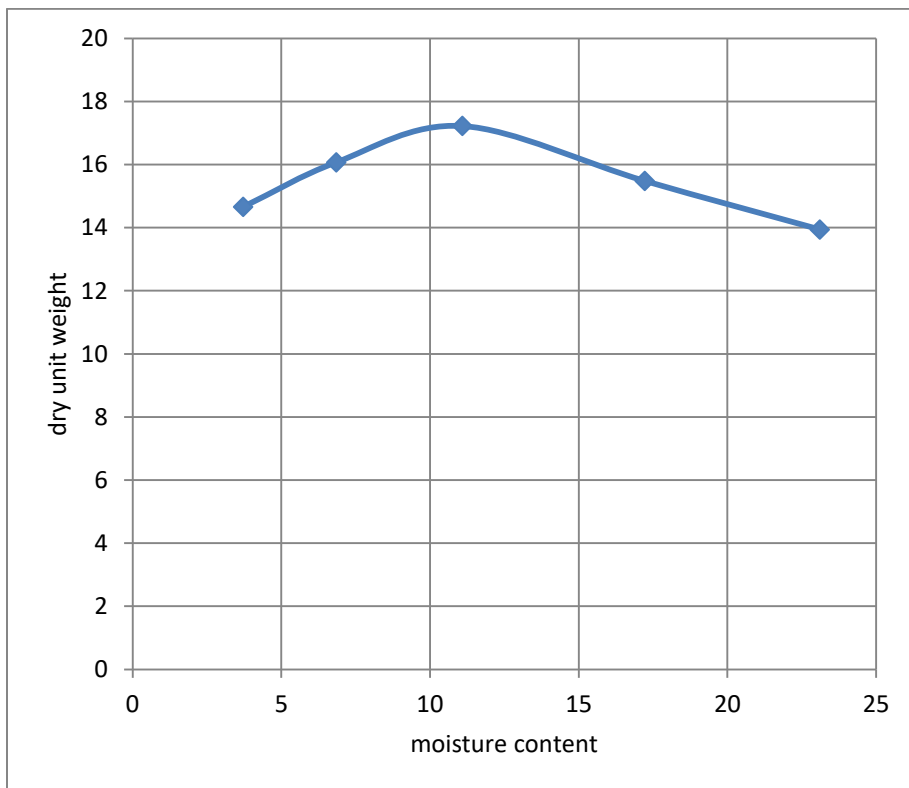
FLYASH -0% ESP -18%

%	VOLUME OF MOULD (M³)	MASS OF MOULD (KG)	MOULD + SAMPLE (KG)	MOISTURE CONTENT (%)	BULK DENSITY	DRY DENSITY
4	0.001	4.2	5.75	3.46	1550	14.26
8	0.001	4.2	5.85	6.65	1750	15.17
12	0.001	4.2	6.10	10.95	2100	17.80
16	0.001	4.2	6.05	16.68	1850	15.53
20	0.001	4.2	5.95	22.91	1750	13.97



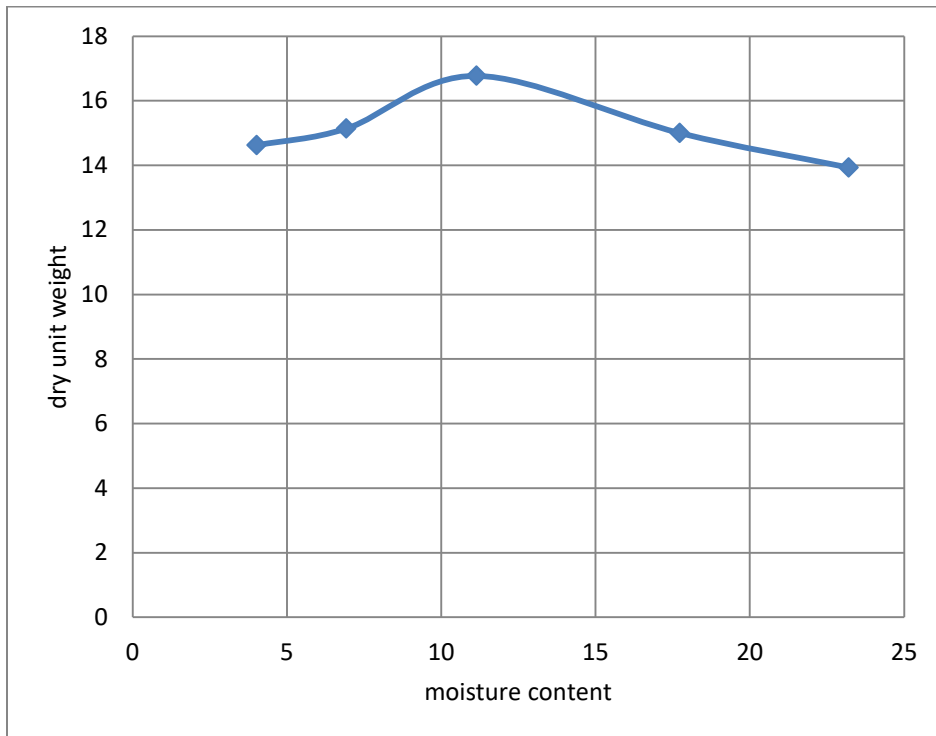
FLYASH – 3% ESP -15%

W _c (%)	VOLUME OF MOULD (M ³)	MASS OF MOULD (KG)	MOULD + SAMPLE (KG)	MOISTURE CONTENT (%)	BULK DENSITY	DRY DENSITY
4	0.001	4.2	5.75	3.72	1550	14.66
8	0.001	4.2	5.95	6.85	1750	16.07
12	0.001	4.2	6.15	10.89	2050	19.02
16	0.001	4.2	6.05	17.22	1850	16.48
20	0.001	4.2	5.95	23.11	1750	13.94



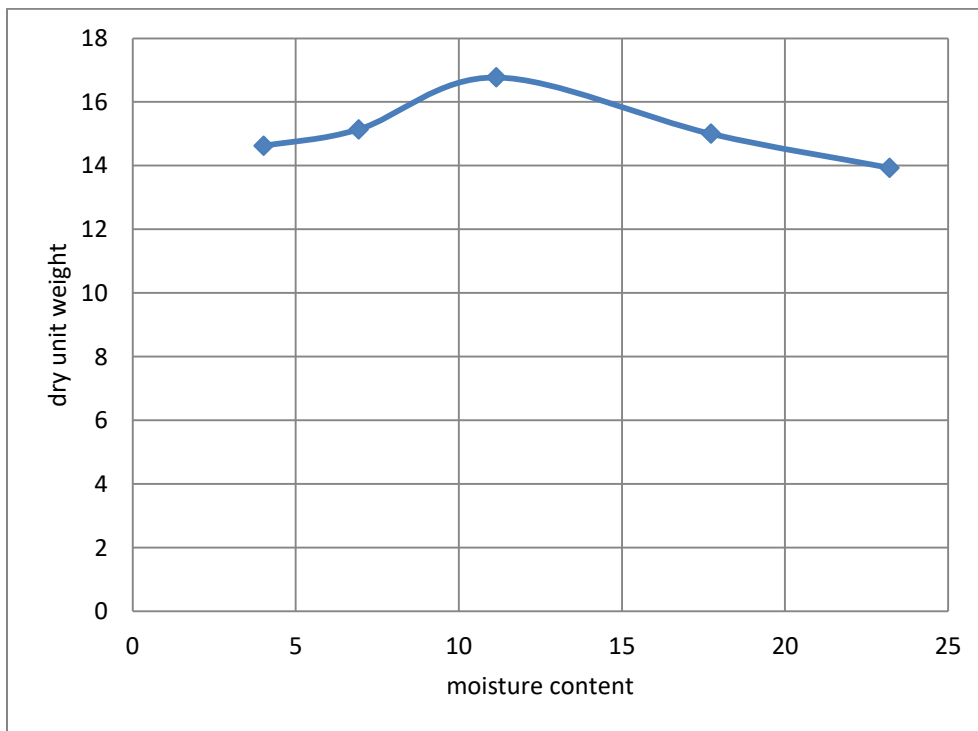
FLYASH -6% ESP -12%

%	VOLUME OF MOULD (M³)	MASS OF MOULD (KG)	MOULD + SAMPLE (KG)	MOISTURE CONTENT (%)	BULK DENSITY	DRY DENSITY
4	0.001	4.2	5.75	4.02	1550	14.62
8	0.001	4.2	5.85	6.93	1850	15.14
12	0.001	4.2	6.10	10.25	2100	18.24
16	0.001	4.2	6.0	17.73	1800	15.00
20	0.001	4.2	5.95	23.21	1750	13.93



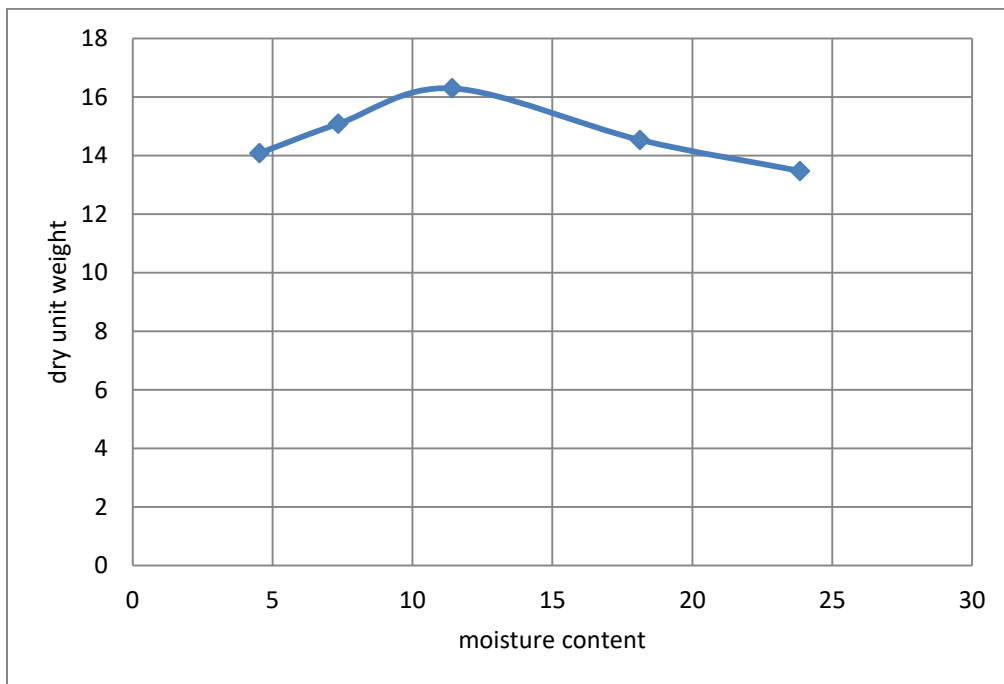
FLYASH -9% ESP -9%

%	VOLUME OF MOULD (M³)	MASS OF MOULD (KG)	MASS OF MOULD + SAMPLE (KG)	MOISTURE CONTENT (%)	BULK DENSITY	DRY DENSITY
4	0.001	4.2	5.70	4.54	1500	14.08
8	0.001	4.2	5.85	7.35	1750	15.08
12	0.001	4.2	6.15	12.02	2000	19.29
16	0.001	4.2	5.95	18.13	1750	14.53
20	0.001	4.2	5.90	23.85	1700	13.47



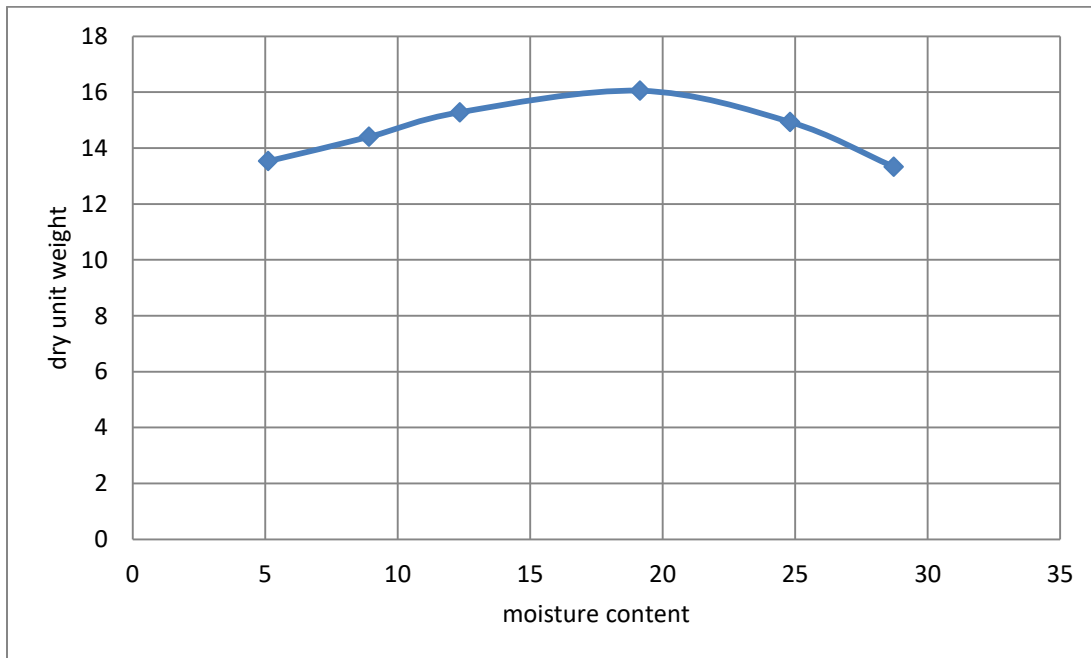
FLYASH -12% ESP -6%

%	VOLUME OF MOULD (M³)	MASS OF MOULD (KG)	MASS OF MOULD + SAMPLE (KG)	MOISTURE CONTENT (%)	BULK DENSITY	DRY DENSITY
4	0.001	4.2	5.75	4.89	1550	14.50
8	0.001	4.2	5.90	8.52	1700	15.36
12	0.001	4.2	6.25	12.81	2150	19.21
16	0.001	4.2	5.95	18.95	1750	14.43
20	0.001	4.2	5.85	24.53	1650	13.00



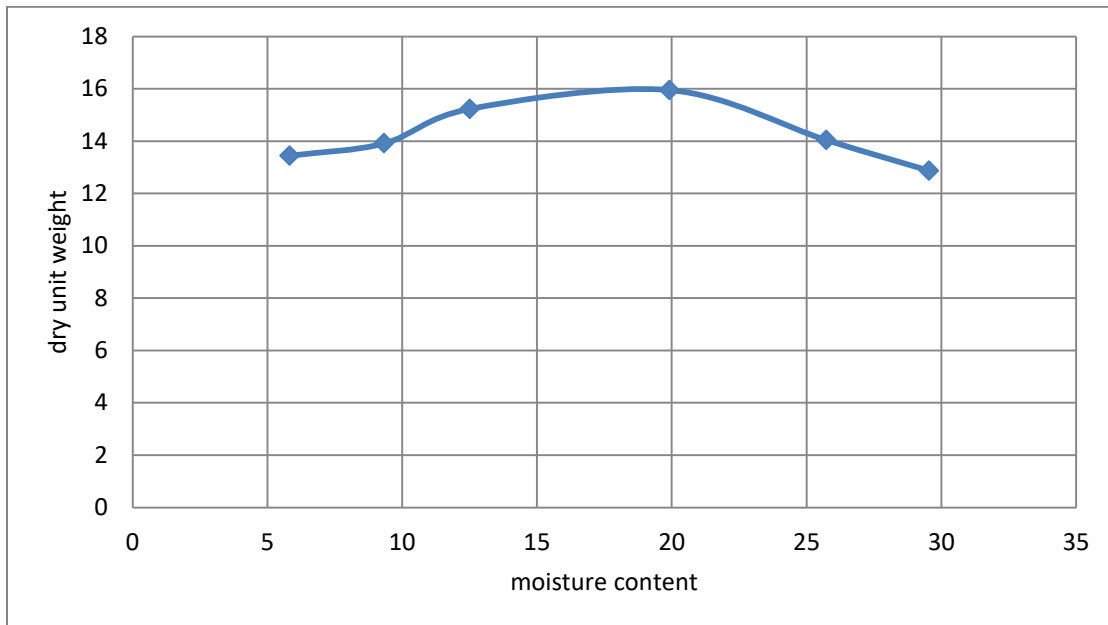
FLYASH -15% ESP -3%

%	VOLUME OF MOULD (M³)	MASS OF MOULD (KG)	MASS OF MOULD + SAMPLE (KG)	MOISTURE CONTENT (%)	BULK DENSITY	DRY DENSITY
4	0.001	4.2	5.65	5.12	1450	13.53
8	0.001	4.2	5.80	8.92	1600	14.4
12	0.001	4.2	5.95	12.35	1750	15.28
16	0.001	4.2	6.25	17.15	2250	19.05
20	0.001	4.2	6.05	24.81	1850	15.93
24	0.001	4.2	5.95	28.72	1750	13.33



FLYASH -18% ESP -0%

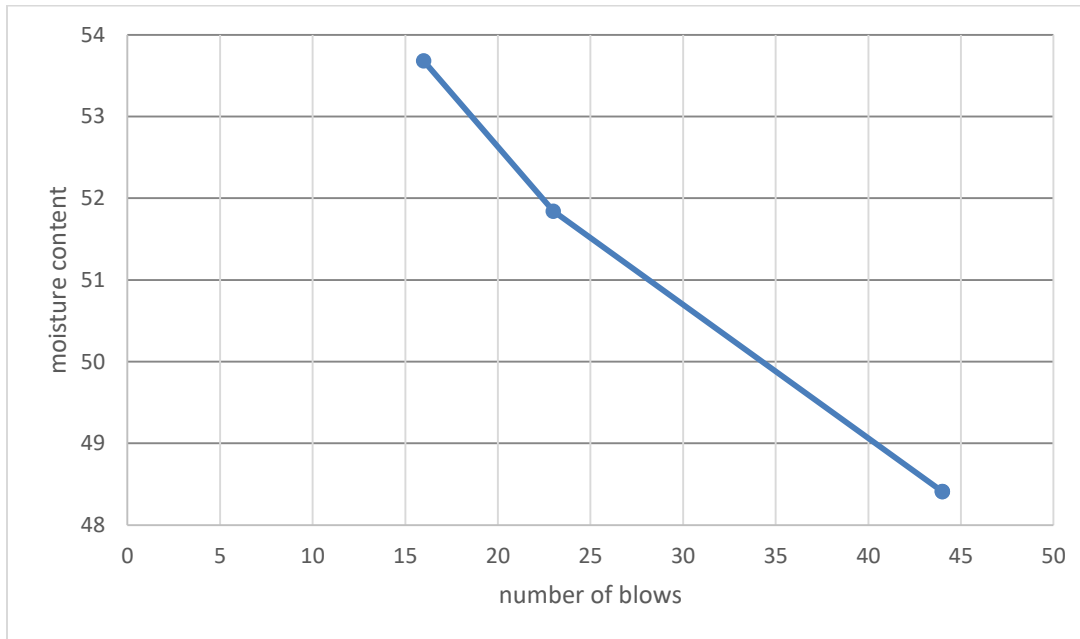
%	VOLUME OF MOULD (M³)	MASS OF MOULD (KG)	MASS OF MOULD + SAMPLE (KG)	MOISTURE CONTENT (%)	BULK DENSITY	DRY DENSITY
4	0.001	4.2	5.65	5.83	1450	13.44
8	0.001	4.2	5.75	9.33	1550	13.91
12	0.001	4.2	5.95	12.51	1750	15.23
16	0.001	4.2	6.15	16.92	2350	17.02
20	0.001	4.2	6.0	25.73	1800	14.04
24	0.001	4.2	5.90	29.54	1700	12.87



ATTERBERG LIMIT (LIQUID LIMIT)

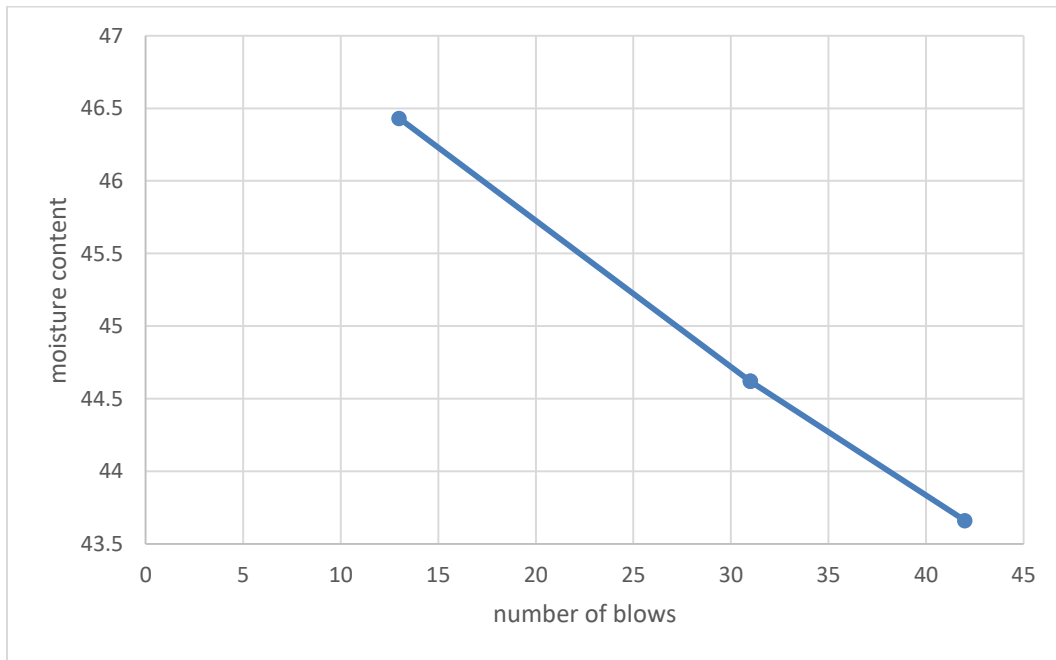
SOIL -100%

WT OF TIN(G)	WT OF TIN + WET SOIL (G)	WT OF SOIL + DRY SOIL	WT OF WET SOIL (G)	WT OF DRY SOIL (G)	MOISTURE CONTENT (%)	NUMBER OF BLOWS
16.10	25.49	22.21	9.39	6.11	53.69	16
14.06	22.70	19.75	8.64	5.61	51.84	23
15.92	23.23	20.81	7.31	4.89	49.49	33
15.09	27.20	23.25	12.11	8.16	48.41	44



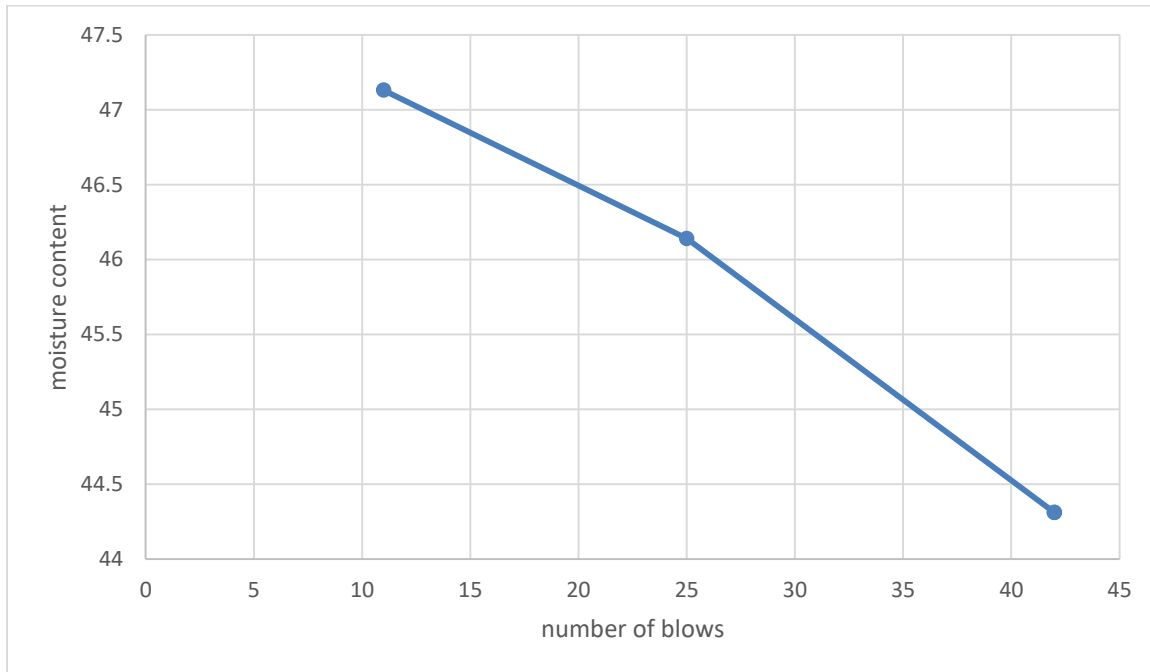
FLYASH 0% ESP 18%

WT OF PAN(G)	WT OF TIN + WET SOIL(G)	WT OF TIN + DRY SOIL(G)	WT OF WET SOIL(G)	WT OF DRY SOIL(G)	MOISTURE CONTENT (%)	NUMBER OF BLOWS
13.68	18.82	17.19	5.14	5.14	46.43	13
16.79	22.07	20.41	5.28	3.62	45.86	25
14.94	20.19	18.57	5.25	3.63	44.62	31
13.76	20.11	18.81	6.35	4.42	43.66	42



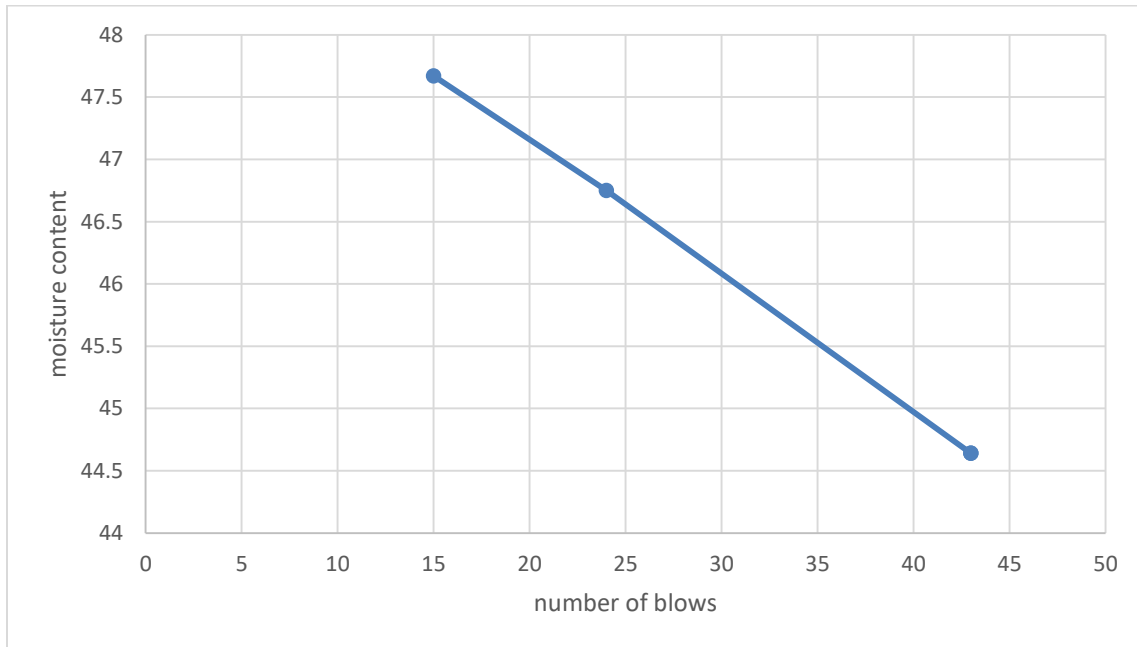
FLYASH 3% ESP 15%

WT OF PAN(G)	WT OF PAN+WET SOIL(G)	WT OF PAN + DRY SOIL(G)	WT OF WET SOIL(G)	WT OF DRY SOIL(G)	MOISTURE CONTENT (%)	NUMBER OF BLOWS
16.88	23.03	21.06	6.15	4.18	47.13	11
16.51	23.51	21.30	7.00	4.79	46.14	25
14.01	19.63	17.67	5.62	3.86	45.60	35
17.15	23.24	21.37	6.09	4.22	44.31	42



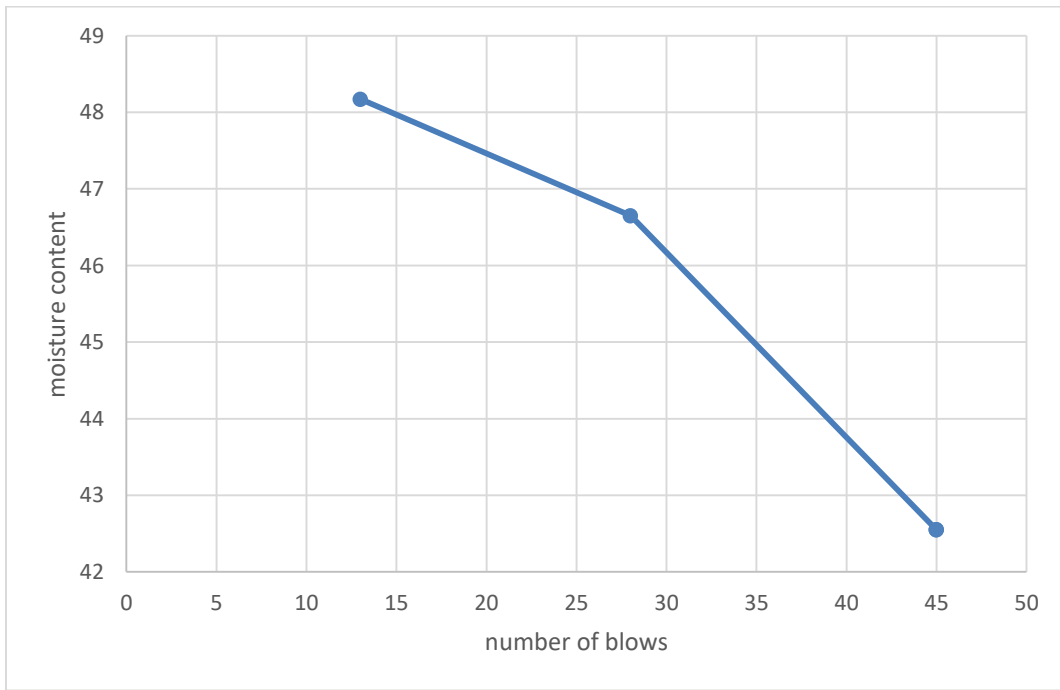
FLYASH 6% ESP 12%

WT OF PAN(G)	WT OF PAN+WET SOIL(G)	WT OF PAN + DRY SOIL(G)	WT OF WET SOIL(G)	WT OF DRY SOIL(G)	MOISTURE CONTENT (%)	NUMBER OF BLOWS
14.80	22.08	19.73	7.28	4.93	47.67	15
17.63	25.54	23.02	7.91	5.39	46.75	24
16.70	25.66	22.85	8.96	6.15	45.02	30
15.53	22.01	20.01	6.48	4.48	44.64	43



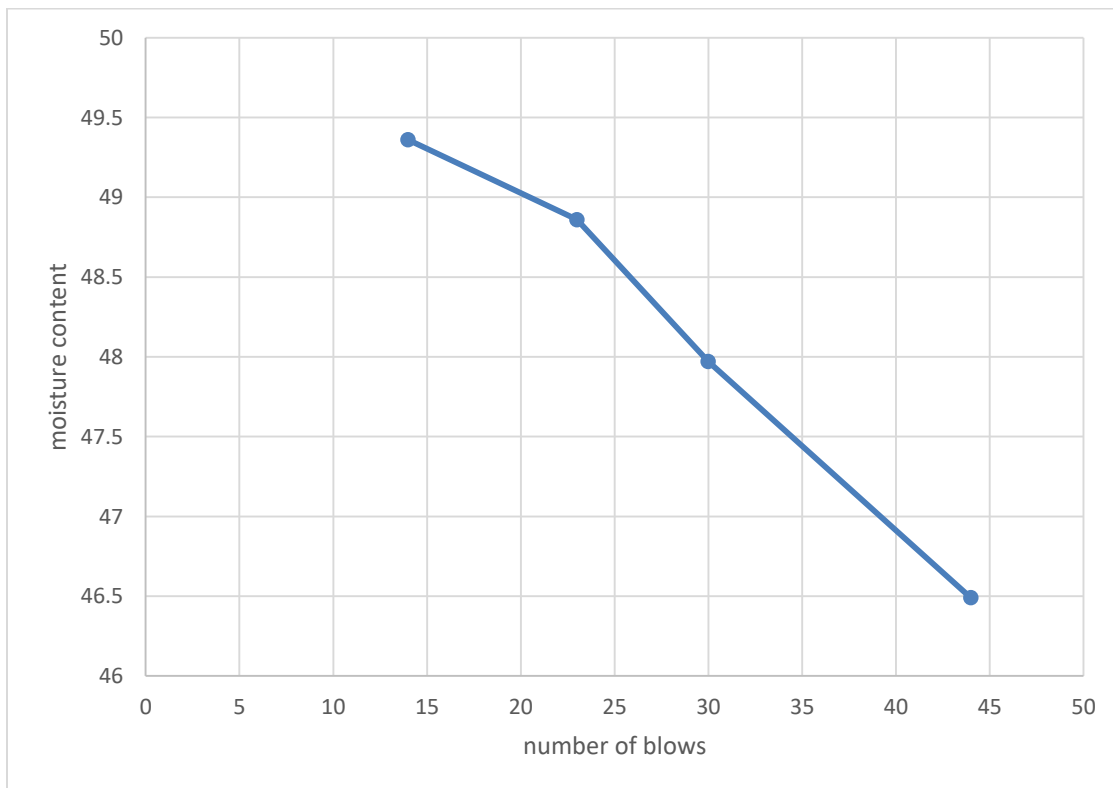
FLYASH 9% ESP 9%

WT OF PAN(G)	WT OF PAN+WET SOIL(G)	WT OF PAN + DRY SOIL(G)	WT OF WET SOIL(G)	WT OF DRY SOIL(G)	MOISTURE CONTENT (%)	NUMBER OF BLOWS
14.80	23.75	20.84	8.95	6.04	48.17	13
14.91	22.15	19.84	7.24	4.93	46.85	28
15.02	23.43	20.85	8.41	5.83	44.25	30
14.41	24.36	21.39	9.95	6.98	42.55	45



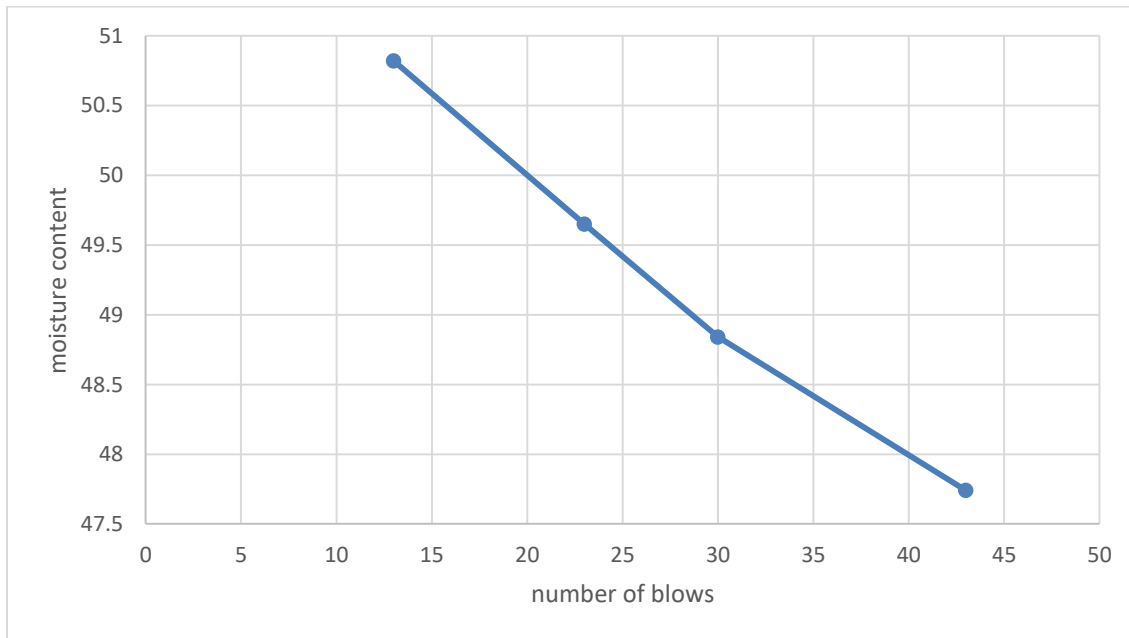
FLYASH 12% ESP 6%

WT OF PAN(G)	WT OF PAN+WET SOIL(G)	WT OF PAN + DRY SOIL(G)	WT OF WET SOIL(G)	WT OF DRY SOIL(G)	MOISTURE CONTENT (%)	NUMBER OF BLOWS
15.53	22.52	20.21	6.99	4.68	49.36	14
16.52	26.97	23.54	10.45	7.02	48.86	23
15.25	23.64	20.92	8.39	5.67	47.97	30
17.01	27.03	23.85	10.02	6.84	46.49	44



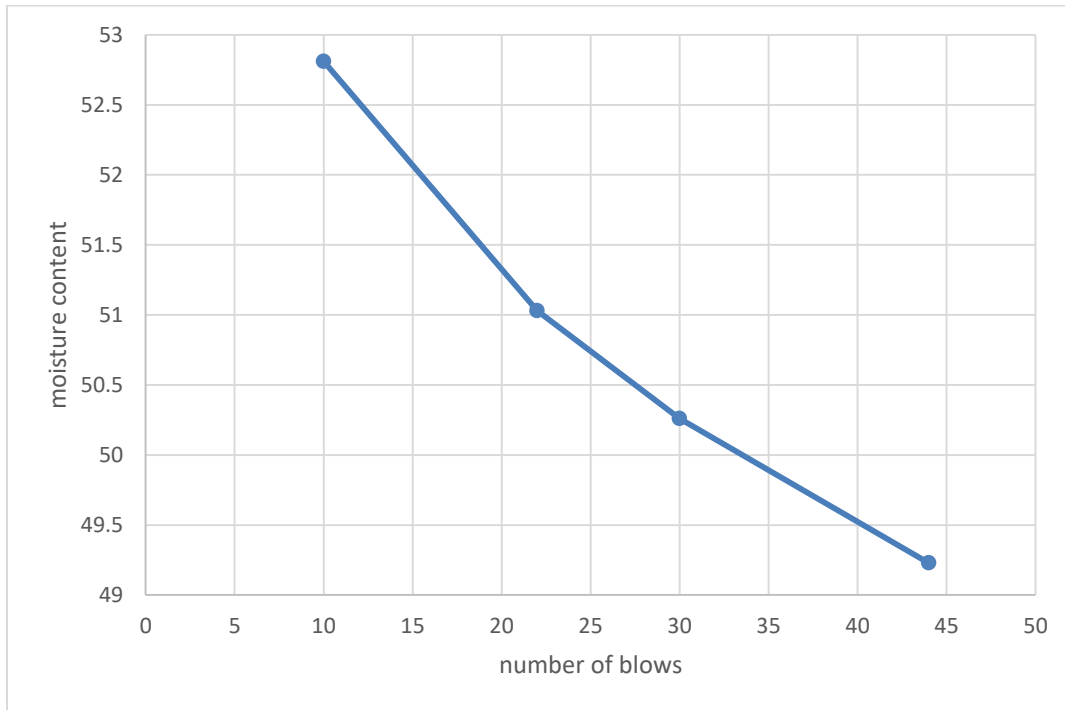
FLYASH 15% ESP 3%

WT OF PAN(G)	WT OF PAN+WET SOIL(G)	WT OF PAN + DRY SOIL(G)	WT OF WET SOIL(G)	WT OF DRY SOIL(G)	MOISTURE CONTENT (%)	NUMBER OF BLOWS
15.09	27.08	23.04	11.99	7.25	50.82	13
15.61	26.31	22.76	10.7	7.15	49.65	23
16.37	25.42	22.45	9.05	6.08	48.84	30
15.65	25.80	22.53	10.15	6.87	47.74	43



FLYASH 18% ESP 0%

WT OF PAN(G)	WT OF PAN+WET SOIL(G)	WT OF PAN + DRY SOIL(G)	WT OF WET SOIL(G)	WT OF DRY SOIL(G)	MOISTURE CONTENT (%)	NUMBER OF BLOWS
14.96	25.55	21.89	10.59	6.93	52.81	10
15.20	29.82	24.7	14.62	9.68	51.03	22
14.33	27.76	23.28	13.43	8.95	50.06	30
15.27	28.81	24.34	13.54	9.07	49.23	44



TRIAXIAL

SOIL 100%

SAMPLE 3

DIVISION	CHANGE IN LENGTH	AXIAL STRAIN	DIVISION(PR OVING RING READING)	APPLIED LOAD *PRC(2.54)	AREA	DEVIATOR STRESS
0	0	0	0	0	12.0073	0
10	0.1	12.5	0.8	2.032	12.0223	0.1690
20	0.2	25	2.2	5.588	12.0374	0.4642
30	0.3	37.5	2.2	5.588	12.0525	0.4642
40	0.4	50	2.3	5.842	12.0676	0.4840
50	0.5	62.5	2.6	6.604	12.0828	0.5470
60	0.6	75	4.0	10.16	12.0980	0.8400
70	0.7	87.5	4.6	11.684	12.1133	0.9560
80	0.8	100	4.8	12.192	12.1236	1.0000
90	0.9	112.5	5.2	13.208	12.1339	1.0880
100	1.0	125	5.6	14.224	12.1543	1.1700
120	1.2	150	5.8	14.73	12.1906	1.2080
140	1.4	175	6.0	15.24	12.2212	1.2470
160	1.6	200	6.9	17.526	12.2524	1.4300
180	1.8	225	14	35.56	12.2836	2.8940
200	2.0	250	18.8	47.752	12.3153	3.7750
240	2.4	300	26.25	66.675	12.3787	5.3870
280	2.8	350	31.4	79.756	12.4425	6.4100
320	3.2	400	35.6	90.424	12.5076	7.2290

360	3.6	450	39.2	99.568	12.5731	7.9190
400	4.0	500	43	109.22	12.6395	8.6410
440	4.4	550	46.8	118.872	12.7061	9.3560
480	4.8	600	50.0	127	12.7737	9.9420
520	5.2	650	53	134.62	12.8430	10.4820
560	5.6	700	55.2	140.208	12.9111	10.8010
600	6.0	750	57.6	146.304	12.9801	11.2710
640	6.4	800	60	152.4	13.0514	11.6770
680	6.8	850	61.8	156.972	13.1227	11.9620
720	7.2	900	63.20	160.528	13.1948	12.1660
760	7.6	950	64.50	163.83	13.2677	12.3480
800	8.0	1000	65.80	167.132	13.3414	12.5270
840	8.4	1050	66.8	169.672	13.4160	12.6470
880	8.8	1100	67.21	170.713	13.4914	12.6530
920	9.2	1150	67.30	170.942	13.5676	12.6000
960	9.6	1200	67	170.18	13.6447	12.4720

SAMPLE 2

DIVISION	CHANGE IN LENGTH	AXIAL STRAIN	DIVISION(PR OVING RING READING)	APPLIED LOAD *PRC(2.54)	AREA	DEVIATOR STRESS
0	0	0	0	0	12.0073	0
10	0.1	12.5	0.8	2.032	12.0223	0.1690
20	0.2	25	2.2	5.588	12.0374	0.4642
30	0.3	37.5	3	7.62	12.0525	0.6322

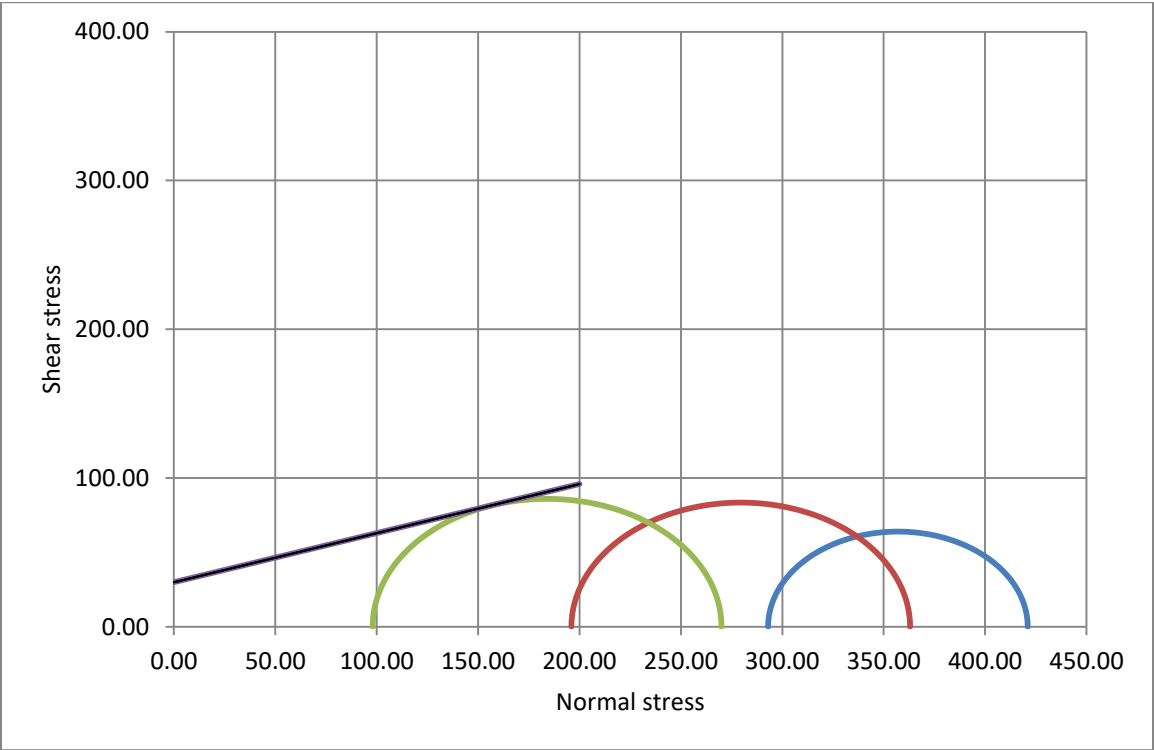
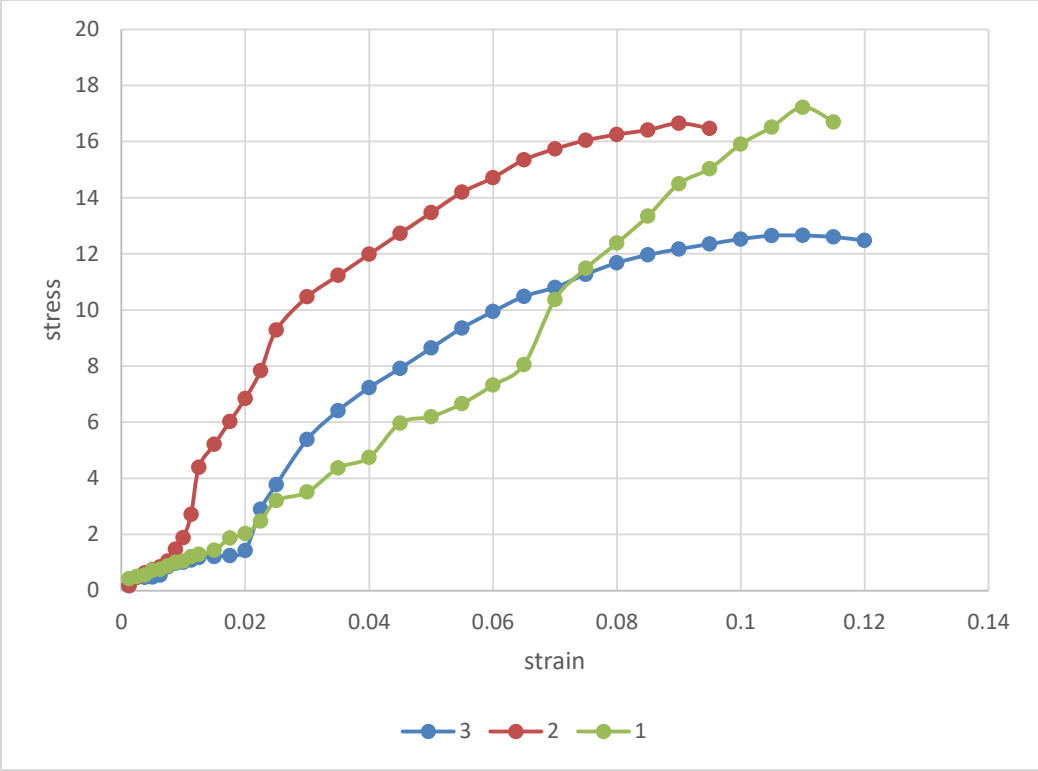
40	0.4	50	3.5	8.89	12.0676	0.7367
50	0.5	62.5	4	10.16	12.0828	0.8409
60	0.6	75	5	12.7	12.0980	1.0498
70	0.7	87.5	7	17.78	12.1133	1.4698
80	0.8	100	9	22.86	12.1236	1.8856
90	0.9	112.5	13	33.02	12.1439	2.7191
100	1.0	125	21	53.34	12.1543	4.3886
120	1.2	150	25	63.5	12.1906	5.0289
140	1.4	175	29	73.66	12.2212	6.6272
160	1.6	200	33	83.82	12.2524	6.8411
180	1.8	225	38	96.52	12.2836	7.8374
200	2.0	250	45	114.3	12.3153	9.2811
240	2.4	300	51	129.54	12.3787	10.4647
280	2.8	350	55	139.7	12.4425	11.2276
320	3.2	400	59	149.86	12.5076	11.9817
360	3.6	450	63	160.02	12.5731	12.7272
400	4.0	500	67	170.18	12.6395	13.4641
440	4.4	550	71	180.34	12.7061	14.1932
480	4.8	600	74	187.96	12.7737	14.7146
520	5.2	650	77.6	197.104	12.8430	15.3472
560	5.6	700	80	203.2	12.9111	15.7383
600	6.0	750	82	208.28	12.9801	16.0461
640	6.4	800	83.5	212.69	13.0514	16.2504
680	6.8	850	84.8	215.39	13.1227	16.4135
720	7.2	900	86.5	219.71	13.1948	16.6513

760 7.6 950 86 218.44 13.2677 16.4640

SAMPLE 1

DIVISION	CHANGE IN LENGTH	AXIAL STRAIN	DIVISION(PR OVING RING READING)	APPLIED LOAD *PRC(2.54)	AREA	DEVIATOR STRESS
0	0	0	0	0	12.0073	0
10	0.1	12.5	2	5.08	12.0223	04225
20	0.2	25	2,4	6.096	12.0374	05056
30	0.3	37.5	2.6	6.604	12.0525	05479
40	0.4	50	3.4	8.636	12.0676	07156
50	0.5	62.5	3.6	9.144	12.0828	07568
60	0.6	75	4.2	10.668	12.0980	08818
70	0.7	87.5	4.8	12.192	12.1133	10065
80	0.8	100	5.0	12.7	12.1236	10475
90	0.9	112.5	5.8	14.732	12.1439	12131
100	1.0	125	6.2	15.748	12.1543	12918
120	1.2	150	6.9	17.526	12.1906	14341
140	1.4	175	9	22.86	12.2212	18658
160	1.6	200	9.8	24.89	12.2524	20263
180	1.8	225	12	30.48	12.2836	24750
200	2.0	250	15.6	39.624	12.3153	32010
240	2.4	300	17.2	43.688	12.3787	35113
280	2.8	350	21.5	54.61	12.4425	43661

320	3.2	400	23.4	59.69	12.5076	47474
360	3.6	450	29.7	75.438	12.5731	59684
400	4.0	500	31.0	78.74	12.6395	61970
440	4.4	550	33.5	85.09	12.7061	6613
480	4.8	600	37	93.98	12.7737	73176
520	5.2	650	45	114.3	12.8430	80528
560	5.6	700	53	134.62	12.9111	103713
600	6.0	750	59	149.86	12.9801	114823
640	6.4	800	64	162.50	13.0514	123831
680	6.8	850	69.3	176.022	13.1227	133403
720	7.2	900	75.7	192.278	13.1948	144922
760	7.6	950	79	200.60	13.2677	150359
800	8.0	1000	84	213.36	13.3414	159034
840	8.4	1050	88	223.52	13.4160	165176
880	8.8	1100	92	233.68	13.4914	172234
920	9.2	1150	89.7	227.84	13.5676	166981



FLYASH 0% ESP 18%**SAMPLE 3**

DIVISION	CHANGE IN LENGTH	AXIAL STRAIN	DIVISION(PRO VING RING READING)	APPLIED LOAD *PRC(2.54)	AREA	DEVIATOR STRESS
0	0	0	0	0	12.0073	0
10	0.1	12.5	0.8	2.032	12.0223	0.1690
20	0.2	25	2.2	5.588	12.0374	0.4646
30	0.3	37.5	2.3	5.842	12.0525	0.4847
40	0.4	50	2.6	6.604	12.0676	0.5473
50	0.5	62.5	4	10.16	12.0828	0.8409
60	0.6	75	4.6	11.684	12.0980	0.9658
70	0.7	87.5	4.8	12.192	12.1133	1.0065
80	0.8	100	5.2	13.308	12.1236	1.0977
90	0.9	112.5	6	15.24	12.1439	1.2550
100	1.0	125	6.9	17.526	12.1543	1.4420
120	1.2	150	14	35.56	12.1906	2.9170
140	1.4	175	18	45.72	12.2212	3.7410
160	1.6	200	21	53.34	12.2524	4.3534
180	1.8	225	25	63.5	12.2836	5.1695
200	2.0	250	27	68.58	12.3153	5.5687
240	2.4	300	31	78.74	12.3787	6.3609
280	2.8	350	34	86.30	12.4425	6.9359
320	3.2	400	37	93.98	12.5076	7.5138
360	3.6	450	42	106.68	12.5731	8.484

400	4.0	500	47	119.38	12.6395	9.4450
440	4.4	550	53	134.62	12.7061	10.5949
480	4.8	600	58	147.32	12.7737	11.5331
520	5.2	650	63	160.02	12.8430	12.4597
560	5.6	700	65.8	167.132	12.9111	12.9448
600	6.0	750	67.8	172.212	12.9801	13.2674
640	6.4	800	68.5	173.99	13.0514	13.3311
680	6.8	850	71.3	181.102	13.1227	13.8007
720	7.2	900	72.4	183.896	13.1948	13.9370
760	7.6	950	73	185.42	13.2677	13.9753
800	8.0	1000	75.4	191.516	13.3414	14.3550
840	8.4	1050	75	190.5	13.4160	14.1995

SAMPLE 2

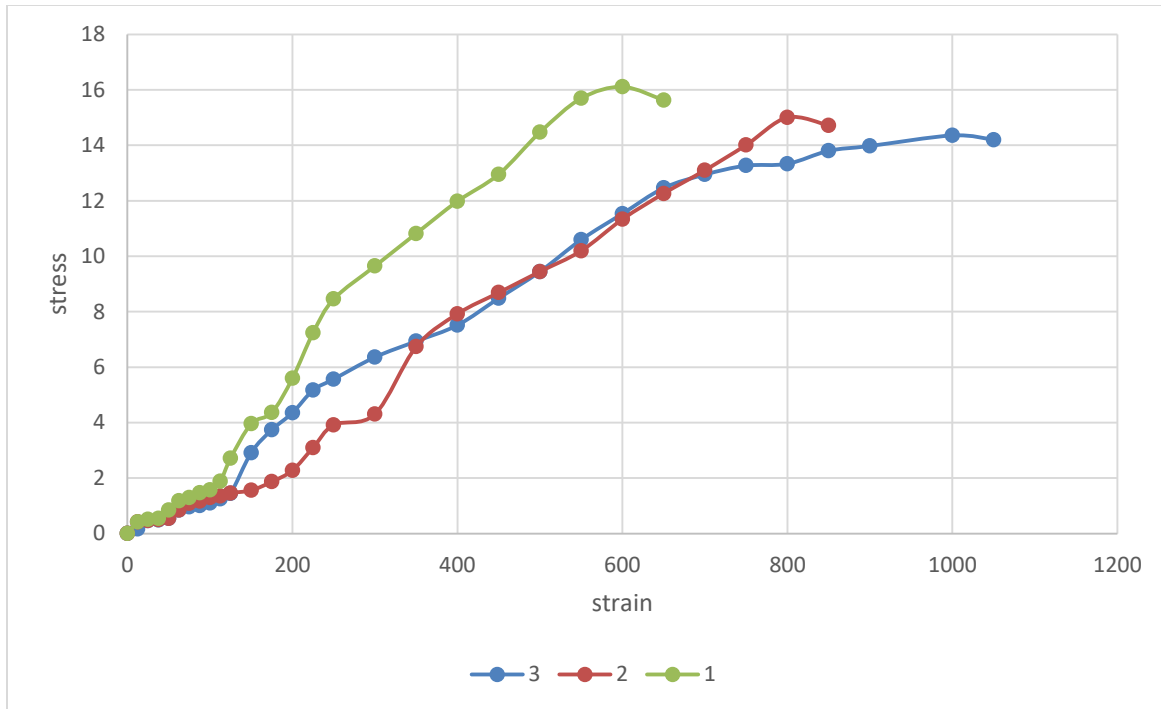
DIVISIO N	CHANGE IN LENGTH	AXIAL STRAIN	DIVISION(PR OVING RING READING)	APPLIED LOAD *PRC(2.54)	AREA	DEVIATOR STRESS
0	0	0	0	0	12.0073	0
10	0.1	12.5	2	5.08	12..0223	0.4225
20	0.2	25	2.2	5.588	12.0374	0.4642
30	0.3	37.5	2.4	6.096	12.0525	0.5058
40	0.4	50	2.6	6.604	12.0676	0.5437
50	0.5	62.5	4	10.16	12.0828	0.8409
60	0.6	75	5.2	13.208	12.0980	1.0918
70	0.7	87.5	5.6	14.224	12.1133	1.1742

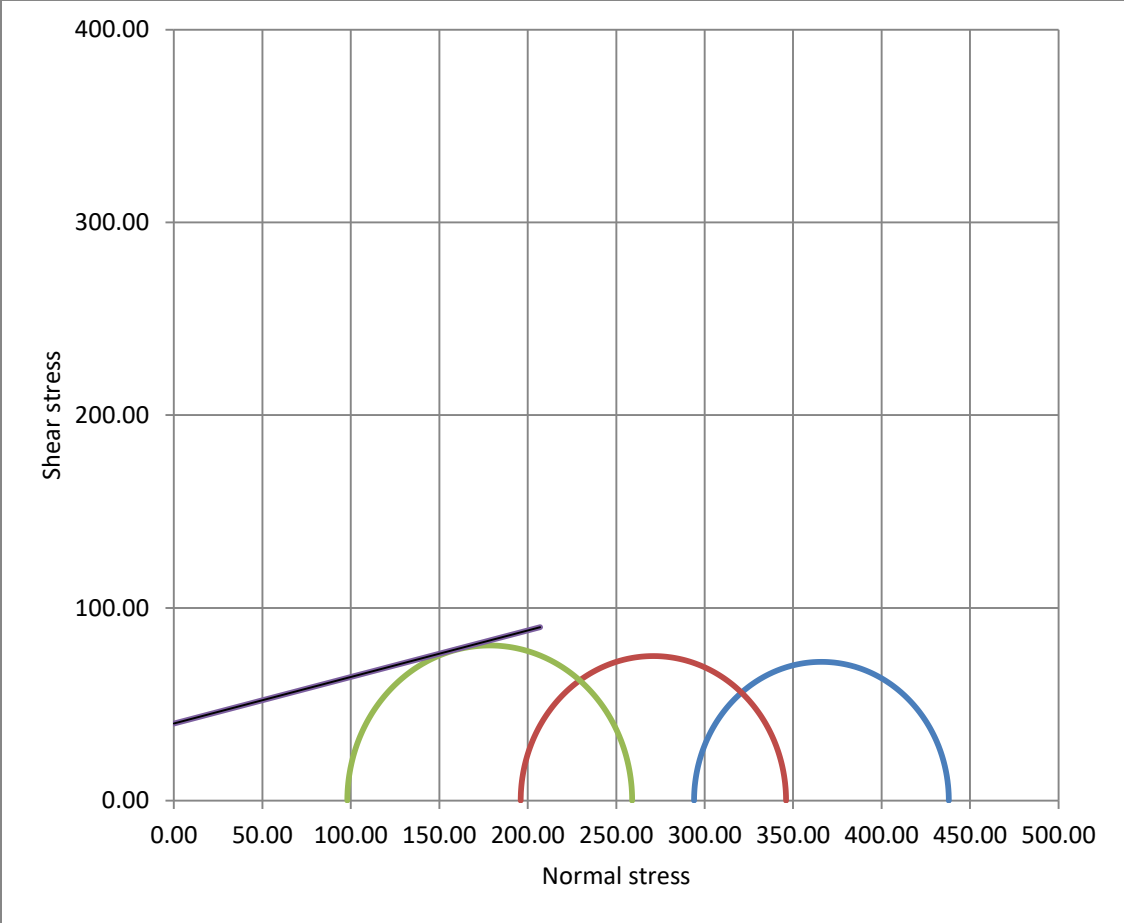
80	0.8	100	6.2	15.748	12.1236	1.2970
90	0.9	112.5	6.5	16.51	12.1439	1.3595
100	1.0	125	7.1	17.78	12.1543	1.4629
120	1.2	150	7.5	19.05	12.1906	1.5627
140	1.4	175	9	22.85	12.2212	1.8697
160	1.6	200	11	27.94	12.2524	2.2804
180	1.8	225	15	38.1	12.2836	3.1017
200	2.0	250	19	48.26	12.3153	3.9187
240	2.4	300	25	53.24	12.3787	4.3090
280	2.8	350	33	83.82	12.4425	6.7366
320	3.2	400	39	99.06	12.5076	7.9200
360	3.6	450	43	109.22	12.5731	8.6868
400	4.0	500	47	119.38	12.6395	9.4450
440	4.4	550	51	129.54	12.7061	10.1951
480	4.8	600	57	144.78	12.7737	11.3342
520	5.2	650	62	157.48	12.8430	12.2619
560	5.6	700	67	170.18	12.9111	13.1009
600	6.0	750	72	182.88	12.9801	14.0093
640	6.4	800	77.5	196.85	13.0514	15.0027
680	6.8	850	76	193.04	13.1227	14.7104

SAMPLE 1

DIVISION	CHANGE IN LENGTH	AXIAL STRAIN	DIVISION(PR OVING RING READING)	APPLIED LOAD *PRC(2.54)	AREA	DEVIATOR STRESS
0	0	0	0	0	12.0073	0
10	0.1	12.5	2	5.08	12.0223	0.4225
20	0.2	25	2.4	6.096	12.0374	0.5064
30	0.3	37.5	2.6	6.604	12.0525	0.5479
40	0.4	50	4	10.16	12.0676	0.8419
50	0.5	62.5	5.6	14.224	12.0828	1.1772
60	0.6	75	6.2	15.748	12.0980	1.3017
70	0.7	87.5	7	17.78	12.1133	1.4678
80	0.8	100	7.5	19.05	12.1236	1.5713
90	0.9	112.5	9	22.86	12.1439	1.8824
100	1.0	125	13	33.02	12.1543	2.7167
120	1.2	150	19	48.26	12.1906	3.9588
140	1.4	175	21	53.34	12.2212	4.3645
160	1.6	200	27	68.58	12.2524	5.5973
180	1.8	225	35	88.9	12.2836	7.2373
200	2.0	250	41	104.14	12.3153	8.4561
240	2.4	300	47	119.38	12.3787	9.6440
280	2.8	350	53	134.62	12.4425	10.8194
320	3.2	400	59	149.86	12.5076	11.9815
360	3.6	450	64	162.56	12.5731	12.9531
400	4.0	500	72	182.86	12.6395	14.4673

440	4.4	550	78.5	199.39	12.7061	15.6925
480	4.8	600	81	205.74	12.7737	16.1065
520	5.2	650	79	200.66	12.8430	15.6241





FLYASH 3% ESP 15%

SAMPLE 3

DIVISION	CHANGE IN LENGTH	AXIAL STRAIN	DIVISION(PR OVING RING READING)	APPLIED LOAD *PRC(2.54)	AREA	DEVIATOR STRESS
0	0	0	0	0	12.0073	0
10	0.1	12.5	2	5.08	12.0223	0.4225
20	0.2	25	2.2	5.588	12.0374	0.4642
30	0.3	37.5	2.4	6.096	12.0525	0.5058
40	0.4	50	4	10.16	12.0676	0.8419
50	0.5	62.5	5	12.7	12.0828	1.2596
60	0.6	75	6.2	15.748	12.0980	1.3017
70	0.7	87.5	7.5	19.055	12.1133	1.5727
80	0.8	100	9	22.86	12.1236	1.8856
90	0.9	112.5	13	33.02	12.1439	2.7191
100	1.0	125	17	43.18	12.1543	3.5527
120	1.2	150	21	53.34	12.1906	4.3755
140	1.4	175	25	63.5	12.2212	5.1959
160	1.6	200	29	73.66	12.2524	6.0119
180	1.8	225	31	78.74	12.2836	6.4102
200	2.0	250	33	83.82	12.3153	6.8062
240	2.4	300	35	88.9	12.3787	7.1817
280	2.8	350	37	93.98	12.4425	7.5531
320	3.2	400	43	109.22	12.5076	8.7323
360	3.6	450	45	114.3	12.5731	9.0908

400	4.0	500	47	119.38	12.6395	9.4450
440	4.4	550	51	129.54	12.7061	10.1951
480	4.8	600	55	139.7	12.7737	10.9365
520	5.2	650	57	144.78	12.8430	11.2731
560	5.6	700	61	154.94	12.9111	12.0005
600	6.0	750	65	165.1	12.9801	12.7195
640	6.4	800	72	182.88	13.0514	14.0123
680	6.8	850	78	198.12	13.1227	15.0975
720	7.2	900	83	210.82	13.1948	15.9775
760	7.6	950	81	203.2	13.2677	15.3154

SAMPLE 2

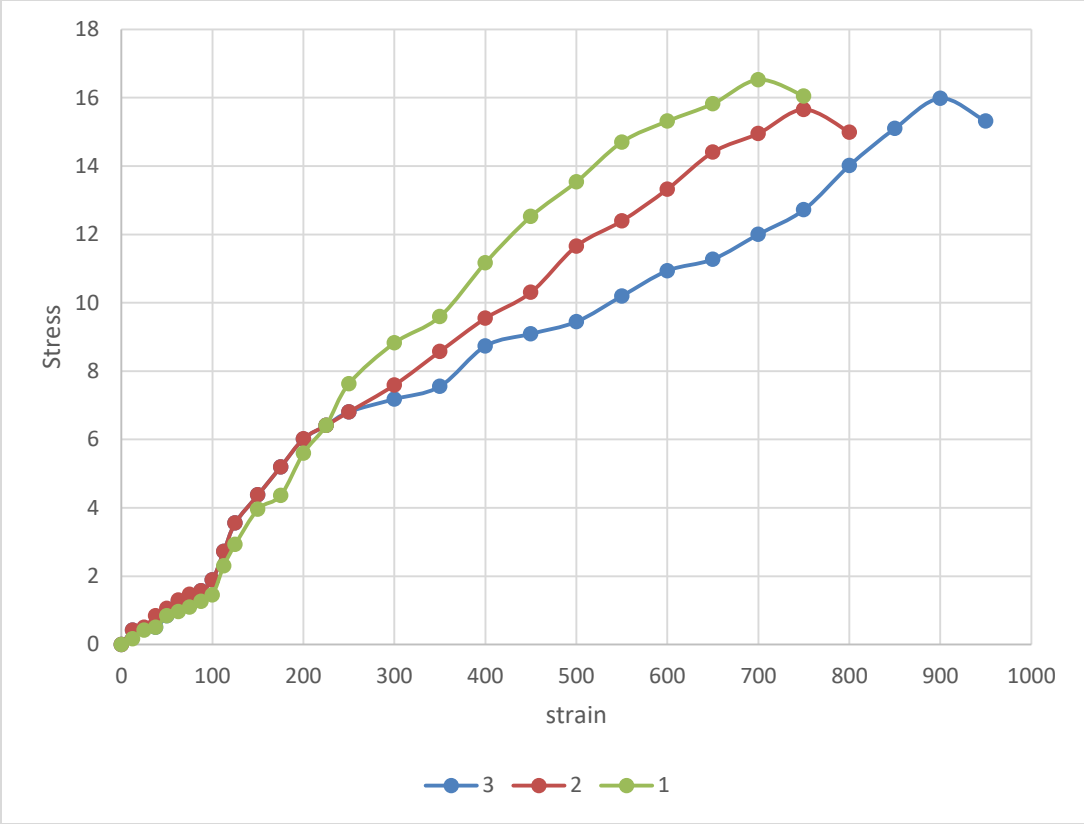
DIVISION	CHANGE IN LENGTH	AXIAL STRAIN	DIVISION(PRO VING RING READING)	APPLIED LOAD *PRC(2.54)	AREA	DEVIATOR STRESS
0	0	0	0	0	12.0073	0
10	0.1	12.5	2	5.08	12.0223	0.4225
20	0.2	25	2.4	6.096	12.0374	0.5064
30	0.3	37.5	4	10.16	12.0525	0.8430
40	0.4	50	5	12.7	12.0676	1.0524
50	0.5	62.5	6.2	15.748	12.0828	1.3033
60	0.6	75	7	17.78	12.0980	1.4697
70	0.7	87.5	7.5	19.05	12.1133	1.5727
80	0.8	100	9	22.86	12.1236	1.8856
90	0.9	112.5	13	33.02	12.1439	2.7191

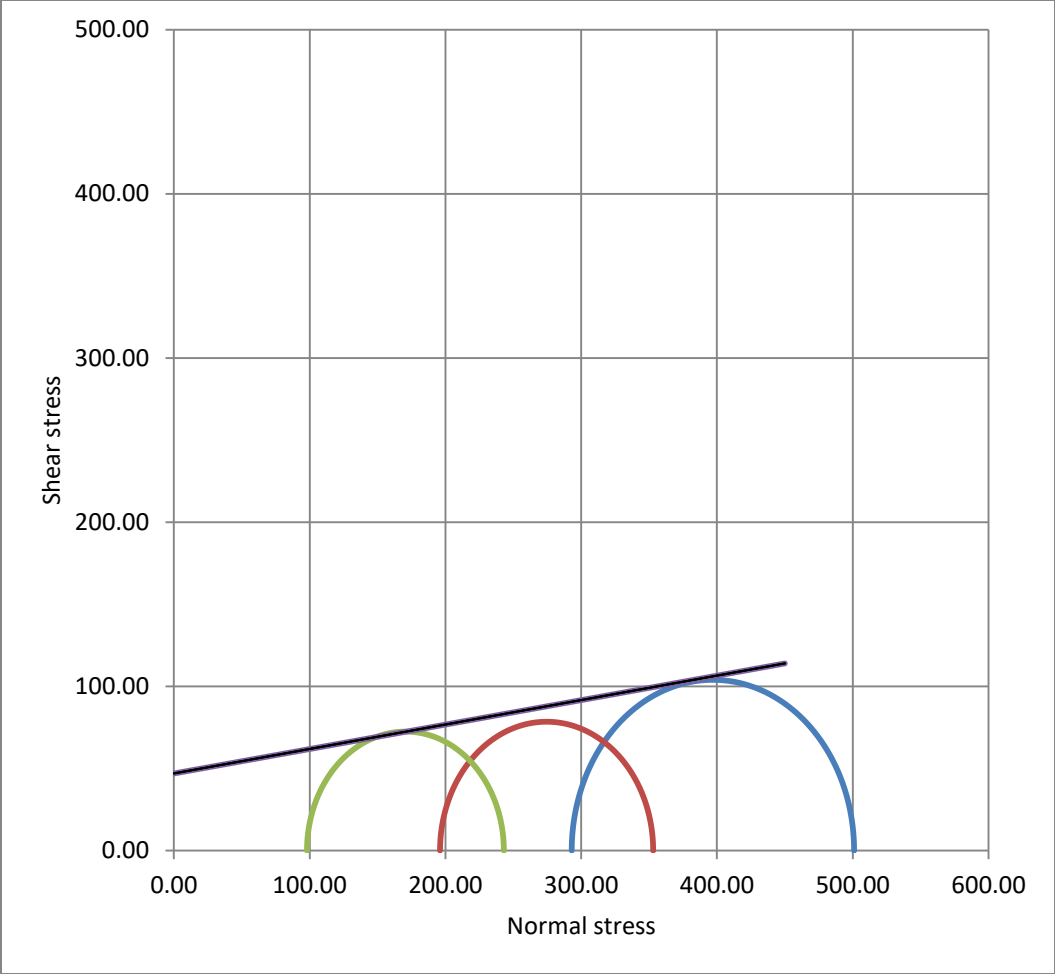
100	1.0	125	17	43.18	12.1543	3.5527
120	1.2	150	21	53.34	12.1906	4.3755
140	1.4	175	25	63.5	12.2212	5.1959
160	1.6	200	29	73.66	12.2524	6.0184
180	1.8	225	31	78.74	12.2836	6.4102
200	2.0	250	33	83.82	12.3153	6.8062
240	2.4	300	37	93.98	12.3787	7.5921
280	2.8	350	42	106.68	12.4425	8.5738
320	3.2	400	47	119.38	12.5076	9.5446
360	3.6	450	51	129.54	12.5731	10.3029
400	4.0	500	58	147.32	12.6395	11.6555
440	4.4	550	62	157.48	12.7061	12.3940
480	4.8	600	67	170.18	12.7737	13.3227
520	5.2	650	71	180.34	12.8430	14.0419
560	5.6	700	76	193.04	12.9111	14.9515
600	6.0	750	80	203.2	12.9801	15.6547
640	6.4	800	77	195.8	13.0514	14.9854

SAMPLE 1

DIVISION	CHANGE IN LENGTH	AXIAL STRAIN	DIVISION(PR OVING RING READING)	APPLIED LOAD *PRC(2.54)	AREA	DEVIATOR STRESS
0	0	0	0	0	12.0037	0
10	0.1	12.5	0.8	2.032	12.0223	0.1690
20	0.2	25	2	5.08	12.0374	0.4220

30	0.3	37.5	2.4	6.096	12.0525	0.5057
40	0.4	50	4	10.16	12.0676	0.8419
50	0.5	62.5	4.6	11.684	12.0828	0.9670
60	0.6	75	5.2	13.208	12.0980	1.0918
70	0.7	87.5	6	15.24	12.1133	1.2581
80	0.8	100	6.9	17.526	12.1236	1.4456
90	0.9	112.5	11	27.94	12.1439	2.3046
100	1.0	125	14	35.56	12.1543	2.9257
120	1.2	150	19	48.26	12.1906	3.9588
140	1.4	175	21	53.34	12.2212	4.3654
160	1.6	200	27	68.58	12.2524	5.5973
180	1.8	225	31	78.74	12.2836	6.4102
200	2.0	250	37	93.98	12.3153	7.6312
240	2.4	300	43	109.22	12.3787	8.8232
280	2.8	350	47	119.38	12.4425	9.5945
320	3.2	400	55	139.7	12.5076	11.1692
360	3.6	450	62	157.48	12.5731	12.5252
400	4.0	500	67	170.18	12.6395	13.4641
440	4.4	550	73	185.42	12.7061	14.5930
480	4.8	600	77	195.58	12.7737	15.3111
520	5.2	650	80	203.2	12.8430	15.8218
560	5.6	700	84	213.36	12.9111	16.5253
600	6.0	750	82	208.28	12.9801	16.0461





FLYASH 6% ESP 12**SAMPLE 3**

DIVISION	CHANGE IN LENGTH	AXIAL STRAIN	DIVISION(PR OVING RING READING)	APPLIED LOAD *PRC(2.54)	AREA	DEVIATOR STRESS
0	0	0	0	0	12.0073	0
10	0.1	12.5	2	5.08	12.0223	0.4225
20	0.2	25	3	7.62	12.0374	0.6330
30	0.3	37.5	5	12.7	12.0525	1.0537
40	0.4	50	5.5	13.37	12.0676	1.1079
50	0.5	62.5	7	17.78	12.0828	1.4715
60	0.6	75	9	22.80	12.0980	1.8846
70	0.7	87.5	13	33.02	12.1133	2.7259
80	0.8	100	21	53.34	12.1236	4.3997
90	0.9	112.5	25	63.5	12.1439	5.2290
100	1.0	125	29	73.60	12.1543	6.0374
120	1.2	150	34	86.30	12.1906	7.0615
140	1.4	175	38	96.52	12.2212	7.8776
160	1.6	200	45	114.3	12.2524	9.3060
180	1.8	225	51	129.54	12.2836	10.5186
200	2.0	250	56	142.24	12.3153	11.4907
240	2.4	300	62	157.48	12.3787	12.6560
280	2.8	350	68	172.72	12.4425	13.8092
320	3.2	400	72	182.88	12.5076	14.4689
360	3.6	450	75	190.5	12.5731	14.9928

400	4.0	500	79`	200.60	12.6395	15.7401
440	4.4	550	81.5	207.01	12.7061	16.1185
480	4.8	600	85	215.9	12.7737	16.7220
520	5.2	650	89	226.06	12.8430	17.4159
560	5.6	700	92	233.68	12.9111	17.9046
600	6.0	750	95	241.3	12.9801	18.3880
640	6.4	800	94	238.76	13.0514	18.0729

SAMPLE 2

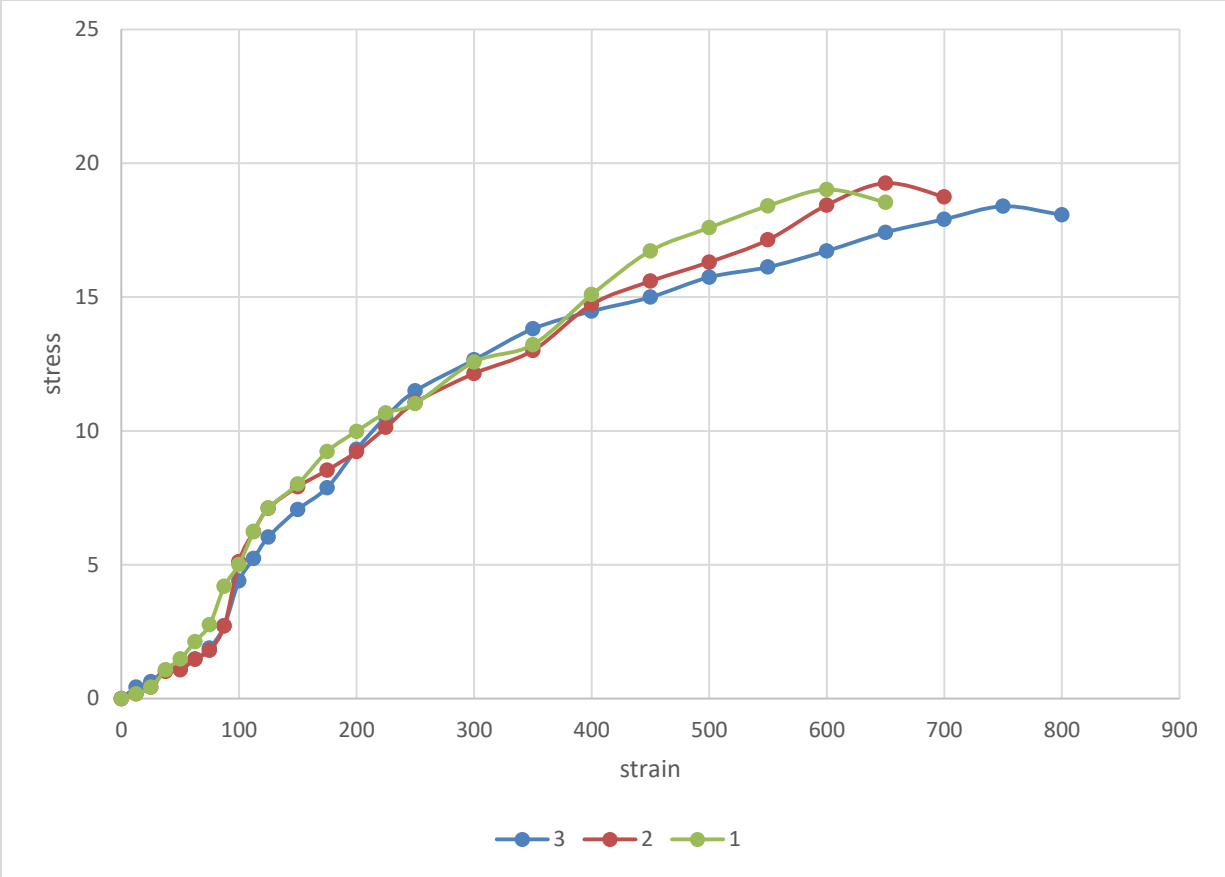
DIVISION	CHANGE IN LENGTH	AXIAL STRAIN	DIVISION(PR OVING RING READING)	APPLIED LOAD *PRC(2.54)	AREA	DEVIATOR STRESS
0	0	0	0	0	12.0073	0
10	0.1	12.5	0.8	2.032	12.0223	0.1690
20	0.2	25	2	5.08	12.0374	0.4225
30	0.3	37.5	4.8	12.22	12.0525	1.0137
40	0.4	50	5.1	12.95	12.0676	1.0735
50	0.5	62.5	7.2	17.78	12.0828	1.4711
60	0.6	75	8.6	21.84	12.0980	1.8052
70	0.7	87.5	12.9	32.85	12.1133	2.7119
80	0.8	100	24.4	61.97	12.1236	5.1120
90	0.9	112.5	29.8	75.71	12.1439	6.2341
100	1.0	125	34.1	86.61	12.1543	7.1046
120	1.2	150	38.1	96.77	12.1906	7.9132
140	1.4	175	41.4	105.15	12.2212	8.5320

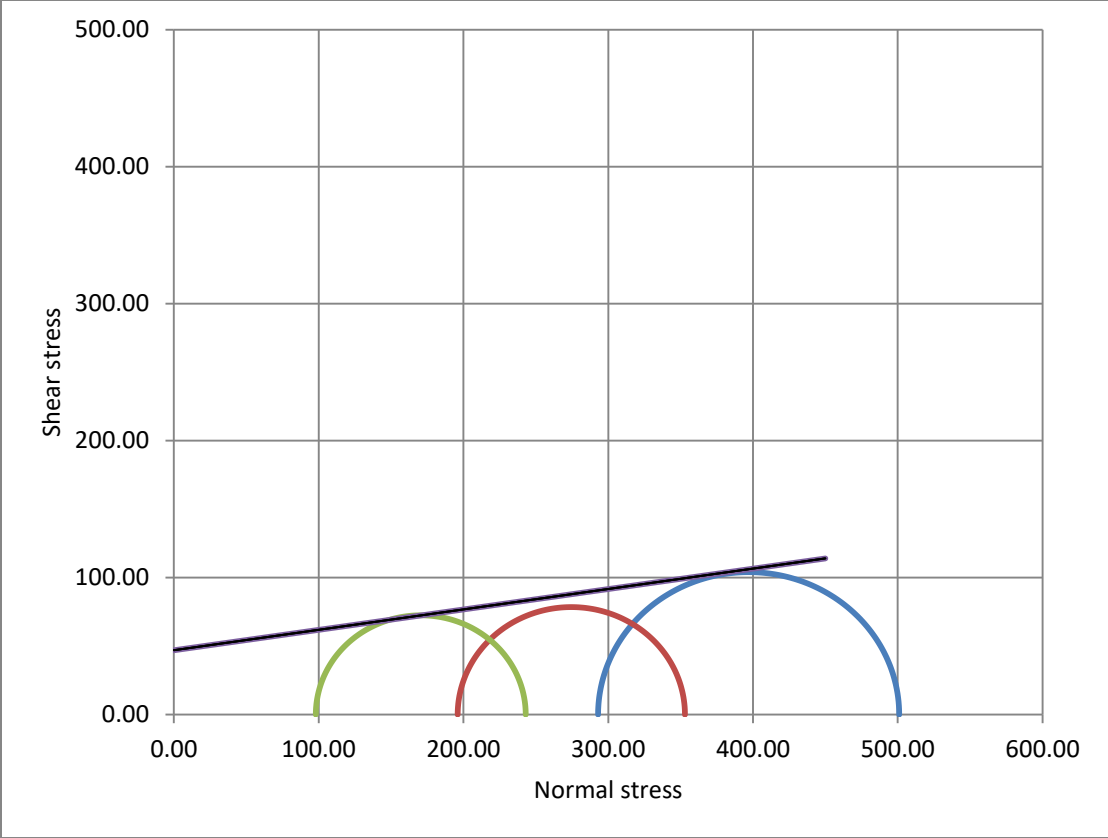
160	1.6	200	44.6	113.28	12.2524	9.2211
180	1.8	225	49.1	124.71	12.2836	10.1267
200	2.0	250	53.9	136.91	12.3153	11.6601
240	2.4	300	59.5	151.10	12.3787	12.1436
280	2.8	350	64	162.63	12.4425	13.0028
320	3.2	400	73.3	186.08	12.5076	14.37228
360	3.6	450	78	198.08	12.5731	15.5891
400	4.0	500	82.3	209.40	12.6395	16.3047
440	4.4	550	87.1	221.23	12.7061	17.1349
480	4.8	600	94.2	239.26	12.7737	18.4332
520	5.2	650	98.9	251.28	12.8430	19.2532
560	5.6	700	96.8	245.83	12.9111	18.7331

SAMPLE 1

DIVISION	CHANGE IN LENGTH	AXIAL STRAIN	DIVISION(PR OVING RING READING)	APPLIED LOAD *PRC(2.54)	AREA	DEVIATOR STRESS
0	0	0	0	0	12.0073	0
10	0.1	12.5	0.8	2.032	12.0223	0.1690
20	0.2	25	2	5.08	12.0374	0.4225
30	0.3	37.5	5.1	12.9	12.0525	1.0735
40	0.4	50	7	17.78	12.0676	1.4733
50	0.5	62.5	10.1	25.65	12.0828	2.1259
60	0.6	75	13.1	33.27	12.0980	2.7562
70	0.7	87.5	20	50.91	12.1133	4.1897

80	0.8	100	23.9	60.71	12.1236	5.0082
90	0.9	112.5	29.8	75.69	12.1439	6.2343
100	1.0	125	34.1	86.75	12.1543	7.1158
120	1.2	150	38.5	97.89	12.1906	8.0101
140	1.4	175	44.5	113.07	12.2212	9.2287
160	1.6	200	48.2	122.60	12.2524	9.9821
180	1.8	225	51.7	131.35	12.2836	10.6654
200	2.0	250	53.7	136.39	12.3153	11.0183
240	2.4	300	61.6	156.47	12.3787	12.5751
280	2.8	350	65.1	165.37	12.4425	13.2215
320	3.2	400	75.1	190.69	12.5076	15.0871
360	3.6	450	83.7	212.489	12.5731	16.7223
400	4.0	500	88.9	225.89	12.6395	17.5891
440	4.4	550	93.59	237.61	12.7061	18.4041
480	4.8	600	97.2	246.82	12.7737	19.0153
520	5.2	650	95.2	241.80	12.8430	18.5321





FLYASH 9% ESP %**SAMPLE 3**

DIVISION	CHANGE IN LENGTH	AXIAL STRAIN	DIVISION(PR OVING RING READING)	APPLIED LOAD *PRC(2.54)	AREA	DEVIATOR STRESS
0	0	0	0	0	12.0073	0
10	0.1	12.5	2	5.08	12.0223	0.4225
20	0.2	25	4	10.16	12.0374	0.8440
30	0.3	37.5	5	12.7	12.0525	1.0537
40	0.4	50	7	17.78	12.0676	1.4734
50	0.5	62.5	9	22.86	12.0828	1.8918
60	0.6	75	11	27.94	12.0980	2.3095
70	0.7	87.5	13	33.02	12.1133	2.7259
80	0.8	100	15	38.1	12.1236	3.1426
90	0.9	112.5	19	48.26	12.1439	3.9740
100	1.0	125	23	58.42	12.1543	4.8065
120	1.2	150	28	71.12	12.1906	5.8340
140	1.4	175	31	78.74	12.2212	6.4429
160	1.6	200	37	93.98	12.2524	7.6703
180	1.8	225	43	109.22	12.2836	8.8915
200	2.0	250	49	124.46	12.3153	10.1061
240	2.4	300	52	132.08	12.3787	10.6699
280	2.8	350	58	147.32	12.4425	11.8401
320	3.2	400	64	162.56	12.5076	12.9969
360	3.6	450	71	180.34	12.5731	14.3433

400	4.0	500	77	195.58	12.6395	15.4737
440	4.4	550	84	213.36	12.7061	16.7919
480	4.8	600	93	236.22	12.7737	18.4927
520	5.2	650	99	251.46	12.8430	19.5795
560	5.6	700	95	243.84	12.9111	18.8861

SAMPLE 2

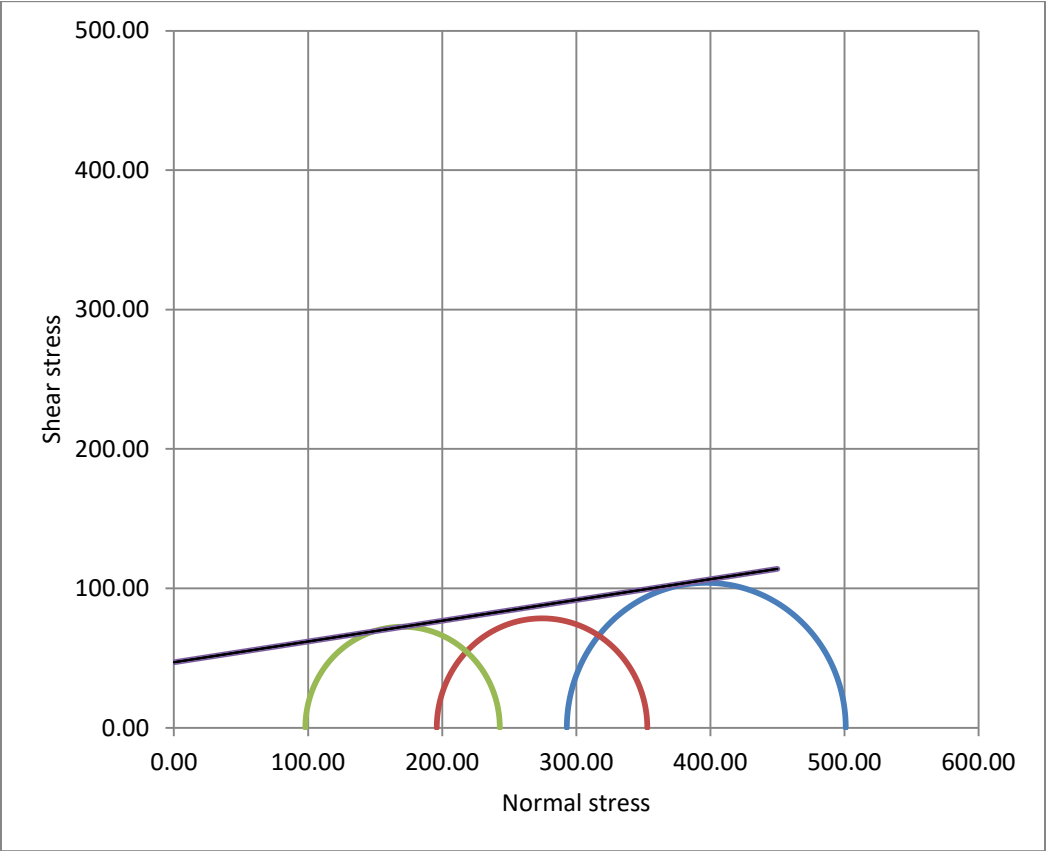
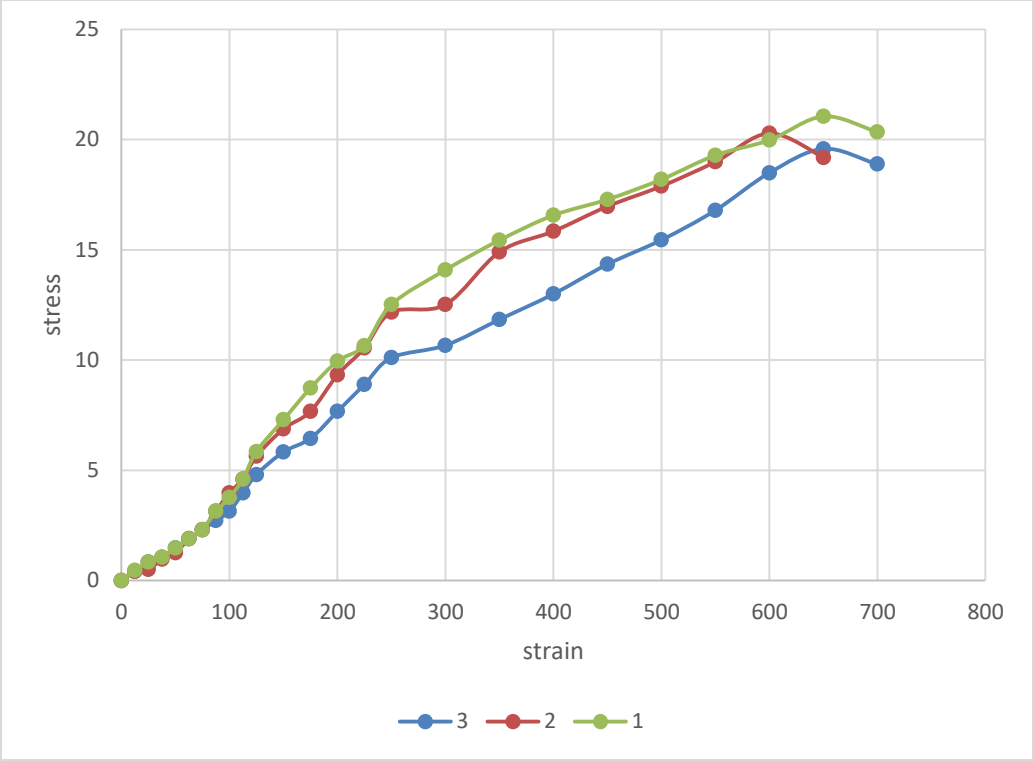
DIVISION	CHANGE IN LENGTH	AXIAL STRAIN	DIVISION(PR OVING RING READING)	APPLIED LOAD *PRC(2.54)	AREA	DEVIATOR STRESS
0	0	0	0	0	12.0073	0
10	0.1	12.5	2	5.08	12.0223	0.4225
20	0.2	25	2.4	6.096	12.0374	0.5064
30	0.3	37.5	4.6	11.684	12.0525	0.9694
40	0.4	50	6	15.24	12.0676	1.2629
50	0.5	62.5	9	22.86	12.0828	1.8919
60	0.6	75	11	27.94	12.0980	2.3095
70	0.7	87.5	15	38.1	12.1133	3.1453
80	0.8	100	19	48.26	12.1236	3.9807
90	0.9	112.5	22	55.88	12.1439	4.6015
100	1.0	125	27	68.58	12.1543	5.6424
120	1.2	150	33	83.82	12.1906	6.8756
140	1.4	175	37	93.98	12.2212	7.6703
160	1.6	200	45	114.3	12.2524	9.3287
180	1.8	225	51	129.54	12.2836	10.5457

200	2.0	250	59	149.86	12.3153	12.1686
240	2.4	300	67	154.94	12.3787	12.5167
280	2.8	350	73	185.42	12.4425	14.9021
320	3.2	400	78	198.12	12.5076	15.8400
360	3.6	450	84	213.36	12.5731	16.9696
400	4.0	500	89	226.06	12.6395	17.8852
440	4.4	550	95	241.3	12.7061	18.9909
480	4.8	600	102	259.08	12.7737	20.2823
520	5.2	650	97	246.38	12.8430	19.1840

SAMPLE 1

DIVISION	CHANGE IN LENGTH	AXIAL STRAIN	DIVISION(PR OVING RING READING)	APPLIED LOAD *PRC(2.54)	AREA	DEVIATOR STRESS
0	0	0	0	0	12.0073	0
10	0.1	12.5	2.2	5.588	12.0223	0.4648
20	0.2	25	4	10.16	12.0374	0.8440
30	0.3	37.5	5	12.7	12.0525	1.0537
40	0.4	50	7	17.78	12.0676	1.4734
50	0.5	62.5	9	22.86	12.0828	1.8919
60	0.6	75	11	27.94	12.0980	2.3095
70	0.7	87.5	15	38.1	12.1133	3.1453
80	0.8	100	18	45.72	12.1236	3.7712
90	0.9	112.5	22	55.88	12.1439	4.6015
100	1.0	125	28	71.12	12.1543	5.8514

120	1.2	150	35	88.9	12.1906	7.2925
140	1.4	175	42	106.68	12.2212	8.7291
160	1.6	200	48	121.92	12.2524	9.9507
180	1.8	225	54	137.16	12.2836	10.6856
200	2.0	250	61	154.94	12.3153	12.5167
240	2.4	300	69	175.26	12.3787	14.0856
280	2.8	350	76	193.04	12.4425	15.4338
320	3.2	400	82	208.28	12.5076	16.5655
360	3.6	450	86	218.44	12.5731	17.2823
400	4.0	500	91	231.14	12.6395	18.1913
440	4.4	550	97	26.38	12.7061	19.2881
480	4.8	600	101	256.54	12.7737	19.9751
520	5.2	650	107	271.78	12.8430	21.0501
560	5.6	700	104	264.16	12.9111	20.3512



FLYASH 12% ESP 6%**SAMPLE 3**

DIVISION	CHANGE IN LENGTH	AXIAL STRAIN	DIVISION(PR OVING RING READING)	APPLIED LOAD *PRC(2.54)	AREA	DEVIATOR STRESS
0	0	0	0	0	12.0073	0
10	0.1	12.5	2	5.08	12.0223	0.4225
20	0.2	25	5	12.7	12.0374	1.0550
30	0.3	37.5	7	17.78	12.0525	1.4752
40	0.4	50	9	22.86	12.0676	1.8943
50	0.5	62.5	11	27.94	12.0828	2.3124
60	0.6	75	12.5	31.75	12.0980	2.6224
70	0.7	87.5	13	33.02	12.1133	2.7259
80	0.8	100	13.5	34.29	12.1236	2.8284
90	0.9	112.5	15	38.1	12.1439	3.1374
100	1.0	125	17	43.18	12.1543	3.5527
120	1.2	150	25	63.5	12.1906	5.2089
140	1.4	175	29	73.66	12.2212	6.0272
160	1.6	200	37	93.98	12.2524	7.6703
180	1.8	225	45	114.3	12.2836	9.3051
200	2.0	250	53	134.62	12.3153	10.9311
240	2.4	300	62	157.48	12.3787	12.7219
280	2.8	350	77	195.58	12.4425	15.7187
320	3.2	400	85	215.9	12.5076	17.2615
360	3.6	450	92	233.68	12.5731	18.5857

400	4.0	500	97	246.38	12.6395	19.4929
440	4.4	550	104	264.16	12.7061	20.7900
480	4.8	600	106	269.24	12.7737	21.0777
520	5.2	650	105.5	267.97	12.8430	20.8651

SAMPLE 2

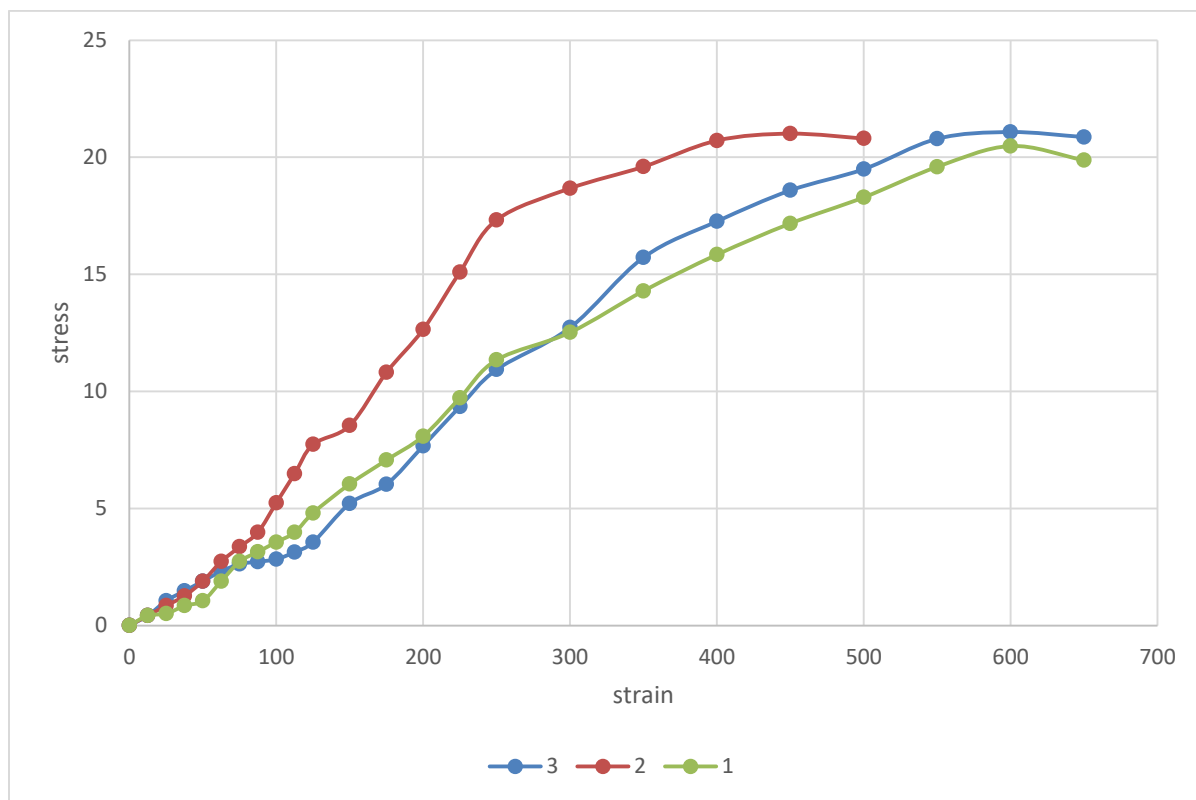
DIVISION	CHANGE IN LENGTH	AXIAL STRAIN	DIVISION(PR OVING RING READING)	APPLIED LOAD *PRC(2.54)	AREA	DEVIATOR STRESS
0	0	0	0	0	12.0073	0
10	0.1	12.5	2	5.08	12.0223	0.4225
20	0.2	25	4	10.19	12.0374	0.8465
30	0.3	37.5	6	15.24	12.0525	1.2645
40	0.4	50	9	22.86	12.0676	1.8943
50	0.5	62.5	13	33.02	12.0828	2.7328
60	0.6	75	16	40.64	12.0980	3.3592
70	0.7	87.5	19	48.26	12.1133	3.9841
80	0.8	100	25	63.5	12.1236	5.2377
90	0.9	112.5	31	78.74	12.1439	6.4839
100	1.0	125	37	93.98	12.1543	7.7322
120	1.2	150	41	104.14	12.1906	8.5426
140	1.4	175	52	132.08	12.2212	10.8074
160	1.6	200	61	154.94	12.2524	12.6457
180	1.8	225	73	185.42	12.2836	15.0949
200	2.0	250	84	213.36	12.3153	17.3248

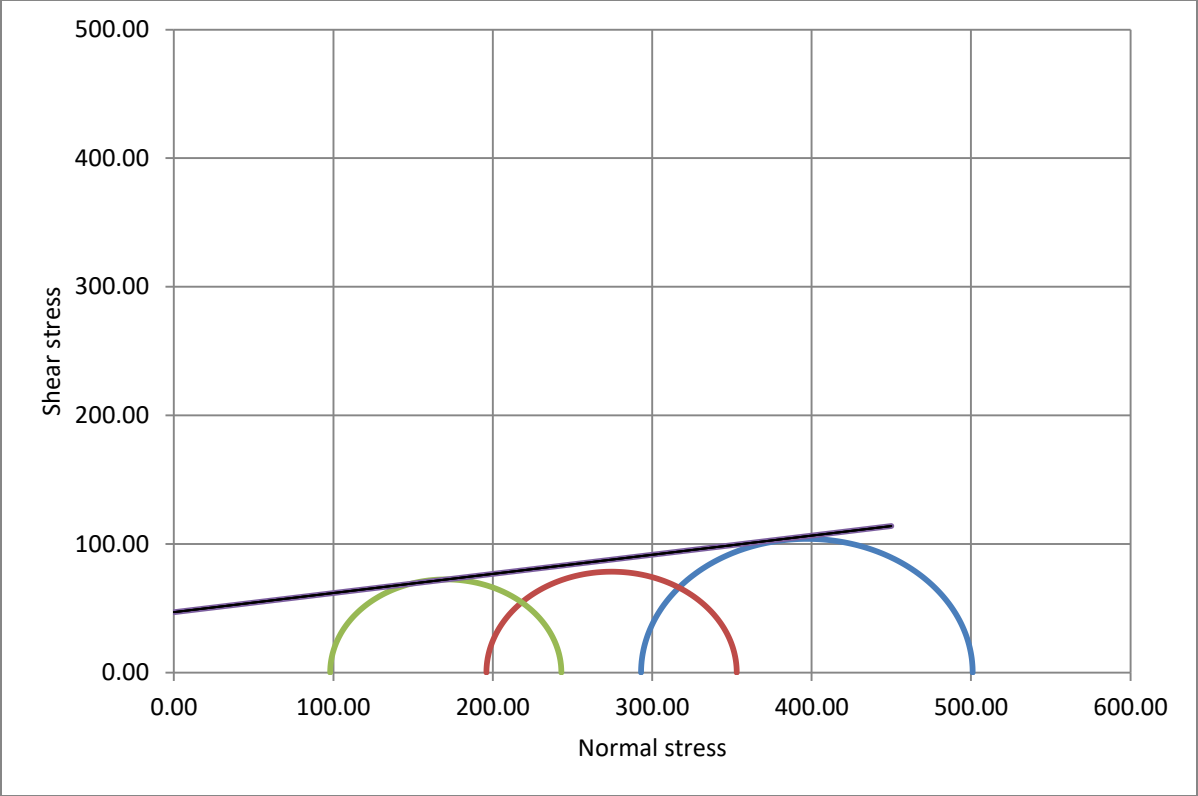
240	2.4	300	91	231.14	12.3787	18.6724
280	2.8	350	96	243.84	12.4425	19.5973
320	3.2	400	102	259.08	12.5076	20.7138
360	3.6	450	104	264.16	12.5731	21.0099
400	4.0	500	103.5	262.89	12.6395	20.7991

SAMPLE 1

DIVISION	CHANGE IN LENGTH	AXIAL STRAIN	DIVISION(PR OVING RING READING)	APPLIED LOAD *PRC(2.54)	AREA	DEVIATOR STRESS
0	0	0	0	0	12.0073	0
10	0.1	12.5	2	5.08	12.0223	0.4225
20	0.2	25	2.4	6.1	12.0374	0.5068
30	0.3	37.5	4	10.16	12.0525	0.8430
40	0.4	50	5	12.7	12.0676	1.0524
50	0.5	62.5	9	22.86	12.0828	1.8919
60	0.6	75	13	33.02	12.0980	2.7294
70	0.7	87.5	15	38.1	12.1133	3..1453
80	0.8	100	17	43.18	12.1236	3.5616
90	0.9	112.5	19	48.26	12.1439	3.9740
100	1.0	125	23	58.42	12.1543	4.8056
120	1.2	150	29	73.66	12.1906	6.0424
140	1.4	175	34	86.36	12.2212	7.0664
160	1.6	200	39	99.06	12.2524	8.0849
180	1.8	225	47	119.38	12.2836	9.7186

200	2.0	250	55	139.7	12.3153	11.3436
240	2.4	300	61	154.94	12.3787	12.5167
280	2.8	350	70	177.8	12.4425	14.2897
320	3.2	400	78	198.12	12.5076	15.8400
360	3.6	450	85	215.9	12.5731	17.1716
400	4.0	500	91	231.14	12.6395	18.2871
440	4.4	550	98	248.92	12.7061	19.5906
480	4.8	600	103	261.62	12.7737	20.4811
520	5.2	650	100.5	255.27	12.8430	19.8762





FLYASH 15% ESP 3%**SAMPLE 3**

DIVISION	CHANGE IN LENGTH	AXIAL STRAIN	DIVISION(PR OVING RING READING)	APPLIED LOAD *PRC(2.54)	AREA	DEVIATOR STRESS
0	0	0	0	0	12.0073	0
10	0.1	12.5	2	5.08	12.0223	0.4225
20	0.2	25	4	10.16	12.0374	0.8440
30	0.3	37.5	7	17.78	12.0525	1.4752
40	0.4	50	9	22.86	12.0676	1.8943
50	0.5	62.5	11	27.94	12.0828	2.3124
60	0.6	75	15	38.1	12.0980	3.1493
70	0.7	87.5	21	53.34	12.1133	4.4034
80	0.8	100	27	68.58	12.1236	5.6624
90	0.9	112.5	35	88.9	12.1439	7.3228
100	1.0	125	41	104.14	12.1543	8.5755
120	1.2	150	49	124.46	12.1906	10.2098
140	1.4	175	58	147.32	12.2212	12.0847
160	1.6	200	65	165.1	12.2524	13.5011
180	1.8	225	71	180.34	12.2836	14.7187
200	2.0	250	80	203.2	12.3153	16.5424
240	2.4	300	87	220.98	12.3787	17.8516
280	2.8	350	95	241.3	12.4425	19.3932
320	3.2	400	102	259.08	12.5076	20.7138
360	3.6	450	109	276.86	12.5731	22.0200

400	4.0	500	115	292.1	12.6395	23.1101
440	4.4	550	112	284.48	12.7061	22.3892

SAMPLE 2

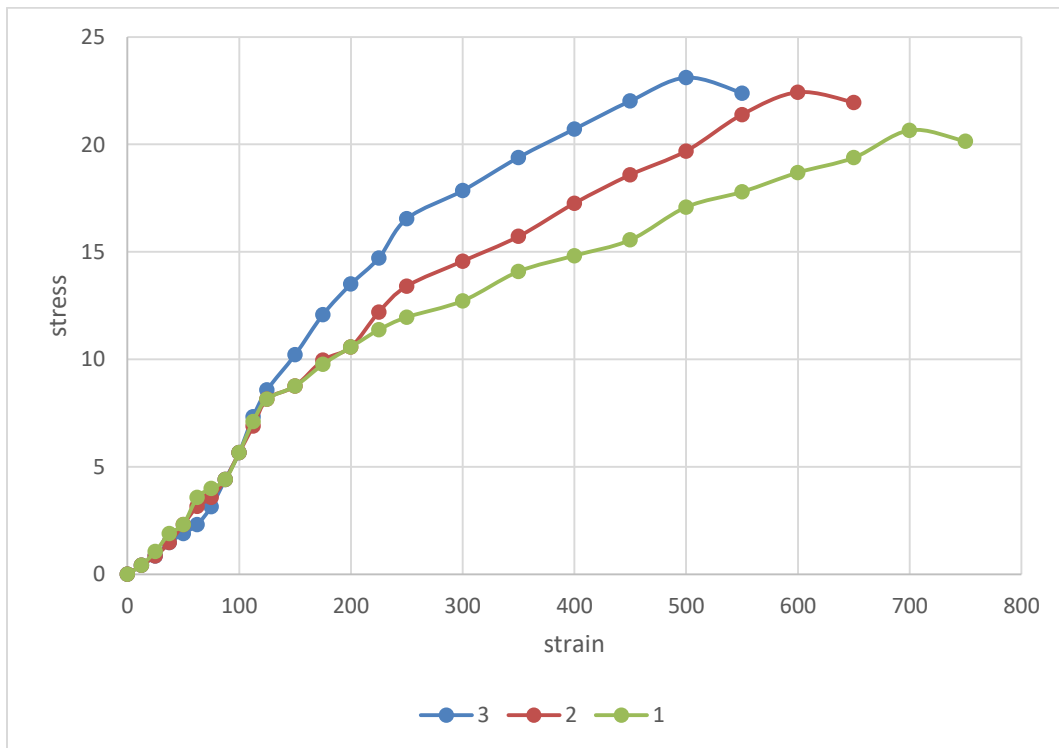
DIVISION	CHANGE IN LENGTH	AXIAL STRAIN	DIVISION(PR OVING RING READING)	APPLIED LOAD *PRC(2.54)	AREA	DEVIATOR STRESS
0	0	0	0	0	12.0073	0
10	0.1	12.5	2	5.08	12.0223	0.4225
20	0.2	25	4	10.16	12.0374	0.8440
30	0.3	37.5	11	17.78	12.0525	1.4752
40	0.4	50	13	27.94	12.0676	2.3153
50	0.5	62.5	15	38.1	12.0828	3.1532
60	0.6	75	17	43.18	12.0980	3.5692
70	0.7	87.5	21	53.34	12.1133	4.4034
80	0.8	100	27	68.58	12.1236	5.6567
90	0.9	112.5	33	83.82	12.1439	6.9022
100	1.0	125	39	99.06	12.1543	8.1502
120	1.2	150	42	106.68	12.1906	8.7510
140	1.4	175	48	121.92	12.2212	9.9565
160	1.6	200	51	129.54	12.2524	10.5726
180	1.8	225	59	149.86	12.2836	12.2000
200	2.0	250	65	165.1	12.3153	13.4061
240	2.4	300	71	180.34	12.3787	14.5686
280	2.8	350	77	195.58	12.4425	15.7187

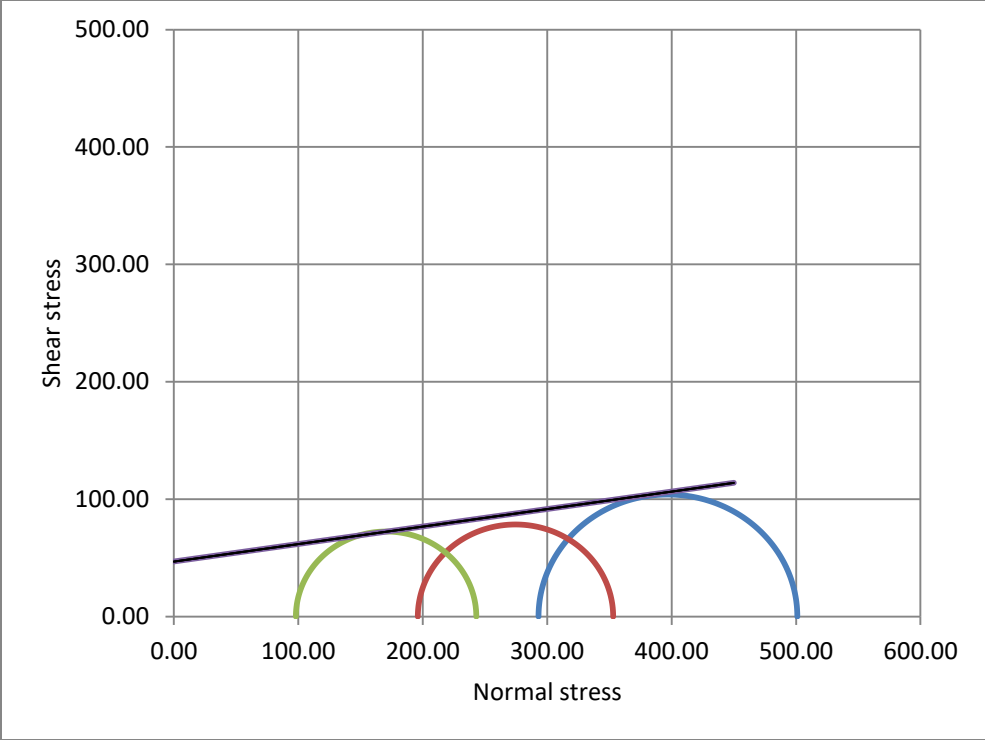
320	3.2	400	85	215.9	12.5076	17.2615
360	3.6	450	92	233.68	12.5731	18.5857
400	4.0	500	98	248.92	12.6395	19.6938
440	4.4	550	107	271.78	12.7061	21.3897
480	4.8	600	112.8	286.51	12.7737	22.4297
520	5.2	650	111	281.94	12.8430	21.9528

SAMPLE 1

DIVISION	CHANGE IN LENGTH	AXIAL STRAIN	DIVISION(PR OVING RING READING)	APPLIED LOAD *PRC(2.54)	AREA	DEVIATOR STRESS
0	0	0	0	0	12.0073	0
10	0.1	12.5	2	5.08	12.0223	0.4225
20	0.2	25	5	12.7	12.0374	1.0550
30	0.3	37.5	9	22.80	12.0525	1.8917
40	0.4	50	11	27.94	12.0676	2.3153
50	0.5	62.5	15	43.18	12.0828	3.5737
60	0.6	75	19	48.26	12.0980	3.9891
70	0.7	87.5	21	53.34	12.1133	4.4034
80	0.8	100	27	68.58	12.1236	5.6567
90	0.9	112.5	34	86.36	12.1439	7.1114
100	1.0	125	39	99.06	12.1543	8.1502
120	1.2	150	42	106.68	12.1906	8.7510
140	1.4	175	47	119.38	12.2212	9.7683
160	1.6	200	51	129.54	12.2524	10.5726

180	1.8	225	55	139.7	12.2836	11.3729
200	2.0	250	58	147.32	12.3153	11.9625
240	2.4	300	62	157.48	12.3787	12.7219
280	2.8	350	69	175.26	12.4425	14.0856
320	3.2	400	73	185.42	12.5076	14.8246
360	3.6	450	77	195.58	12.5731	15.5554
400	4.0	500	85	215.9	12.6395	17.0814
440	4.4	550	89	226.06	12.7061	17.7915
480	4.8	600	94	238.76	12.7737	18.6915
520	5.2	650	98	248.92	12.8430	19.3818
560	5.6	700	105	266.7	12.9111	20.6566
600	6.0	750	103	261.62	12.9801	20.1555





FLYASH 18% ESP 0%**SAMPLE 3**

DIVISION	CHANGE IN LENGTH	AXIAL STRAIN	DIVISION(PR OVING RING READING)	APPLIED LOAD *PRC(2.54)	AREA	DEVIATOR STRESS
0	0	0	0	0	12.0073	0
10	0.1	12.5	5	12.7	12.0223	1.0564
20	0.2	25	9	22.86	12.0374	1.8991
30	0.3	37.5	15	38.1	12.0525	3.1612
40	0.4	50	21	53.34	12.0676	4.4201
50	0.5	62.5	26	66.04	12.0828	5.4656
60	0.6	75	33	83.82	12.0980	6.9284
70	0.7	87.5	38	96.52	12.1133	7.9681
80	0.8	100	44	111.76	12.1236	9.2184
90	0.9	112.5	51	129.54	12.1439	10.6671
100	1.0	125	57	144.78	12.1543	11.9118
120	1.2	150	63	160.02	12.1906	13.1265
140	1.4	175	68	172.72	12.2212	14.1328
160	1.6	200	74	187.96	12.2524	15.3407
180	1.8	225	77	195.58	12.2836	15.9220
200	2.0	250	85	215.8	12.3153	17.5229
240	2.4	300	91	231.14	12.3787	18.6724
280	2.8	350	98	248.92	12.4425	20.0056
320	3.2	400	105	266.7	12.5076	21.3230
360	3.6	450	116	294.64	12.5731	23.4342

400	4.0	500	122	309.88	12.6395	24.5168
440	4.4	550	118	299.72	12.7061	23.5887

SAMPLE 2

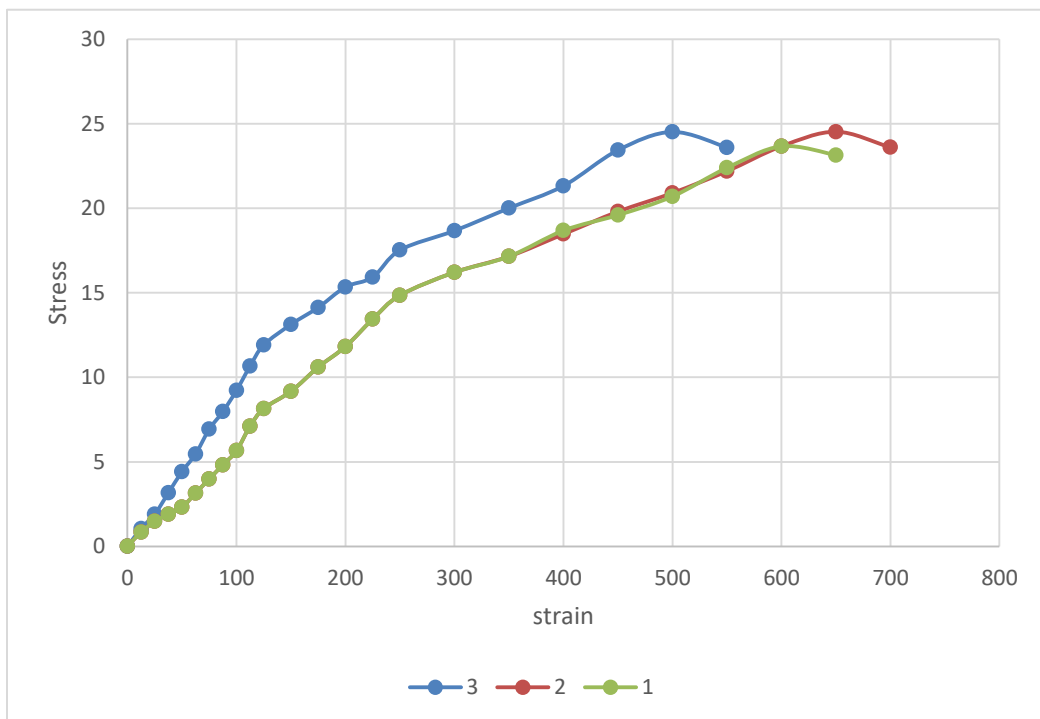
DIVISION	CHANGE IN LENGTH	AXIAL STRAIN	DIVISION(PR OVING RING READING)	APPLIED LOAD *PRC(2.54)	AREA	DEVIATOR STRESS
0	0	0	0	0	12.0073	0
10	0.1	12.5	4	10.16	12.0223	0.8451
20	0.2	25	7	17.78	12.0374	1.4771
30	0.3	37.5	9	22.86	12.0525	1.9010
40	0.4	50	11	27.94	12.0676	2.3153
50	0.5	62.5	15	38.1	12.0828	3.1532
60	0.6	75	19	48.26	12.0980	3.9891
70	0.7	87.5	23	58.42	12.1133	4.8228
80	0.8	100	27	68.58	12.1236	5.6567
90	0.9	112.5	34	86.36	12.1439	7.1114
100	1.0	125	39	99.06	12.1543	8.1502
120	1.2	150	44	111.76	12.1906	9.1677
140	1.4	175	51	129.54	12.2212	10.5996
160	1.6	200	57	144.78	12.2524	11.8165
180	1.8	225	65	165.1	12.2836	13.4407
200	2.0	250	72	182.88	12.3153	14.8498
240	2.4	300	79	200.66	12.3787	16.2101
280	2.8	350	84	213.36	12.4425	17.1477

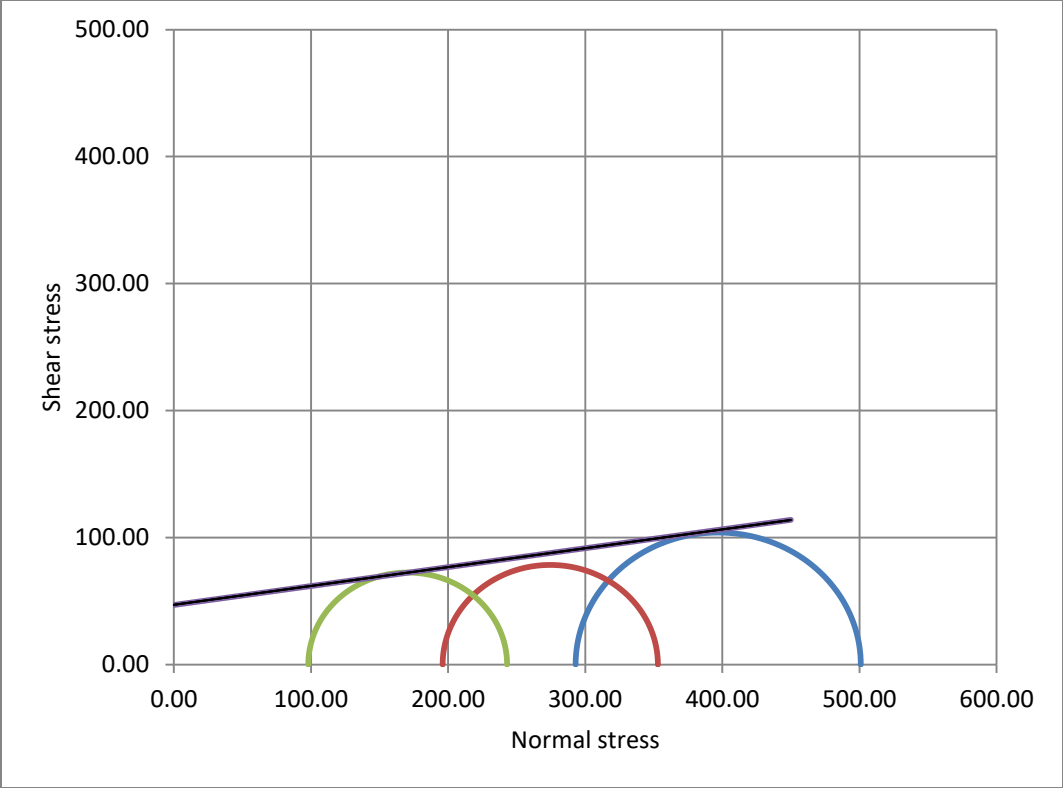
320	3.2	400	91	231.14	12.5076	18.4800
360	3.6	450	98	248.92	12.5731	19.7978
400	4.0	500	104	261.16	12.6395	20.8996
440	4.4	550	111	281.94	12.7061	22.1893
480	4.8	600	119	302.26	12.7737	23.6627
520	5.2	650	124	314.96	12.8430	24.5239
560	5.6	700	120	304.8	12.9111	23.6076

SAMPLE 1

DIVISION	CHANGE IN LENGTH	AXIAL STRAIN	DIVISION(PR OVING RING READING)	APPLIED LOAD *PRC(2.54)	AREA	DEVIATOR STRESS
0	0	0	0	0	12.0073	0
10	0.1	12.5	4	10.16	12.0223	0.8451
20	0.2	25	7	17.78	12.0374	1.4771
30	0.3	37.5	9	22.86	12.0525	1.9010
40	0.4	50	11	27.94	12.0676	2.3153
50	0.5	62.5	15	38.1	12.0828	3.1532
60	0.6	75	19	48.26	12.0980	3.9891
70	0.7	87.5	23	58.42	12.1133	4.8228
80	0.8	100	27	68.58	12.1236	5.6567
90	0.9	112.5	34	86.36	12.1439	7.1114
100	1.0	125	39	99.06	12.1543	8.1502
120	1.2	150	44	111.76	12.1906	9.1677
140	1.4	175	51	129.54	12.2212	10.5996

160	1.6	200	57	144.78	12.2524	11.8165
180	1.8	225	65	165.1	12.2836	13.4407
200	2.0	250	72	182.88	12.3153	14.8498
240	2.4	300	79	200.66	12.3787	16.2101
280	2.8	350	84	213.36	12.4425	17.1477
320	3.2	400	92	233.68	12.5076	18.6830
360	3.6	450	97	246.38	12.5731	19.5958
400	4.0	500	103	261.62	12.6395	20.6986
440	4.4	550	112	284.48	12.7061	22.3892
480	4.8	600	119	302.26	12.7737	23.6627
520	5.2	650	117	297.180	12.8430	23.1395

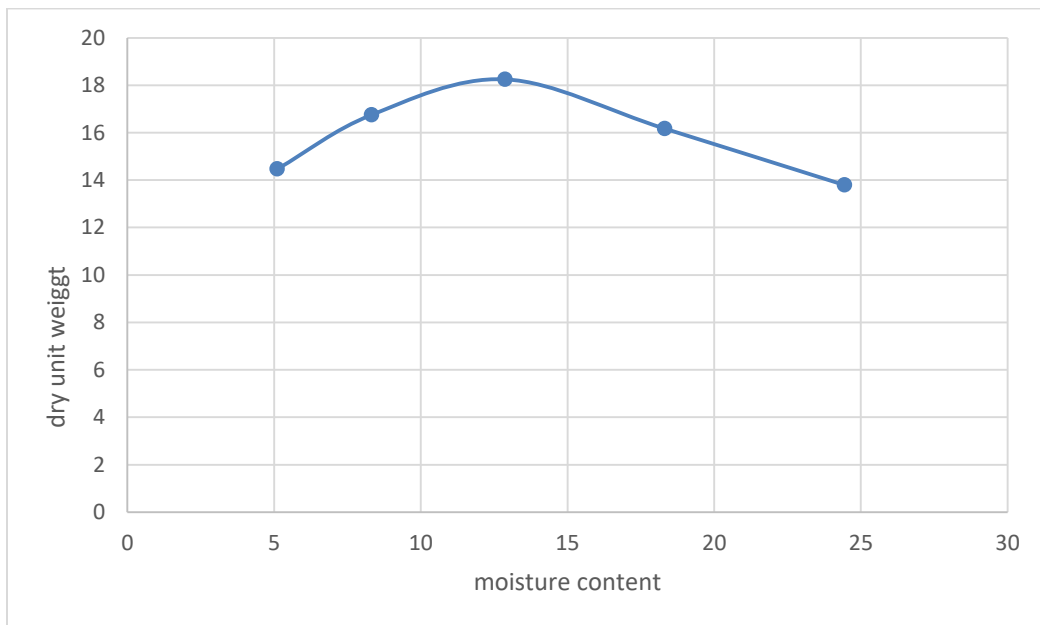




APPENDIX 2
CLAY EE2
COMPACTION

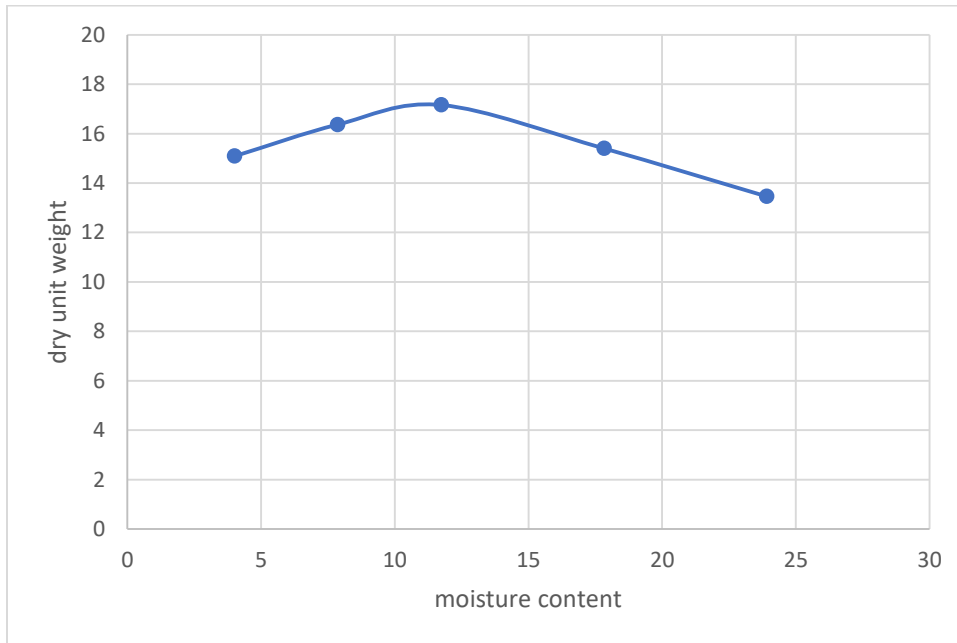
SOIL – 100%

%	VOLUME OF MOULD (M³)	MASS OF MOULD (KG)	MOULD + SAMPLE (KG)	MOISTURE CONTENT (%)	BULK DENSITY	DRY DENSITY
4	0.001	4.2	5.75	5.11	1550	14.47
8	0.001	4.2	6.05	8.30	1850	16.75
12	0.001	4.2	6.25	12.87	2100	18.25
16	0.001	4.2	6.15	18.32	1950	16.17
20	0.001	4.2	5.95	24.45	1750	13.79



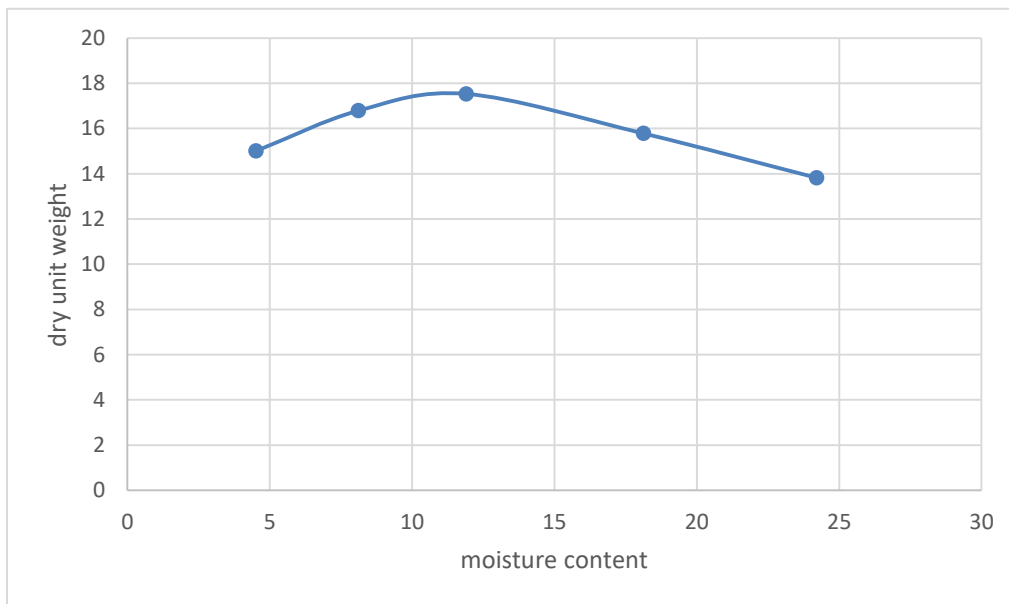
FLYASH -0% ESP -18%

%	VOLUME OF MOULD (M³)	MASS OF MOULD (KG)	MOULD + SAMPLE (KG)	MOISTURE CONTENT (%)	BULK DENSITY	DRY DENSITY
4	0.001	4.2	5.80	4.01	1600	15.09
8	0.001	4.2	6.0	7.87	1800	16.37
12	0.001	4.2	6.15	1174	1950	17.16
16	0.001	4.2	6.0	17.83	1850	15.40
20	0.001	4.2	5.90	23.91	1700	13.46



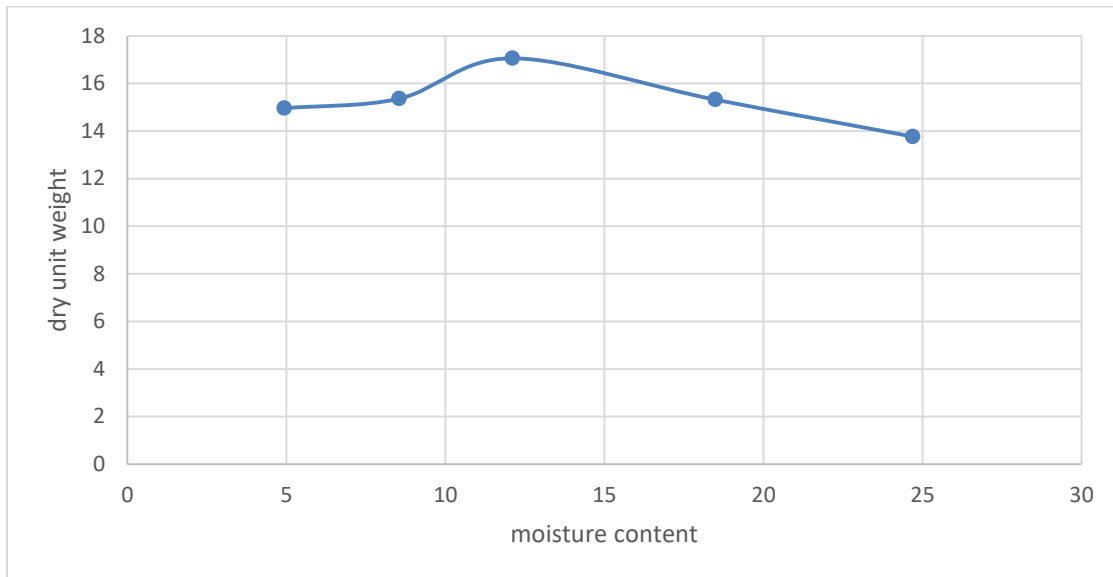
FLYASH – 3% ESP -15%

%	VOLUME OF MOULD (M³)	MASS OF MOULD (KG)	MOULD + SAMPLE (KG)	MOISTURE CONTENT (%)	BULK DENSITY	DRY DENSITY
4	0.001	4.2	5.80	4.52	1600	15.01
8	0.001	4.2	6.0	8.12	1850	16.79
12	0.001	4.2	6.20	11.91	2000	17.53
16	0.001	4.2	6.10	18.13	1900	15.78
20	0.001	4.2	5.95	24.21	1750	13.82



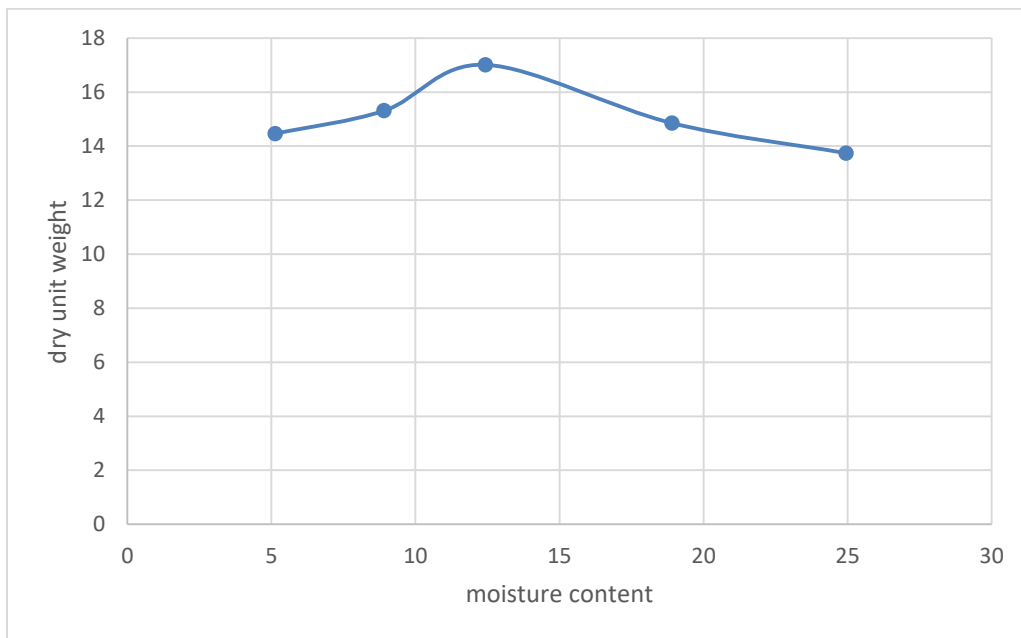
FLYASH -6% ESP -12%

%	VOLUME OF MOULD (M³)	MASS OF MOULD (KG)	MOULD + SAMPLE (KG)	MOISTURE CONTENT (%)	BULK DENSITY	DRY DENSITY
4	0.001	4.2	5.80	4.93	1600	14.96
8	0.001	4.2	5.90	8.54	1700	15.36
12	0.001	4.2	6.25	11.71	1950	18.00
16	0.001	4.2	6.05	18.49	1850	15.32
20	0.001	4.2	5.95	24.69	1750	13.77



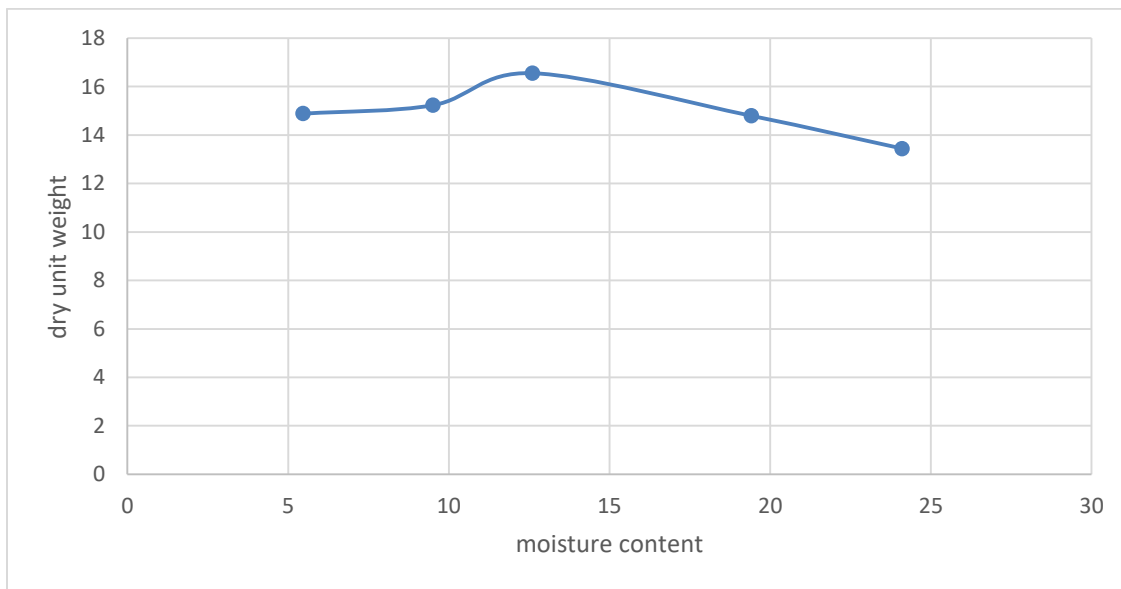
FLYASH -9% ESP -9%

%	VOLUME OF MOULD (M³)	MASS OF MOULD (KG)	MASS OF MOULD + SAMPLE (KG)	MOISTURE CONTENT (%)	BULK DENSITY	DRY DENSITY
4	0.001	4.2	5.75	5.13	1550	14.46
8	0.001	4.2	5.90	8.91	1700	15.31
12	0.001	4.2	6.15	11.43	2050	18.05
16	0.001	4.2	6.00	18.91	1800	14.85
20	0.001	4.2	5.95	23.95	1750	13.74



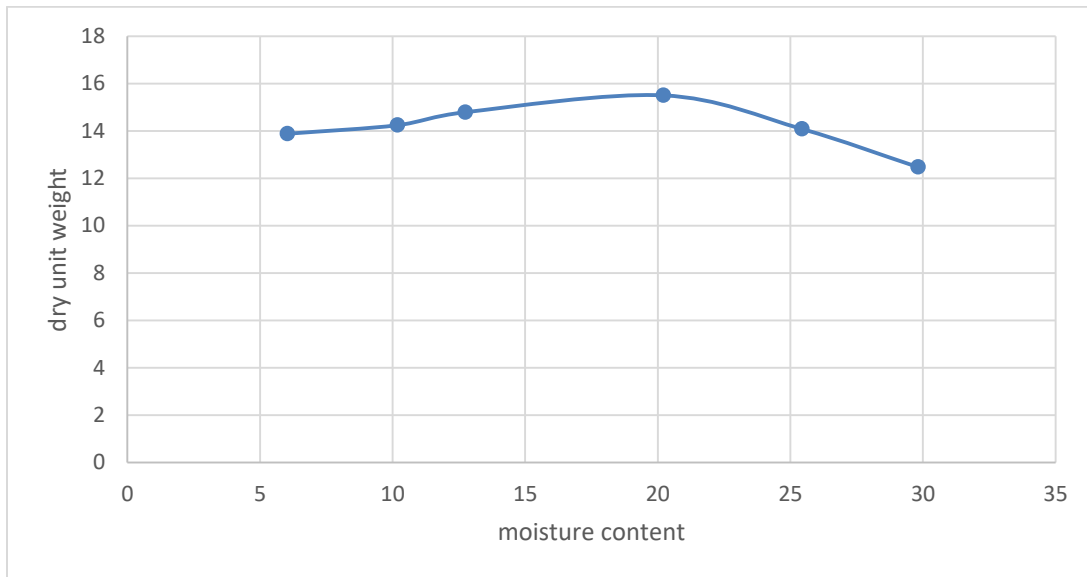
FLYASH -12% ESP -6%

%	VOLUME OF MOULD (M³)	MASS OF MOULD (KG)	MASS OF MOULD + SAMPLE (KG)	MOISTURE CONTENT (%)	BULK DENSITY	DRY DENSITY
4	0.001	4.2	5.80	5.47	1600	14.88
8	0.001	4.2	5.90	9.51	1700	15.23
12	0.001	4.2	6.20	11.61	2100	18.49
16	0.001	4.2	6.00	17.42	1800	15.79
20	0.001	4.2	5.90	24.11	1700	13.44



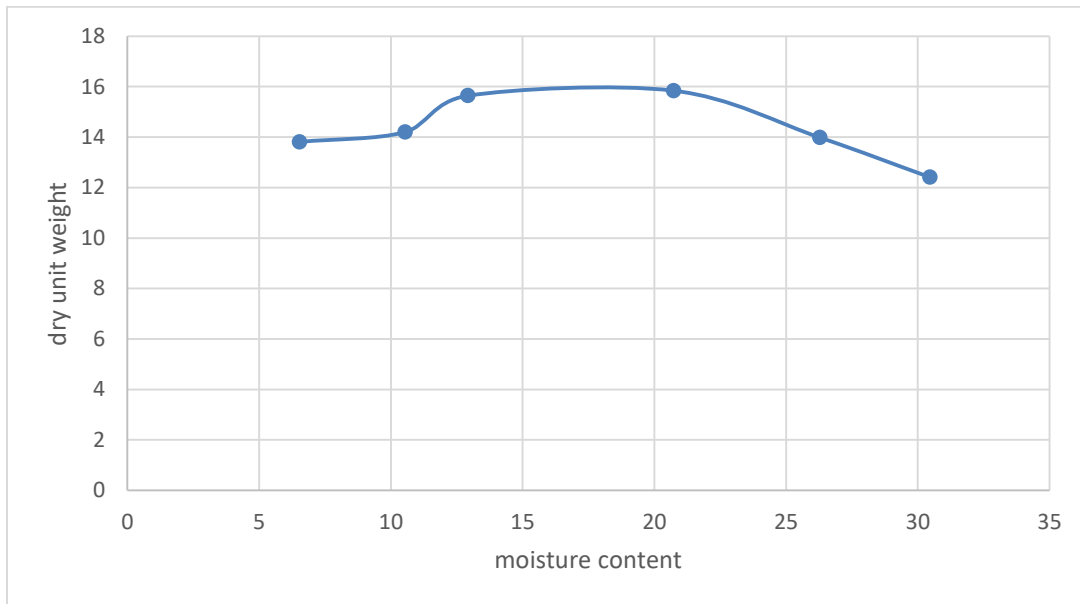
FLYASH -15% ESP -3%

%	VOLUME OF MOULD (M³)	MASS OF MOULD (KG)	MASS OF MOULD + SAMPLE (KG)	MOISTURE CONTENT (%)	BULK DENSITY	DRY DENSITY
4	0.001	4.2	5.70	6.04	1500	13.88
8	0.001	4.2	5.80	10.19	1600	14.24
12	0.001	4.2	5.90	12.75	1700	14.79
16	0.001	4.2	6.10	18.22	1900	18.67
20	0.001	4.2	6.00	25.44	1800	14.08
24	0.001	4.2	5.85	29.82	1650	12.47



FLYASH -18% ESP -0%

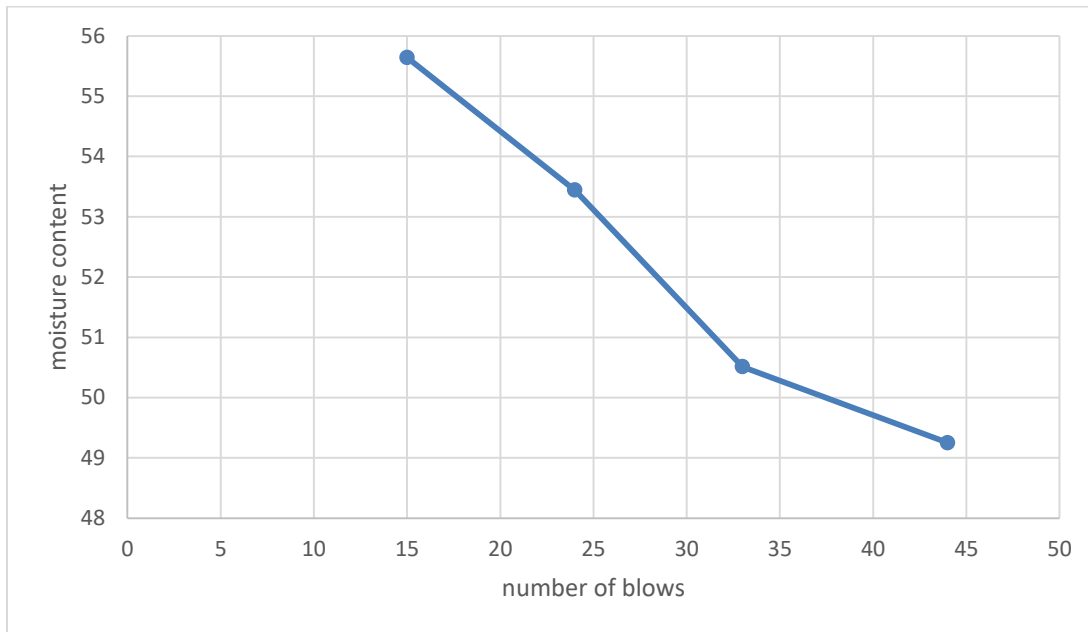
%	VOLUME OF MOULD (M³)	MASS OF MOULD (KG)	MASS OF MOULD + SAMPLE (KG)	MOISTURE CONTENT (%)	BULK DENSITY	DRY DENSITY
4	0.001	4.2	5.70	6.53	1500	13.81
8	0.001	4.2	5.80	10.54	1600	14.20
12	0.001	4.2	6.00	12.92	1800	15.64
16	0.001	4.2	6.15	17.22	1950	18.83
20	0.001	4.2	6.00	29.29	1800	15.98
24	0.001	4.2	5.85	30.46	1650	12.41



ATTERBERG LIMIT (LIQUID LIMIT)

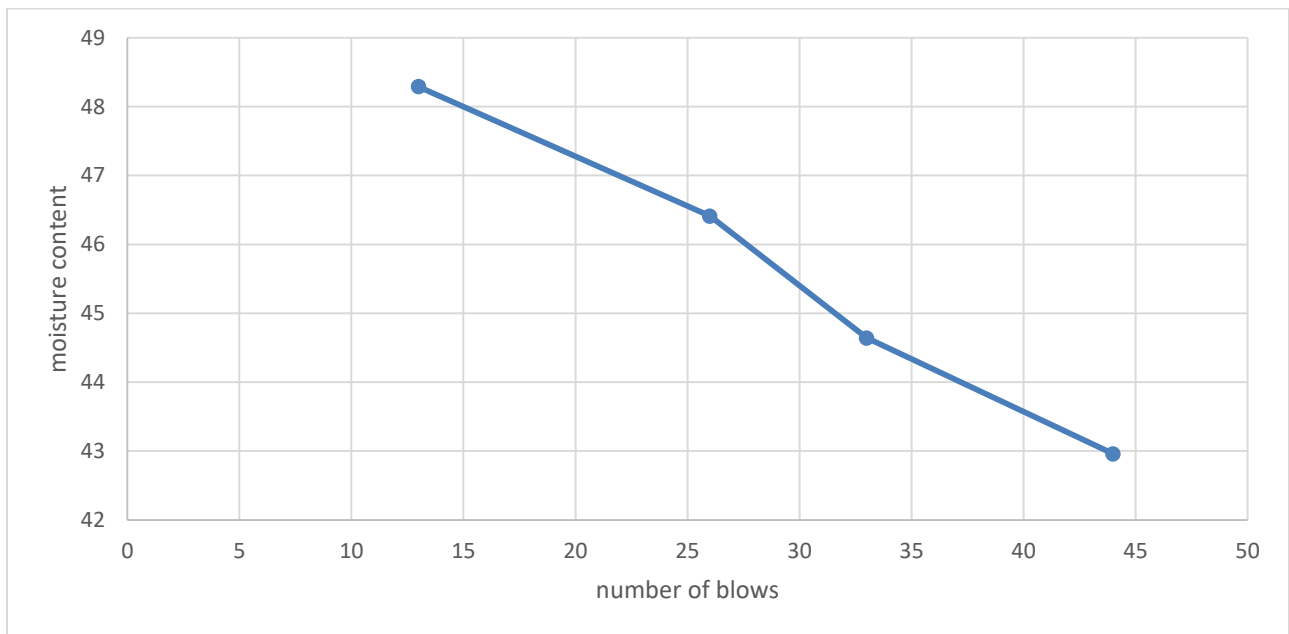
SOIL 100%

WT OF PAN(G)	WT OF PAN+WET SOIL(G)	WT OF PAN + DRY SOIL(G)	WT OF WET SOIL(G)	WT OF DRY SOIL(G)	MOISTURE CONTENT (%)	NUMBER OF BLOWS
16.72	27.49	23.64	10.77	6.92	55.64	15
15.98	24.79	21.09	7.81	5.09	53.44	24
15.03	23.96	20.93	8.88	5.9	50.51	33
14.14	25.16	21.51	11.00	7.37	49.25	44



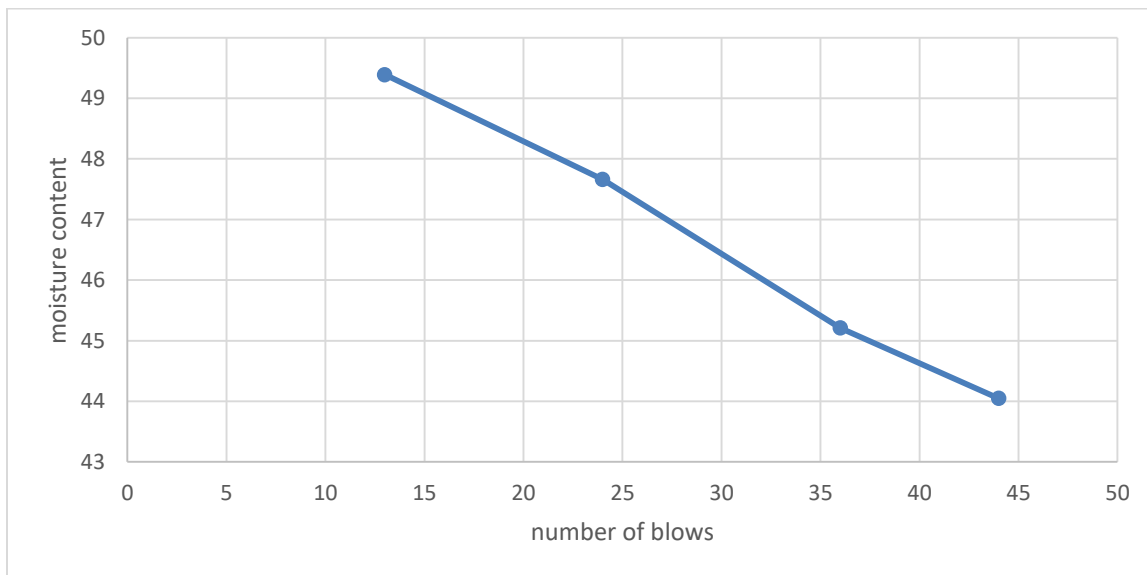
FLYASH 0% ESP 18%

WT OF PAN(G)	WT OF PAN+WET SOIL(G)	WT OF PAN + DRY SOIL(G)	WT OF WET SOIL(G)	WT OF DRY SOIL(G)	MOISTURE CONTENT (%)	NUMBER OF BLOWS
13.68	20.22	18.09	6.54	4.41	48.29	13
16.79	23.21	21.16	6.42	4.37	46.41	26
14.94	20.99	19.33	6.35	4.39	44.64	33
13.76	21.08	18.88	7.32	5.12	42.96	44



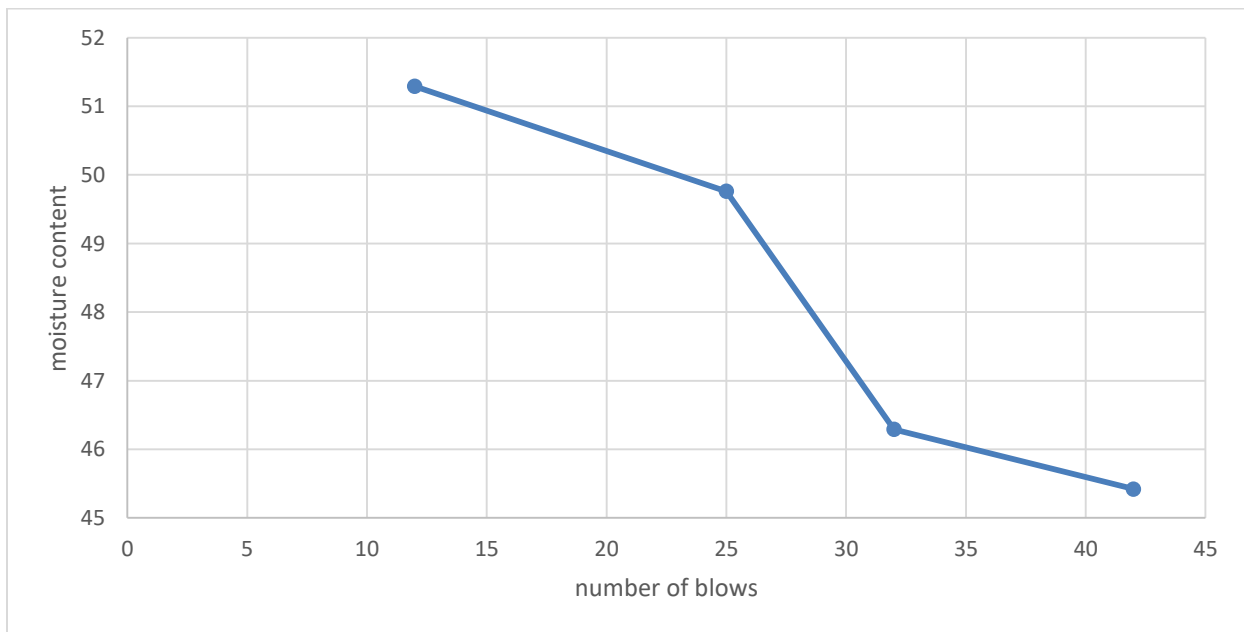
FLYASH 3% ESP 15%

WT OF PAN(G)	WT OF PAN+WET SOIL(G)	WT OF PAN + DRY SOIL(G)	WT OF WET SOIL(G)	WT OF DRY SOIL(G)	MOISTURE CONTENT (%)	NUMBER OF BLOWS
14.80	22.15	19.72	7.35	4.92	49.39	13
17.63	26.18	23.42	8.55	5.79	47.66	24
16.70	23.83	21.61	7.13	4.11	45.21	36
15.53	22.79	20.57	7.26	5.04	44.05	44



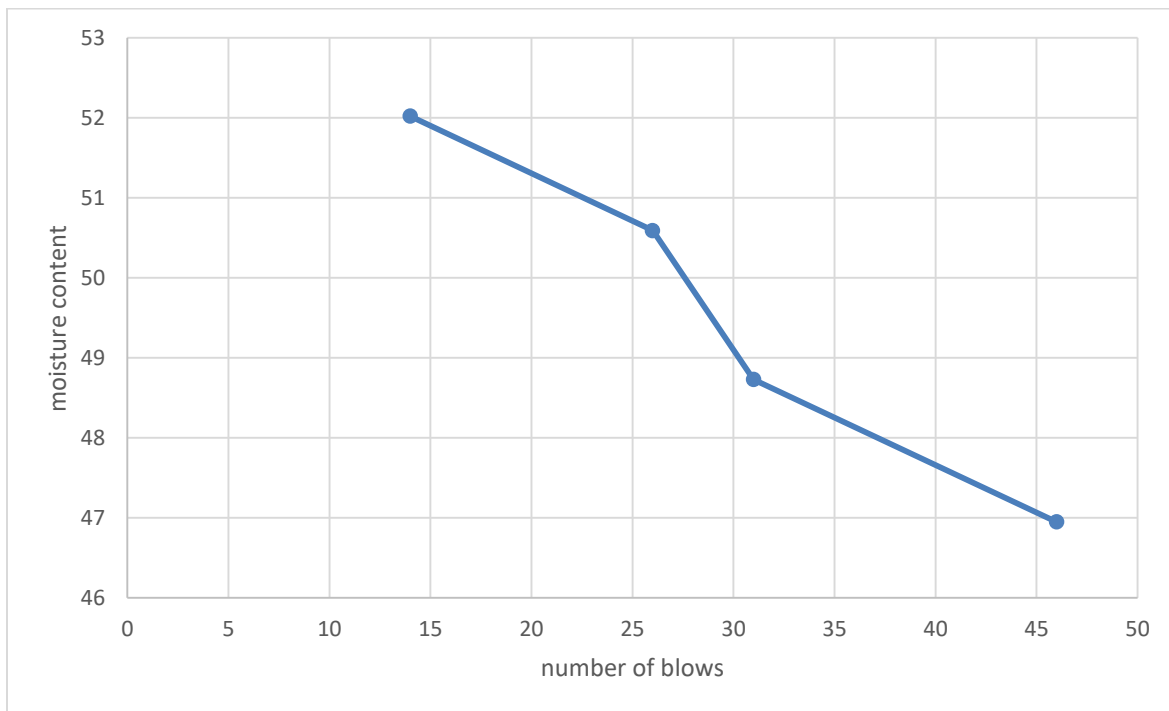
FLYASH 6% ESP 12%

WT OF PAN(G)	WT OF PAN+WET SOIL(G)	WT OF PAN + DRY SOIL(G)	WT OF WET SOIL(G)	WT OF DRY SOIL(G)	MOISTURE CONTENT (%)	NUMBER OF BLOWS
15.09	23.82	20.86	8.73	5.77	51.29	12
15.61	25.12	21.96	9.51	6.35	49.76	25
16.37	26.83	23.52	10.46	7.15	46.29	32
15.65	23.43	21.00	7.78	5.35	45.42	42



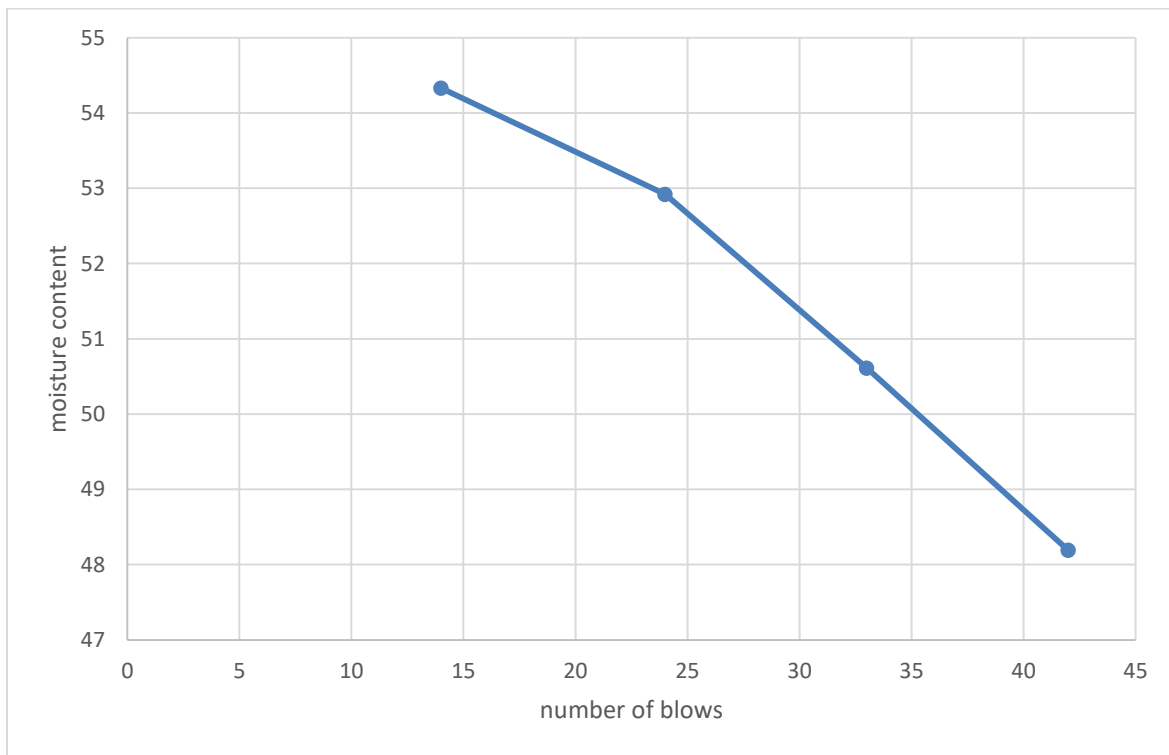
FLYASH 9% ESP 9%

WT OF PAN(G)	WT OF PAN+WET SOIL(G)	WT OF PAN + DRY SOIL(G)	WT OF WET SOIL(G)	WT OF DRY SOIL(G)	MOISTURE CONTENT (%)	NUMBER OF BLOWS
4.80	25.35	21.74	10.55	6.94	52.02	14
6.70	25.54	22.57	8.84	5.87	50.59	26
17.63	27.61	24.34	9.98	6.71	48.73	31
15.09	26.04	22.54	10.95	7.45	46.95	46



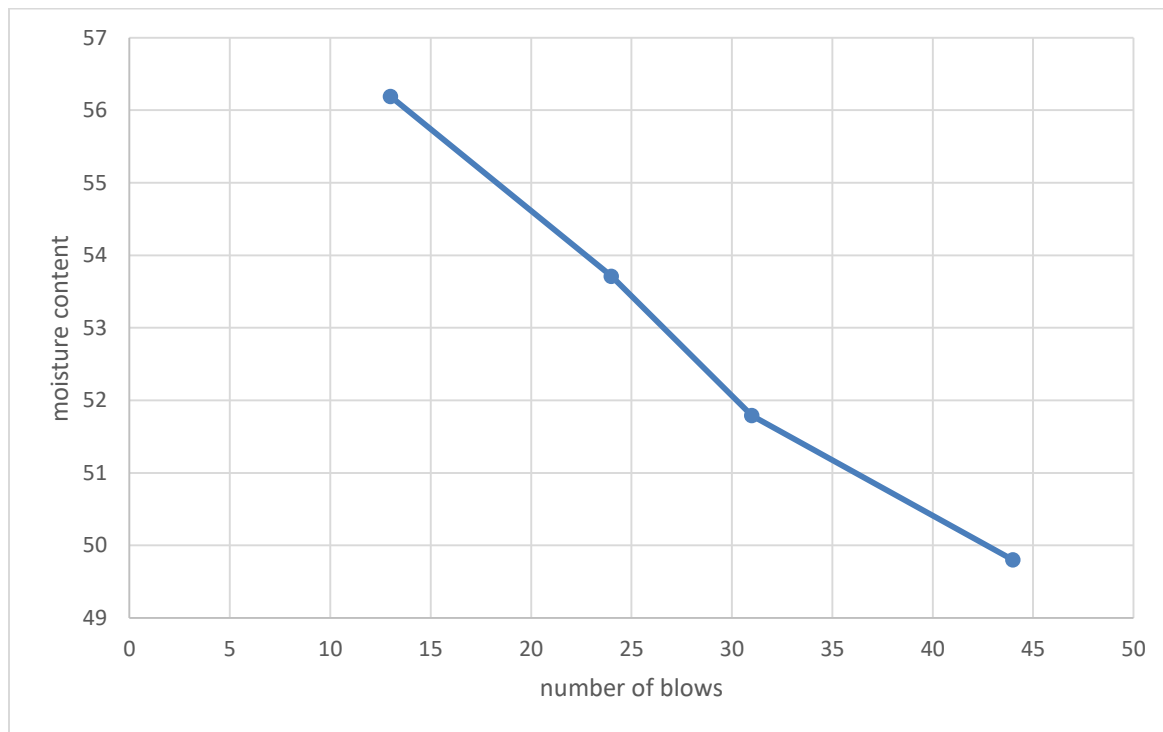
FLYASH 12% ESP 6%

WT OF PAN(G)	WT OF PAN+WET SOIL(G)	WT OF PAN + DRY SOIL(G)	WT OF WET SOIL(G)	WT OF DRY SOIL(G)	MOISTURE CONTENT (%)	NUMBER OF BLOWS
15.53	24.08	21.07	8.55	5.54	54.33	14
16.52	28.47	24.3	11.95	7.78	52.92	24
14.62	24.44	21.14	9.82	6.52	50.61	33
16.87	28.34	24.61	11.47	7.74	48.19	42



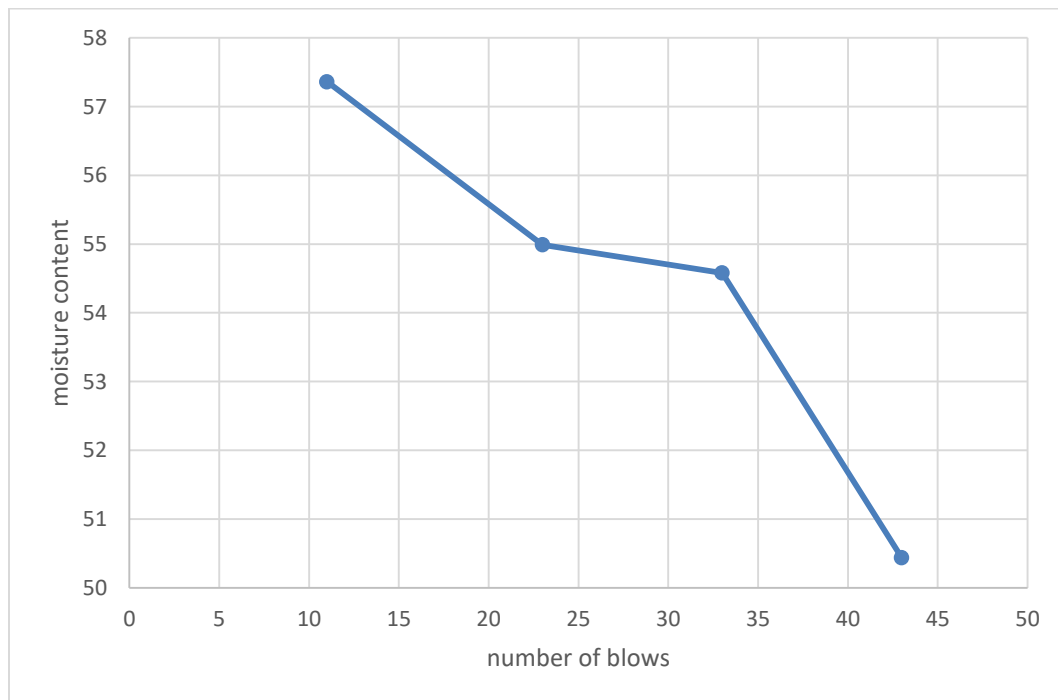
FLYASH 15% ESP 3%

WT OF PAN(G)	WT OF PAN+WET SOIL(G)	WT OF PAN + DRY SOIL(G)	WT OF WET SOIL(G)	WT OF DRY SOIL(G)	MOISTURE CONTENT (%)	NUMBER OF BLOWS
17.05	30.67	25.77	13.62	8.72	56.19	13
16.74	28.96	24.69	12.22	7.95	53.71	24
13.76	24.31	20.71	10.55	6.95	51.79	31
14.94	26.55	22.69	11.61	7.75	49.80	45



FLYASH 18% ESP 0%

WT OF PAN(G)	WT OF PAN+WET SOIL(G)	WT OF PAN + DRY SOIL(G)	WT OF WET SOIL(G)	WT OF DRY SOIL(G)	MOISTURE CONTENT (%)	NUMBER OF BLOWS
16.10	28.39	23.91	12.29	7.81	57.36	11
14.06	30.21	24.48	16.15	10.42	54.99	23
15.92	30.95	25.77	15.03	9.85	52.58	33
15.09	30.54	25.36	15.45	10.27	50.44	43



TRIAXIAL

SOIL 100%

SAMPLE 3

DIVISION	CHANGE IN LENGTH	AXIAL STRAIN	DIVISION(PRO VING RING READING)	APPLIED LOAD *PRC(2.54)	AREA	DEVIATOR STRESS
0	0	0	0	0	12.0073	0
10	0.1	12.5	0.8	2.032	12.0223	0.1690
20	0.2	25	2.2	5.588	12.0374	0.4642
30	0.3	37.5	2.2	5.588	12.0525	0.4642
40	0.4	50	2.3	5.842	12.0676	0.4840
50	0.5	62.5	2.6	6.604	12.0828	0.5470
60	0.6	75	4.0	10.16	12.0980	0.8400
70	0.7	87.5	4.6	11.684	12.1133	0.9560
80	0.8	100	4.8	12.192	12.1236	1.0000
90	0.9	112.5	5.2	13.208	12.1339	1.0880
100	1.0	125	5.6	14.224	12.1543	1.1700
120	1.2	150	5.8	14.73	12.1906	1.2080
140	1.4	175	6.0	15.24	12.2212	1.2470
160	1.6	200	6.9	17.526	12.2524	1.4300
180	1.8	225	14	35.56	12.2836	2.8940
200	2.0	250	18.8	47.752	12.3153	3.7750
240	2.4	300	26.25	66.675	12.3787	5.3870
280	2.8	350	31.4	79.756	12.4425	6.4100
320	3.2	400	35.6	90.424	12.5076	7.2290

360	3.6	450	39.2	99.568	12.5731	7.9190
400	4.0	500	43	109.22	12.6395	8.6410
440	4.4	550	44	111.76	12.7061	8.7958
480	4.8	600	47.2	119.888	12.7737	9.3855
520	5.2	650	50	127	12.8430	9.8887
560	5.6	700	52.5	133.35	12.9111	10.3283
600	6.0	750	54.2	137.668	12.9801	10.6628
640	6.4	800	58.3	148.082	13.0514	11.4084
680	6.8	850	61	154.98	13.1227	11.8746
720	7.2	900	62.3	158.242	13.1948	12.0586
760	7.6	950	64	162.56	13.2677	12.3200
800	8.0	1000	65.8	167.132	13.3414	12.5273
840	8.4	1050	67.2	170.688	13.4160	12.7227
880	8.8	1100	68.3	173.482	13.4914	12.8587
920	9.2	1150	68.5	173.99	13.5676	12.8239
960	9.6	1200	68	172.72	13.6447	12.6584

SAMPLE 2

DIVISION	CHANGE IN LENGTH	AXIAL STRAIN	DIVISION(PRO VING RING READING)	APPLIED LOAD *PRC(2.54)	AREA	DEVIATOR STRESS
0	0	0	0	0	12.0073	0
10	0.1	12.5	0.8	2.032	12.0223	0.1690
20	0.2	25	2.2	5.588	12.0374	0.4642
30	0.3	37.5	3	7.62	12.0525	0.6322

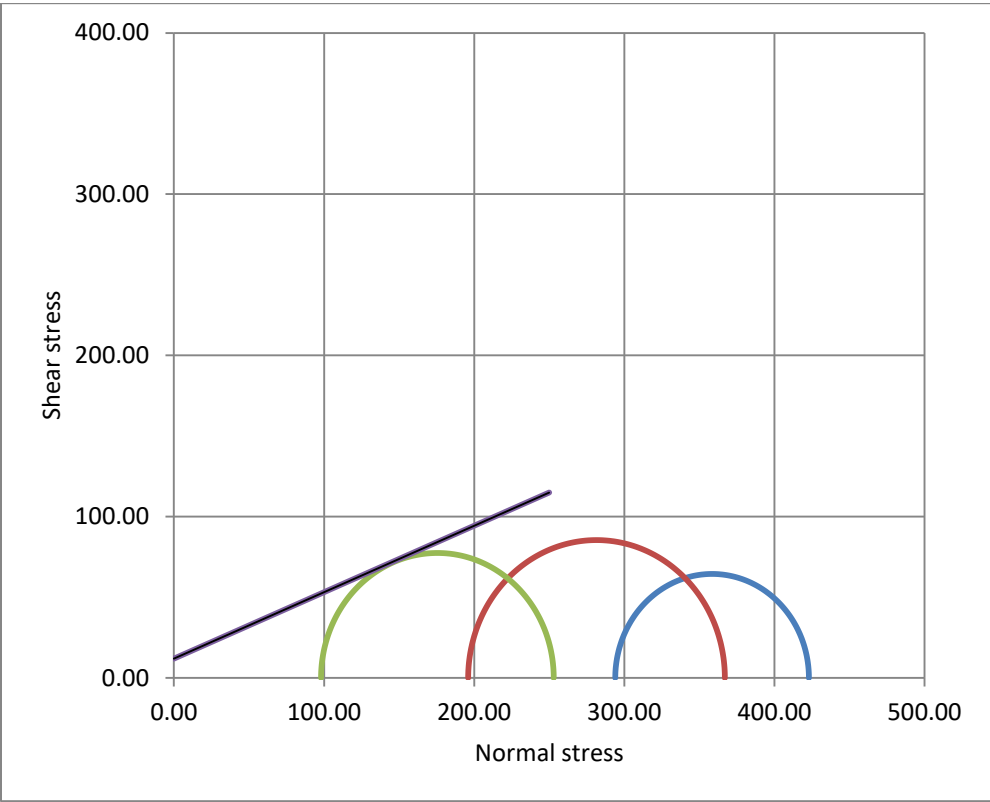
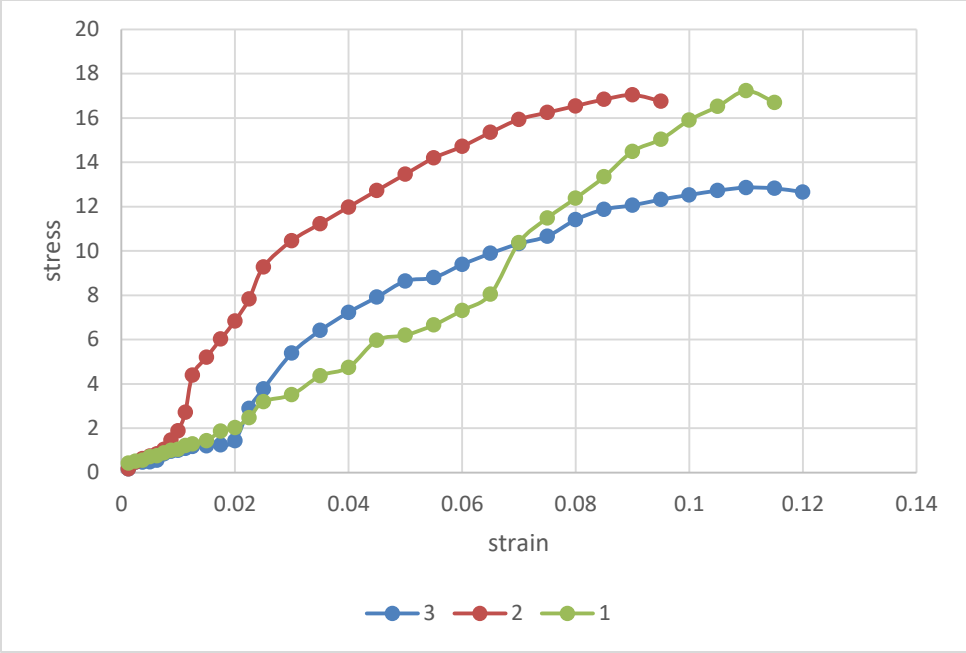
40	0.4	50	3.5	8.89	12.0676	0.7367
50	0.5	62.5	4	10.16	12.0828	0.8409
60	0.6	75	5	12.7	12.0980	1.0498
70	0.7	87.5	7	17.78	12.1133	1.4698
80	0.8	100	9	22.86	12.1236	1.8856
90	0.9	112.5	13	33.02	12.1439	2.7191
100	1.0	125	21	53.34	12.1543	4.3886
120	1.2	150	25	63.5	12.1906	5.0289
140	1.4	175	29	73.66	12.2212	6.6272
160	1.6	200	33	83.82	12.2524	6.8411
180	1.8	225	38	96.52	12.2836	7.8374
200	2.0	250	45	114.3	12.3153	9.2811
240	2.4	300	51	129.54	12.3787	10.4647
280	2.8	350	55	139.7	12.4425	11.2276
320	3.2	400	59	149.86	12.5076	11.9817
360	3.6	450	63	160.02	12.5731	12.7272
400	4.0	500	67	170.18	12.6395	13.4641
440	4.4	550	71	180.34	12.7061	14.1932
480	4.8	600	74	187.96	12.7737	14.7146
520	5.2	650	77.6	197.104	12.8430	15.3472
560	5.6	700	81	205.74	12.9111	15.9351
600	6.0	750	83	210.82	12.9801	16.2418
640	6.4	800	85	215.9	13.0514	16.5423
680	6.8	850	87	220.98	13.1227	16.8375
720	7.2	900	89	226.06	13.1948	17.0384

760 7.6 950 88 223.52 13.2677 16.7539

SAMPLE 1

DIVISION	CHANGE IN LENGTH	AXIAL STRAIN	DIVISION(PR OVING RING READING)	APPLIED LOAD *PRC(2.54)	AREA	DEVIATOR STRESS
0	0	0	0	0	12.0073	0
10	0.1	12.5	2	5.08	12.0223	04225
20	0.2	25	2.4	6.096	12.0374	05056
30	0.3	37.5	2.6	6.604	12.0525	05479
40	0.4	50	3.4	8.636	12.0676	07156
50	0.5	62.5	3.6	9.144	12.0828	07568
60	0.6	75	4.2	10.668	12.0980	08818
70	0.7	87.5	4.8	12.192	12.1133	10065
80	0.8	100	5.0	12.7	12.1236	10475
90	0.9	112.5	5.8	14.732	12.1439	12131
100	1.0	125	6.2	15.748	12.1543	12918
120	1.2	150	6.9	17.526	12.1906	14341
140	1.4	175	9	22.86	12.2212	18658
160	1.6	200	9.8	24.89	12.2524	20263
180	1.8	225	12	30.48	12.2836	24750
200	2.0	250	15.6	39.624	12.3153	32010
240	2.4	300	17.2	43.688	12.3787	35113
280	2.8	350	21.5	54.61	12.4425	43661
320	3.2	400	23.4	59.69	12.5076	47474

360	3.6	450	29.7	75.438	12.5731	59684
400	4.0	500	31.0	78.74	12.6395	61970
440	4.4	550	33.5	85.09	12.7061	6613
480	4.8	600	37	93.98	12.7737	73176
520	5.2	650	45	114.3	12.8430	80528
560	5.6	700	53	134.62	12.9111	103713
600	6.0	750	59	149.86	12.9801	114823
640	6.4	800	64	162.50	13.0514	123831
680	6.8	850	69.3	176.022	13.1227	133403
720	7.2	900	75.7	192.278	13.1948	144922
760	7.6	950	79	200.60	13.2677	150359
800	8.0	1000	84	213.36	13.3414	159034
840	8.4	1050	88	223.52	13.4160	165176
880	8.8	1100	92	233.68	13.4914	172234
920	9.2	1150	89.7	227.84	13.5676	166981



FLYASH 0% ESP 18%

SAMPLE 3

DIVISION	CHANGE IN LENGTH	AXIAL STRAIN	DIVISION(PRO VING RING READING)	APPLIED LOAD *PRC(2.54)	AREA	DEVIATOR STRESS
0	0	0	0	0	12.0073	0
10	0.1	12.5	0.8	2.032	12.0223	0.1690
20	0.2	25	2.2	5.588	12.0374	0.4646
30	0.3	37.5	2.3	5.842	12.0525	0.4847
40	0.4	50	2.6	6.604	12.0676	0.5473
50	0.5	62.5	4	10.16	12.0828	0.8409
60	0.6	75	4.6	11.684	12.0980	0.9658
70	0.7	87.5	4.8	12.192	12.1133	1.0065
80	0.8	100	5.2	13.308	12.1236	1.0977
90	0.9	112.5	6	15.24	12.1439	1.2550
100	1.0	125	6.9	17.526	12.1543	1.4420
120	1.2	150	14	35.56	12.1906	2.9170
140	1.4	175	18	45.72	12.2212	3.7410
160	1.6	200	21	53.34	12.2524	4.3534
180	1.8	225	25	63.5	12.2836	5.1695
200	2.0	250	27	68.58	12.3153	5.5687
240	2.4	300	31	78.74	12.3787	6.3609
280	2.8	350	34	86.30	12.4425	6.9359
320	3.2	400	37	93.98	12.5076	7.5138
360	3.6	450	42	106.68	12.5731	8.484

400	4.0	500	47	119.38	12.6395	9.4450
440	4.4	550	53	134.62	12.7061	10.5949
480	4.8	600	58	147.32	12.7737	11.5331
520	5.2	650	63	160.02	12.8430	12.4597
560	5.6	700	65.8	167.132	12.9111	12.9448
600	6.0	750	68.3	173.482	12.9801	13.3652
640	6.4	800	69	175.26	13.0514	13.4284
680	6.8	850	72	182.88	13.1227	13.9362
720	7.2	900	73	185.42	13.1948	14.0525
760	7.6	950	75	190.5	13.2677	14.3582
800	8.0	1000	77.4	196.596	13.3414	14.7358
840	8.4	1050	76	193.04	13.4160	14.3888

SAMPLE 2

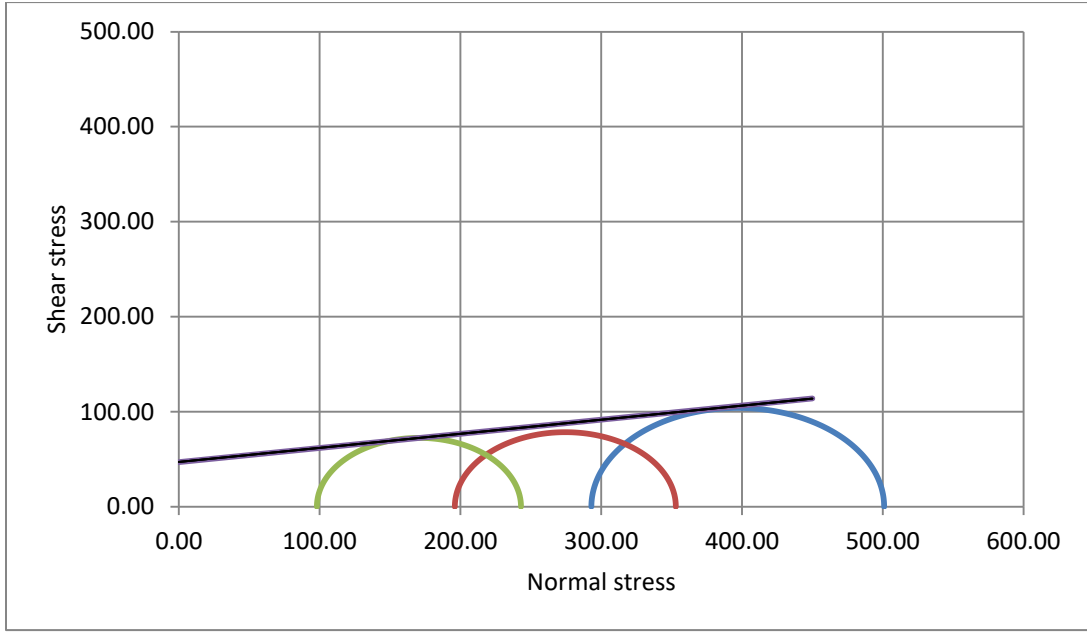
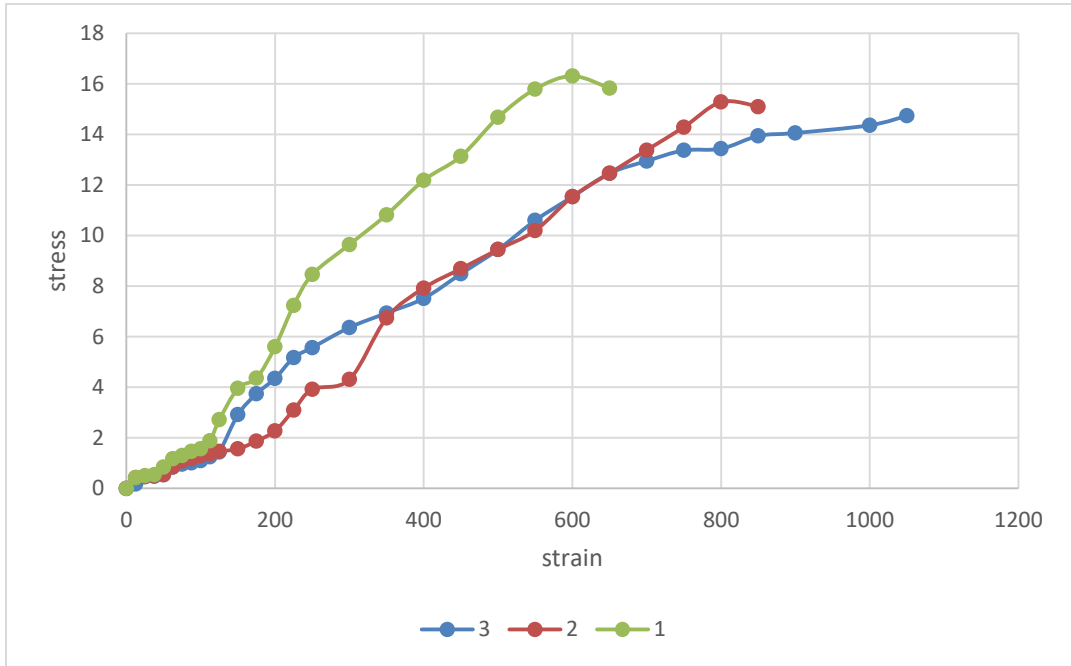
DIVISION	CHANGE IN LENGTH	AXIAL STRAIN	DIVISION(PR OVING RING READING)	APPLIED LOAD *PRC(2.54)	AREA	DEVIATOR STRESS
0	0	0	0	0	12.0073	0
10	0.1	12.5	2	5.08	12.0223	0.4225
20	0.2	25	2.2	5.588	12.0374	0.4642
30	0.3	37.5	2.4	6.096	12.0525	0.5058
40	0.4	50	2.6	6.604	12.0676	0.5437
50	0.5	62.5	4	10.16	12.0828	0.8409
60	0.6	75	5.2	13.208	12.0980	1.0918
70	0.7	87.5	5.6	14.224	12.1133	1.1742

80	0.8	100	6.2	15.748	12.1236	1.2970
90	0.9	112.5	6.5	16.51	12.1439	1.3595
100	1.0	125	7.1	17.78	12.1543	1.4629
120	1.2	150	7.5	19.05	12.1906	1.5627
140	1.4	175	9	22.85	12.2212	1.8697
160	1.6	200	11	27.94	12.2524	2.2804
180	1.8	225	15	38.1	12.2836	3.1017
200	2.0	250	19	48.26	12.3153	3.9187
240	2.4	300	25	53.24	12.3787	4.3090
280	2.8	350	33	83.82	12.4425	6.7366
320	3.2	400	39	99.06	12.5076	7.9200
360	3.6	450	43	109.22	12.5731	8.6868
400	4.0	500	47	119.38	12.6395	9.4450
440	4.4	550	51	129.54	12.7061	10.1951
480	4.8	600	58	147.32	12.7737	11.5331
520	5.2	650	63	160.02	12.8430	12.4597
560	5.6	700	68	172.72	12.9111	13.3776
600	6.0	750	73	185.42	12.9801	14.2849
640	6.4	800	78.5	199.39	13.0514	15.2773
680	6.8	850	77	198.12	13.1227	15.0975

SAMPLE 1

DIVISION	CHANGE IN LENGTH	AXIAL STRAIN	DIVISION(PRO VING RING READING)	APPLIED LOAD *PRC(2.54)	AREA	DEVIATOR STRESS
0	0	0	0	0	12.0073	0
10	0.1	12.5	2	5.08	12.0223	0.4225
20	0.2	25	2.4	6.096	12.0374	0.5064
30	0.3	37.5	2.6	6.604	12.0525	0.5479
40	0.4	50	4	10.16	12.0676	0.8419
50	0.5	62.5	5.6	14.224	12.0828	1.1772
60	0.6	75	6.2	15.748	12.0980	1.3017
70	0.7	87.5	7	17.78	12.1133	1.4678
80	0.8	100	7.5	19.05	12.1236	1.5713
90	0.9	112.5	9	22.86	12.1439	1.8824
100	1.0	125	13	33.02	12.1543	2.7167
120	1.2	150	19	48.26	12.1906	3.9588
140	1.4	175	21	53.34	12.2212	4.3645
160	1.6	200	27	68.58	12.2524	5.5973
180	1.8	225	35	88.9	12.2836	7.2373
200	2.0	250	41	104.14	12.3153	8.4561
240	2.4	300	47	119.38	12.3787	9.6440
280	2.8	350	53	134.62	12.4425	10.8194
320	3.2	400	60	152.4	12.5076	12.1846
360	3.6	450	65	165.1	12.5731	13.1312
400	4.0	500	73	185.42	12.6395	14.6699

440	4.4	550	79	200.66	12.7061	15.7924
480	4.8	600	82	208.28	12.7737	16.3054
520	5.2	650	80	203.2	12.8430	15.8218



FLYASH 3% ESP 15%**SAMPLE 3**

DIVISION	CHANGE IN LENGTH	AXIAL STRAIN	DIVISION(PRO VING RING READING)	APPLIED LOAD *PRC(2.54)	AREA	DEVIATOR STRESS
0	0	0	0	0	12.0073	0
10	0.1	12.5	2	5.08	12.0223	0.4225
20	0.2	25	2.2	5.588	12.0374	0.4642
30	0.3	37.5	2.4	6.096	12.0525	0.5058
40	0.4	50	4	10.16	12.0676	0.8419
50	0.5	62.5	5	12.7	12.0828	1.2596
60	0.6	75	6.2	15.748	12.0980	1.3017
70	0.7	87.5	7.5	19.055	12.1133	1.5727
80	0.8	100	9	22.86	12.1236	1.8856
90	0.9	112.5	13	33.02	12.1439	2.7191
100	1.0	125	17	43.18	12.1543	3.5527
120	1.2	150	21	53.34	12.1906	4.3755
140	1.4	175	25	63.5	12.2212	5.1959
160	1.6	200	29	73.66	12.2524	6.0119
180	1.8	225	31	78.74	12.2836	6.4102
200	2.0	250	33	83.82	12.3153	6.8062
240	2.4	300	35	88.9	12.3787	7.1817
280	2.8	350	37	93.98	12.4425	7.5531
320	3.2	400	43	109.22	12.5076	8.7323
360	3.6	450	45	114.3	12.5731	9.0908

400	4.0	500	47	119.38	12.6395	9.4450
440	4.4	550	51	129.54	12.7061	10.1951
480	4.8	600	55	139.7	12.7737	10.9365
520	5.2	650	57	144.78	12.8430	11.2731
560	5.6	700	63	160.02	12.9111	12.3940
600	6.0	750	67	170.18	12.9801	13.1108
640	6.4	800	73	185.42	13.0514	14.2069
680	6.8	850	79	200.66	13.1227	15.2911
720	7.2	900	84	213.36	13.1948	16.1700
760	7.6	950	82	208.28	13.2677	15.6945

SAMPLE 2

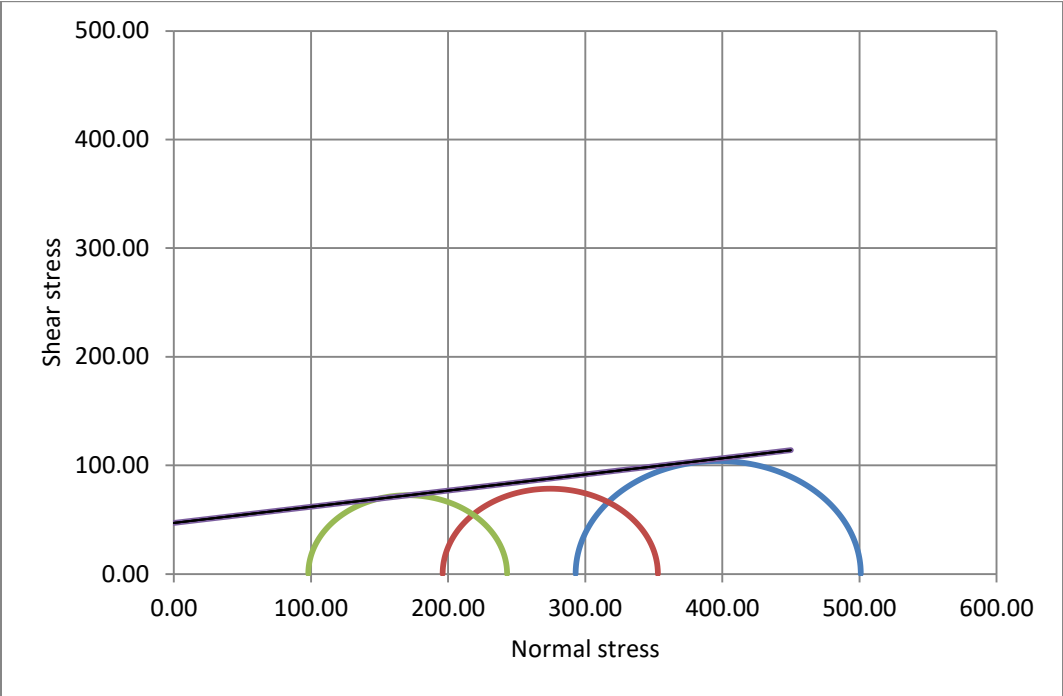
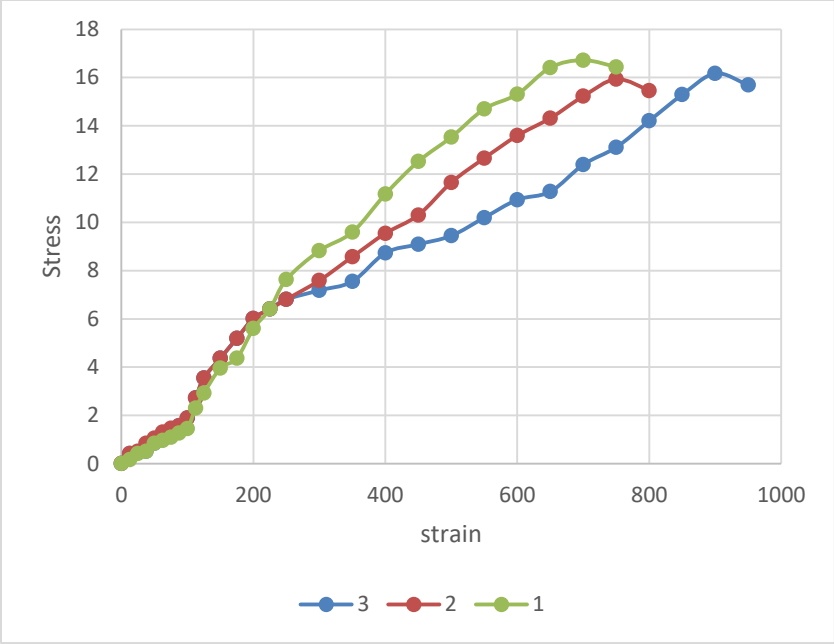
DIVISION	CHANGE IN LENGTH	AXIAL STRAIN	DIVISION(PR OVING RING READING)	APPLIED LOAD *PRC(2.54)	AREA	DEVIATOR STRESS
0	0	0	0	0	12.0073	0
10	0.1	12.5	2	5.08	12.0223	0.4225
20	0.2	25	2.4	6.096	12.0374	0.5064
30	0.3	37.5	4	10.16	12.0525	0.8430
40	0.4	50	5	12.7	12.0676	1.0524
50	0.5	62.5	6.2	15.748	12.0828	1.3033
60	0.6	75	7	17.78	12.0980	1.4697
70	0.7	87.5	7.5	19.05	12.1133	1.5727
80	0.8	100	9	22.86	12.1236	1.8856
90	0.9	112.5	13	33.02	12.1439	2.7191

100	1.0	125	17	43.18	12.1543	3.5527
120	1.2	150	21	53.34	12.1906	4.3755
140	1.4	175	25	63.5	12.2212	5.1959
160	1.6	200	29	73.66	12.2524	6.0184
180	1.8	225	31	78.74	12.2836	6.4102
200	2.0	250	33	83.82	12.3153	6.8062
240	2.4	300	37	93.98	12.3787	7.5921
280	2.8	350	42	106.68	12.4425	8.5738
320	3.2	400	47	119.38	12.5076	9.5446
360	3.6	450	51	129.54	12.5731	10.3029
400	4.0	500	58	147.32	12.6395	11.6555
440	4.4	550	63	160.02	12.7061	12.6603
480	4.8	600	68	172.72	12.7737	13.5935
520	5.2	650	72	182.88	12.8430	14.3169
560	5.6	700	77	195.58	12.9111	15.2285
600	6.0	750	91	205.74	12.9801	15.9351
640	6.4	800	79	200.66	13.0514	15.4590

SAMPLE 1

DIVISION	CHANGE IN LENGTH	AXIAL STRAIN	DIVISION(PROV ING RING READING)	APPLIED LOAD *PRC(2.54)	AREA	DEVIATOR STRESS
0	0	0	0	0	12.0037	0
10	0.1	12.5	0.8	2.032	12.0223	0.1690
20	0.2	25	2	5.08	12.0374	0.4220

30	0.3	37.5	2.4	6.096	12.0525	0.5057
40	0.4	50	4	10.16	12.0676	0.8419
50	0.5	62.5	4.6	11.684	12.0828	0.9670
60	0.6	75	5.2	13.208	12.0980	1.0918
70	0.7	87.5	6	15.24	12.1133	1.2581
80	0.8	100	6.9	17.526	12.1236	1.4456
90	0.9	112.5	11	27.94	12.1439	2.3046
100	1.0	125	14	35.56	12.1543	2.9257
120	1.2	150	19	48.26	12.1906	3.9588
140	1.4	175	21	53.34	12.2212	4.3654
160	1.6	200	27	68.58	12.2524	5.5973
180	1.8	225	31	78.74	12.2836	6.4102
200	2.0	250	37	93.98	12.3153	7.6312
240	2.4	300	43	109.22	12.3787	8.8232
280	2.8	350	47	119.38	12.4425	9.5945
320	3.2	400	55	139.7	12.5076	11.1692
360	3.6	450	62	157.48	12.5731	12.5252
400	4.0	500	67	170.18	12.6395	13.4641
440	4.4	550	73	185.42	12.7061	14.5930
480	4.8	600	77	195.58	12.7737	15.3111
520	5.2	650	83	210.82	12.8430	16.4152
560	5.6	700	85	215.9	12.9111	16.7220
600	6.0	750	84	213.36	12.9801	16.4375



FLYASH 6% ESP 12%**SAMPLE 3**

DIVISION	CHANGE IN LENGTH	AXIAL STRAIN	DIVISION(PR OVING RING READING)	APPLIED LOAD *PRC(2.54)	AREA	DEVIATOR STRESS
0	0	0	0	0	12.0073	0
10	0.1	12.5	2	5.08	12.0223	0.4225
20	0.2	25	3	7.62	12.0374	0.6330
30	0.3	37.5	5	12.7	12.0525	1.0537
40	0.4	50	5.5	13.37	12.0676	1.1079
50	0.5	62.5	7	17.78	12.0828	1.4715
60	0.6	75	9	22.80	12.0980	1.8846
70	0.7	87.5	13	33.02	12.1133	2.7259
80	0.8	100	21	53.34	12.1236	4.3997
90	0.9	112.5	25	63.5	12.1439	5.2290
100	1.0	125	29	73.60	12.1543	6.0374
120	1.2	150	34	86.30	12.1906	7.0615
140	1.4	175	38	96.52	12.2212	7.8776
160	1.6	200	45	114.3	12.2524	9.3060
180	1.8	225	51	129.54	12.2836	10.5186
200	2.0	250	56	142.24	12.3153	11.4907
240	2.4	300	62	157.48	12.3787	12.6560
280	2.8	350	68	172.72	12.4425	13.8092
320	3.2	400	72	182.88	12.5076	14.4689
360	3.6	450	75	190.5	12.5731	14.9928

400	4.0	500	79	200.60	12.6395	15.7401
440	4.4	550	83	210.82	12.7061	16.5920
480	4.8	600	86	218.44	12.7737	17.1008
520	5.2	650	91	231.14	12.8430	17.9974
560	5.6	700	94	238.76	12.9111	18.4926
600	6.0	750	97	246.38	12.9801	18.9814
640	6.4	800	95	241.3	13.0514	18.4884

SAMPLE 2

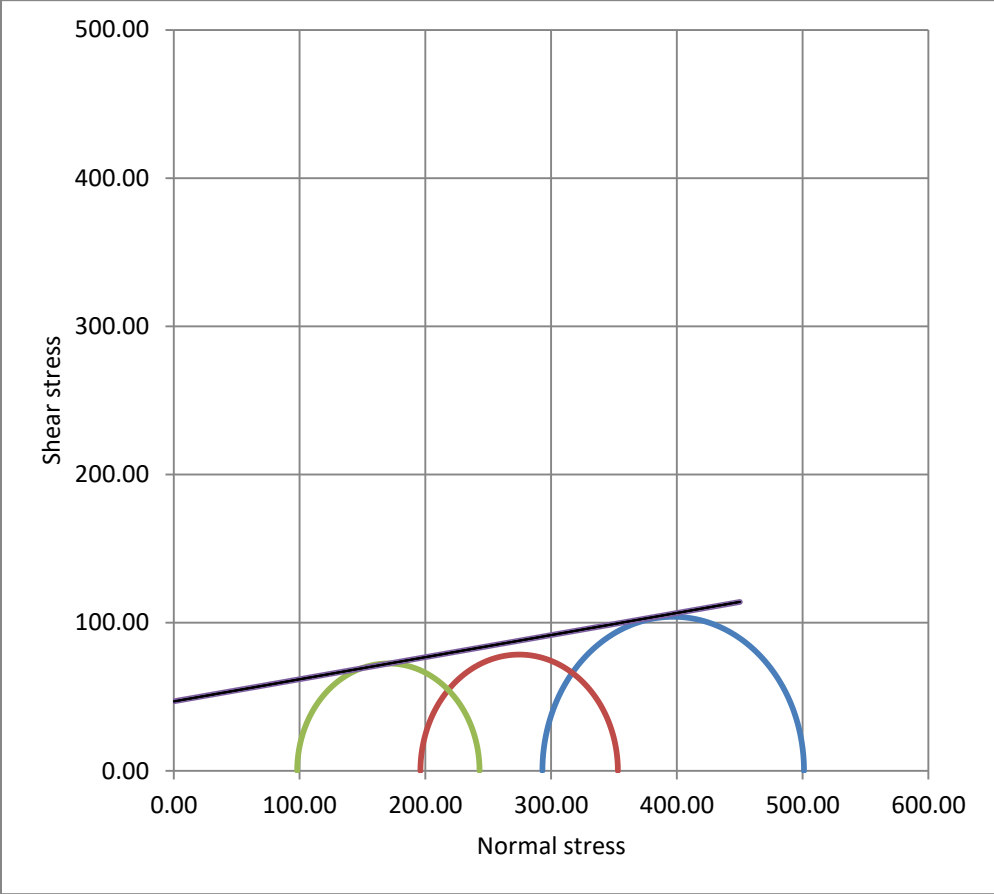
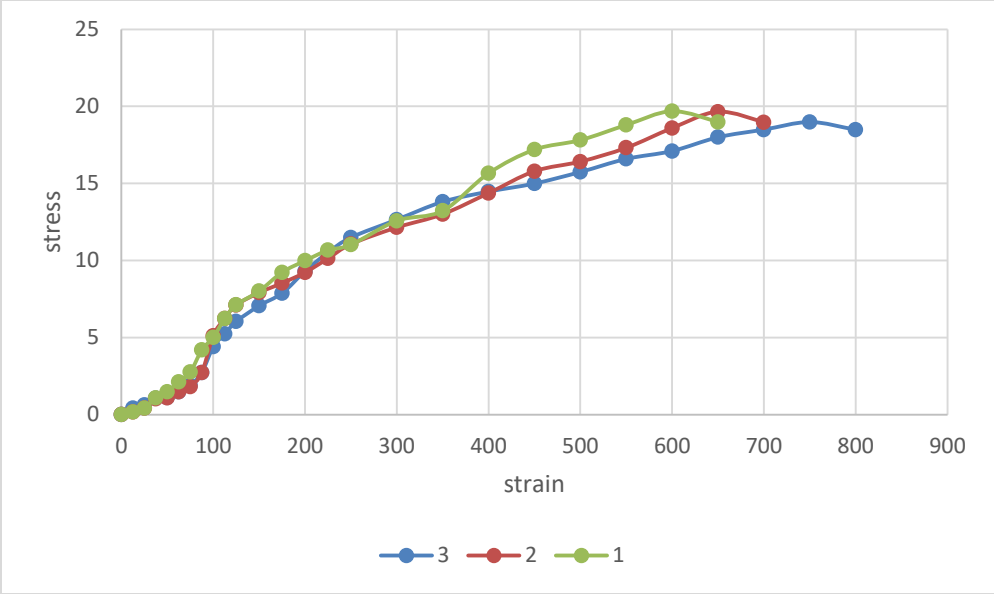
DIVISION	CHANGE IN LENGTH	AXIAL STRAIN	DIVISION(PR OVING RING READING)	APPLIED LOAD *PRC(2.54)	AREA	DEVIATOR STRESS
0	0	0	0	0	12.0073	0
10	0.1	12.5	0.8	2.032	12..0223	0.1690
20	0.2	25	2	5.08	12.0374	0.4225
30	0.3	37.5	4.8	12.22	12.0525	1.0137
40	0.4	50	5.1	12.95	12.0676	1.0735
50	0.5	62.5	7.2	17.78	12.0828	1.4711
60	0.6	75	8.6	21.84	12.0980	1.8052
70	0.7	87.5	12.9	32.85	12.1133	2.7119
80	0.8	100	24.4	61.97	12.1236	5.1120
90	0.9	112.5	29.8	75.71	12.1439	6.2341
100	1.0	125	34.1	86.61	12.1543	7.1046
120	1.2	150	38.1	96.77	12.1906	7.9132
140	1.4	175	41.4	105.15	12.2212	8.5320

160	1.6	200	44.6	113.28	12.2524	9.2211
180	1.8	225	49.1	124.71	12.2836	10.1267
200	2.0	250	53.9	136.91	12.3153	11.6601
240	2.4	300	59.5	151.10	12.3787	12.1436
280	2.8	350	64	162.63	12.4425	13.0028
320	3.2	400	73.3	186.08	12.5076	14.37228
360	3.6	450	79	200.66	12.5731	15.7924
400	4.0	500	83	210.82	12.6395	16.4152
440	4.4	550	88	223.52	12.7061	17.3122
480	4.8	600	95	241.3	12.7737	18.5900
520	5.2	650	101	256.54	12.8430	19.6561
560	5.6	700	98	248.92	12.9111	18.9687

SAMPLE 1

DIVISION	CHANGE IN LENGTH	AXIAL STRAIN	DIVISION(PR OVING RING READING)	APPLIED LOAD *PRC(2.54)	AREA	DEVIATOR STRESS
0	0	0	0	0	12.0073	0
10	0.1	12.5	0.8	2.032	12.0223	0.1690
20	0.2	25	2	5.08	12.0374	0.4225
30	0.3	37.5	5.1	12.9	12.0525	1.0735
40	0.4	50	7	17.78	12.0676	1.4733
50	0.5	62.5	10.1	25.65	12.0828	2.1259
60	0.6	75	13.1	33.27	12.0980	2.7562
70	0.7	87.5	20	50.91	12.1133	4.1897

80	0.8	100	23.9	60.71	12.1236	5.0082
90	0.9	112.5	29.8	75.69	12.1439	6.2343
100	1.0	125	34.1	86.75	12.1543	7.1158
120	1.2	150	38.5	97.89	12.1906	8.0101
140	1.4	175	44.5	113.07	12.2212	9.2287
160	1.6	200	48.2	122.60	12.2524	9.9821
180	1.8	225	51.7	131.35	12.2836	10.6654
200	2.0	250	53.7	136.39	12.3153	11.0183
240	2.4	300	61.6	156.47	12.3787	12.5751
280	2.8	350	65.1	165.37	12.4425	13.2215
320	3.2	400	77	197.89	12.5076	15.6565
360	3.6	450	85	215.9	12.5731	17.1925
400	4.0	500	89	228.73	12.6395	17.8097
440	4.4	550	94	238.76	12.7061	18.7910
480	4.8	600	99	251.46	12.7737	19.6857
520	5.2	650	96	243.84	12.8430	18.9862



FLYASH 9% ESP 9%**SAMPLE 3**

DIVISION	CHANGE IN LENGTH	AXIAL STRAIN	DIVISION(PRO VING RING READING)	APPLIED LOAD *PRC(2.54)	AREA	DEVIATOR STRESS
0	0	0	0	0	12.0073	0
10	0.1	12.5	2	5.08	12.0223	0.4225
20	0.2	25	4	10.16	12.0374	0.8440
30	0.3	37.5	5	12.7	12.0525	1.0537
40	0.4	50	7	17.78	12.0676	1.4734
50	0.5	62.5	9	22.86	12.0828	1.8918
60	0.6	75	11	27.94	12.0980	2.3095
70	0.7	87.5	13	33.02	12.1133	2.7259
80	0.8	100	15	38.1	12.1236	3.1426
90	0.9	112.5	19	48.26	12.1439	3.9740
100	1.0	125	23	58.42	12.1543	4.8065
120	1.2	150	28	71.12	12.1906	5.8340
140	1.4	175	31	78.74	12.2212	6.4429
160	1.6	200	37	93.98	12.2524	7.6703
180	1.8	225	43	109.22	12.2836	8.8915
200	2.0	250	49	124.46	12.3153	10.1061
240	2.4	300	52	132.08	12.3787	10.6699
280	2.8	350	58	147.32	12.4425	11.8401
320	3.2	400	64	162.56	12.5076	12.9969
360	3.6	450	71	180.34	12.5731	14.3433

400	4.0	500	77	195.58	12.6395	15.4737
440	4.4	550	85	215.9	12.7061	16.9918
480	4.8	600	95	241.3	12.7737	18.8904
520	5.2	650	101	256.54	12.8430	19.8194
560	5.6	700	97	246.38	12.9111	19.0828

SAMPLE 2

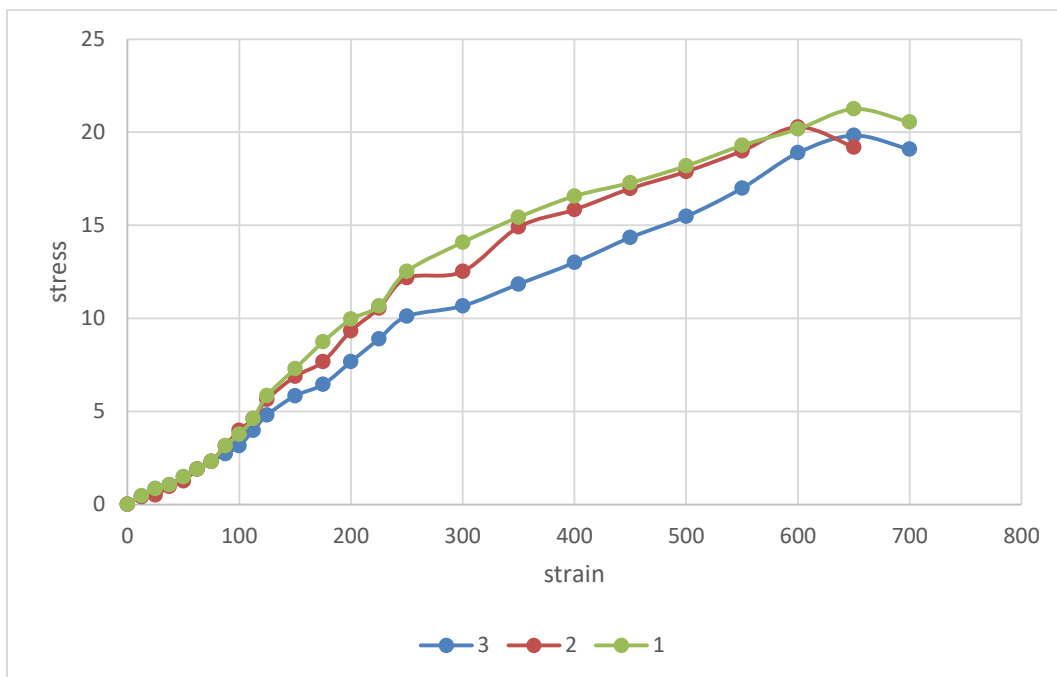
DIVISION	CHANGE IN LENGTH	AXIAL STRAIN	DIVISION(P ROVING RING READING)	APPLIED LOAD *PRC(2.54)	AREA	DEVIATOR STRESS
0	0	0	0	0	12.0073	0
10	0.1	12.5	2	5.08	12..0223	0.4225
20	0.2	25	2.4	6.096	12.0374	0.5064
30	0.3	37.5	4.6	11.684	12.0525	0.9694
40	0.4	50	6	15.24	12.0676	1.2629
50	0.5	62.5	9	22.86	12.0828	1.8919
60	0.6	75	11	27.94	12.0980	2.3095
70	0.7	87.5	15	38.1	12.1133	3.1453
80	0.8	100	19	48.26	12.1236	3.9807
90	0.9	112.5	22	55.88	12.1439	4.6015
100	1.0	125	27	68.58	12.1543	5.6424
120	1.2	150	33	83.82	12.1906	6.8756
140	1.4	175	37	93.98	12.2212	7.6703
160	1.6	200	45	114.3	12.2524	9.3287
180	1.8	225	51	129.54	12.2836	10.5457

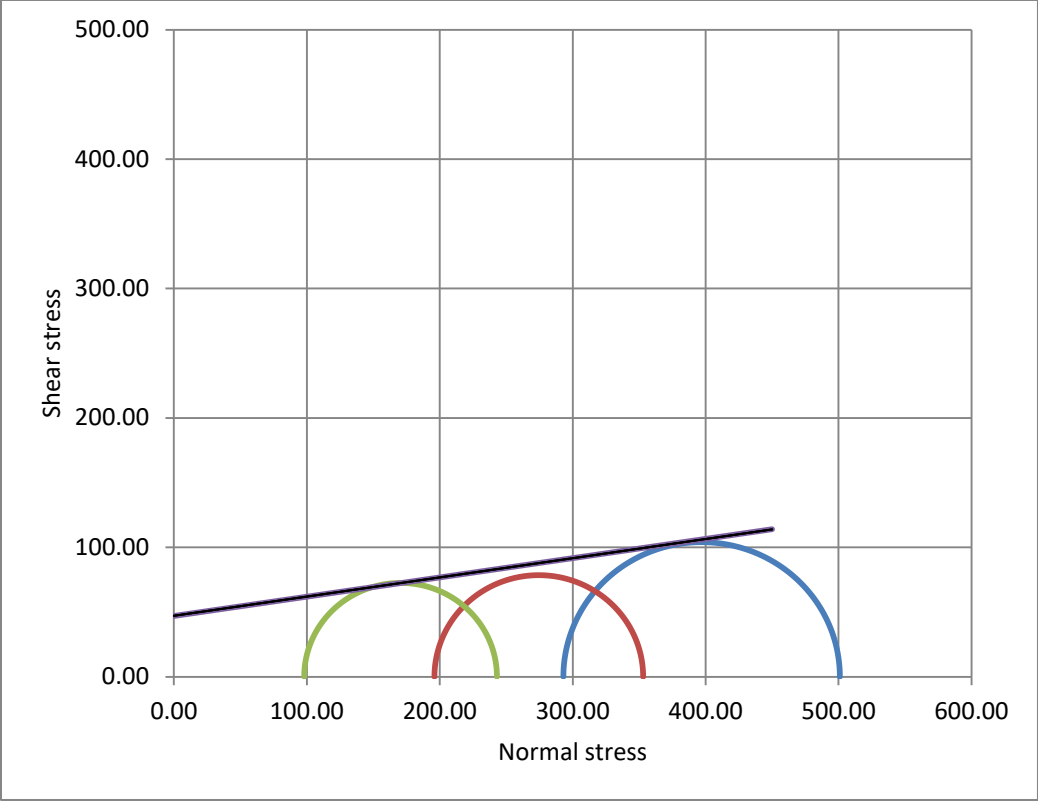
200	2.0	250	59	149.86	12.3153	12.1686
240	2.4	300	67	154.94	12.3787	12.5167
280	2.8	350	73	185.42	12.4425	14.9021
320	3.2	400	78	198.12	12.5076	15.8400
360	3.6	450	84	213.36	12.5731	16.9696
400	4.0	500	89	226.06	12.6395	17.8852
440	4.4	550	95	241.3	12.7061	18.9909
480	4.8	600	102	259.08	12.7737	20.2823
520	5.2	650	97	246.38	12.8430	19.1840

SAMPLE 1

DIVISION	CHANGE IN LENGTH	AXIAL STRAIN	DIVISION(P ROVING RING READING)	APPLIED LOAD *PRC(2.54)	AREA	DEVIATOR STRESS
0	0	0	0	0	12.0073	0
10	0.1	12.5	2.2	5.588	12.0223	0.4648
20	0.2	25	4	10.16	12.0374	0.8440
30	0.3	37.5	5	12.7	12.0525	1.0537
40	0.4	50	7	17.78	12.0676	1.4734
50	0.5	62.5	9	22.86	12.0828	1.8919
60	0.6	75	11	27.94	12.0980	2.3095
70	0.7	87.5	15	38.1	12.1133	3.1453
80	0.8	100	18	45.72	12.1236	3.7712
90	0.9	112.5	22	55.88	12.1439	4.6015
100	1.0	125	28	71.12	12.1543	5.8514

120	1.2	150	35	88.9	12.1906	7.2925
140	1.4	175	42	106.68	12.2212	8.7291
160	1.6	200	48	121.92	12.2524	9.9507
180	1.8	225	54	137.16	12.2836	10.6856
200	2.0	250	61	154.94	12.3153	12.5167
240	2.4	300	69	175.26	12.3787	14.0856
280	2.8	350	76	193.04	12.4425	15.4338
320	3.2	400	82	208.28	12.5076	16.5655
360	3.6	450	86	218.44	12.5731	17.2823
400	4.0	500	91	231.14	12.6395	18.1913
440	4.4	550	97	248.92	12.7061	19.2881
480	4.8	600	102	259.08	12.7737	20.1729
520	5.2	650	108	274.32	12.8430	21.2468
560	5.6	700	105	266.7	12.9111	20.5468





FLYASH 12% ESP 6%**SAMPLE 3**

DIVISION	CHANGE IN LENGTH	AXIAL STRAIN	DIVISION(PR OVING RING READING)	APPLIED LOAD *PRC(2.54)	AREA	DEVIATOR STRESS
0	0	0	0	0	12.0073	0
10	0.1	12.5	2	5.08	12.0223	0.4225
20	0.2	25	5	12.7	12.0374	1.0550
30	0.3	37.5	7	17.78	12.0525	1.4752
40	0.4	50	9	22.86	12.0676	1.8943
50	0.5	62.5	11	27.94	12.0828	2.3124
60	0.6	75	12.5	31.75	12.0980	2.6224
70	0.7	87.5	13	33.02	12.1133	2.7259
80	0.8	100	13.5	34.29	12.1236	2.8284
90	0.9	112.5	15	38.1	12.1439	3.1374
100	1.0	125	17	43.18	12.1543	3.5527
120	1.2	150	25	63.5	12.1906	5.2089
140	1.4	175	29	73.66	12.2212	6.0272
160	1.6	200	37	93.98	12.2524	7.6703
180	1.8	225	45	114.3	12.2836	9.3051
200	2.0	250	53	134.62	12.3153	10.9311
240	2.4	300	62	157.48	12.3787	12.7219
280	2.8	350	77	195.58	12.4425	15.7187
320	3.2	400	85	215.9	12.5076	17.2615
360	3.6	450	92	233.68	12.5731	18.5857

400	4.0	500	97	246.38	12.6395	19.4929
440	4.4	550	105	266.7	12.7061	20.9899
480	4.8	600	108	274.32	12.7737	21.4754
520	5.2	650	107	271.78	12.8430	21.1617

SAMPLE 2

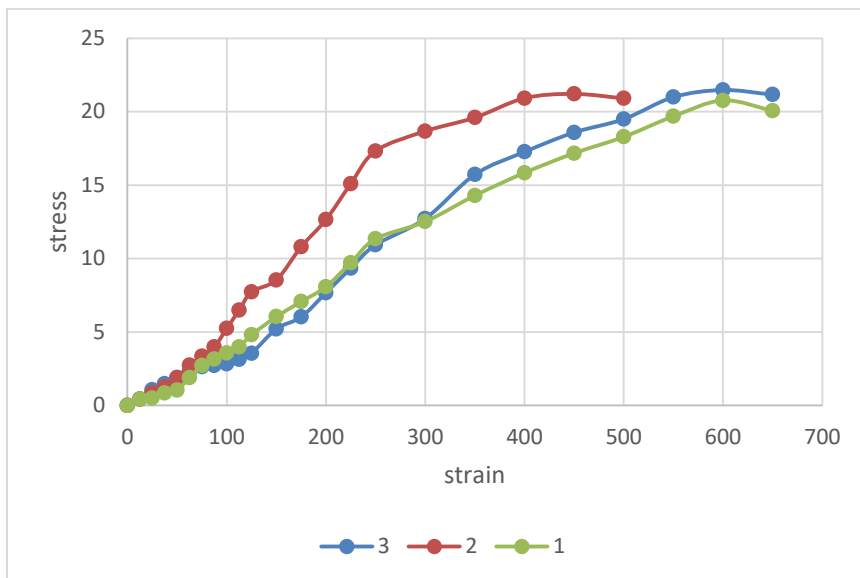
DIVISION	CHANGE IN LENGTH	AXIAL STRAIN	DIVISION(PR OVING RING READING)	APPLIED LOAD *PRC(2.54)	AREA	DEVIATOR STRESS
0	0	0	0	0	12.0073	0
10	0.1	12.5	2	5.08	12.0223	0.4225
20	0.2	25	4	10.19	12.0374	0.8465
30	0.3	37.5	6	15.24	12.0525	1.2645
40	0.4	50	9	22.86	12.0676	1.8943
50	0.5	62.5	13	33.02	12.0828	2.7328
60	0.6	75	16	40.64	12.0980	3.3592
70	0.7	87.5	19	48.26	12.1133	3.9841
80	0.8	100	25	63.5	12.1236	5.2377
90	0.9	112.5	31	78.74	12.1439	6.4839
100	1.0	125	37	93.98	12.1543	7.7322
120	1.2	150	41	104.14	12.1906	8.5426
140	1.4	175	52	132.08	12.2212	10.8074
160	1.6	200	61	154.94	12.2524	12.6457
180	1.8	225	73	185.42	12.2836	15.0949
200	2.0	250	84	213.36	12.3153	17.3248

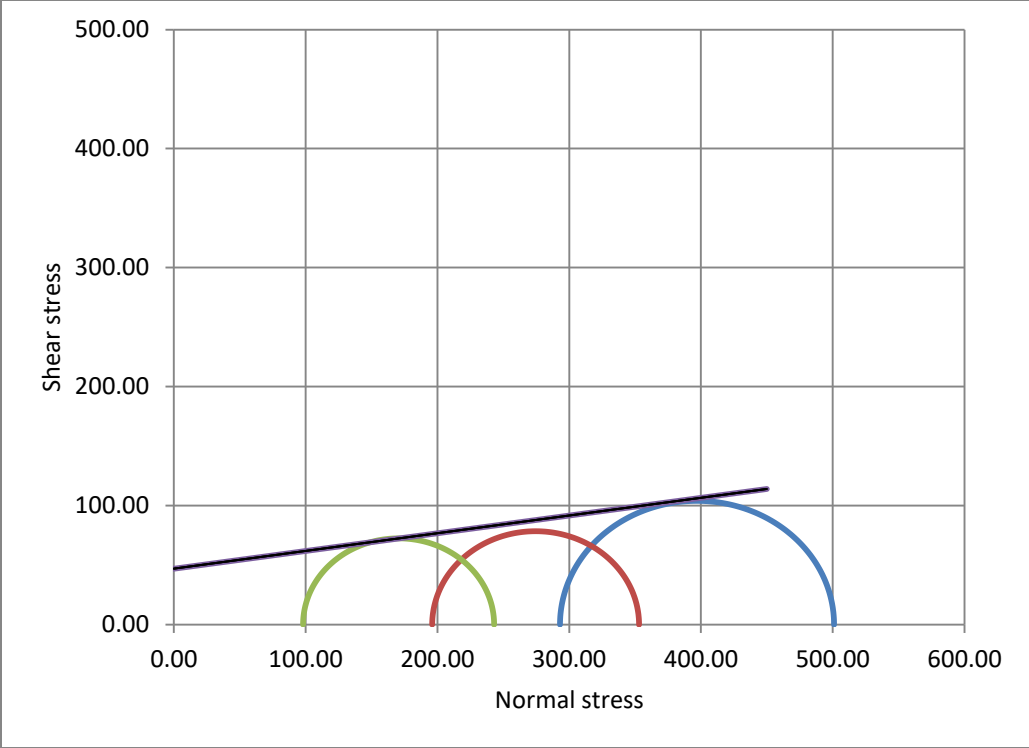
240	2.4	300	91	231.14	12.3787	18.6724
280	2.8	350	96	243.84	12.4425	19.5973
320	3.2	400	103	261.62	12.5076	20.9169
360	3.6	450	105	266.7	12.5731	21.2120
400	4.0	500	104	264.16	12.6395	20.8996

SAMPLE 1

DIVISION	CHANGE IN LENGTH	AXIAL STRAIN	DIVISION(PR OVING RING READING)	APPLIED LOAD *PRC(2.54)	AREA	DEVIATOR STRESS
0	0	0	0	0	12.0073	0
10	0.1	12.5	2	5.08	12.0223	0.4225
20	0.2	25	2.4	6.1	12.0374	0.5068
30	0.3	37.5	4	10.16	12.0525	0.8430
40	0.4	50	5	12.7	12.0676	1.0524
50	0.5	62.5	9	22.86	12.0828	1.8919
60	0.6	75	13	33.02	12.0980	2.7294
70	0.7	87.5	15	38.1	12.1133	3..1453
80	0.8	100	17	43.18	12.1236	3.5616
90	0.9	112.5	19	48.26	12.1439	3.9740
100	1.0	125	23	58.42	12.1543	4.8056
120	1.2	150	29	73.66	12.1906	6.0424
140	1.4	175	34	86.36	12.2212	7.0664
160	1.6	200	39	99.06	12.2524	8.0849
180	1.8	225	47	119.38	12.2836	9.7186

200	2.0	250	55	139.7	12.3153	11.3436
240	2.4	300	61	154.94	12.3787	12.5167
280	2.8	350	70	177.8	12.4425	14.2897
320	3.2	400	78	198.12	12.5076	15.8400
360	3.6	450	85	215.9	12.5731	17.1716
400	4.0	500	91	231.14	12.6395	18.2871
440	4.4	550	99	251.46	12.7061	19.6858
480	4.8	600	105	266.7	12.7737	20.7662
520	5.2	650	102	259.08	12.8430	20.0665





FLYASH 15% ESP 3%

SAMPLE 3

DIVISION	CHANGE IN LENGTH	AXIAL STRAIN	DIVISION(PRO VING RING READING)	APPLIED LOAD *PRC(2.54)	AREA	DEVIATOR STRESS
0	0	0	0	0	12.0073	0
10	0.1	12.5	2	5.08	12.0223	0.4225
20	0.2	25	4	10.16	12.0374	0.8440
30	0.3	37.5	7	17.78	12.0525	1.4752
40	0.4	50	9	22.86	12.0676	1.8943
50	0.5	62.5	11	27.94	12.0828	2.3124
60	0.6	75	15	38.1	12.0980	3.1493
70	0.7	87.5	21	53.34	12.1133	4.4034
80	0.8	100	27	68.58	12.1236	5.6624
90	0.9	112.5	35	88.9	12.1439	7.3228
100	1.0	125	41	104.14	12.1543	8.5755
120	1.2	150	49	124.46	12.1906	10.2098
140	1.4	175	58	147.32	12.2212	12.0847
160	1.6	200	65	165.1	12.2524	13.5011
180	1.8	225	71	180.34	12.2836	14.7187
200	2.0	250	80	203.2	12.3153	16.5424
240	2.4	300	87	220.98	12.3787	17.8516
280	2.8	350	95	241.3	12.4425	19.3932
320	3.2	400	103	261.62	12.5076	20.9169
360	3.6	450	110	279.4	12.5731	22.2220

400	4.0	500	116	294.64	12.6395	23.3110
440	4.4	550	114	289.56	12.7061	22.7891

SAMPLE 2

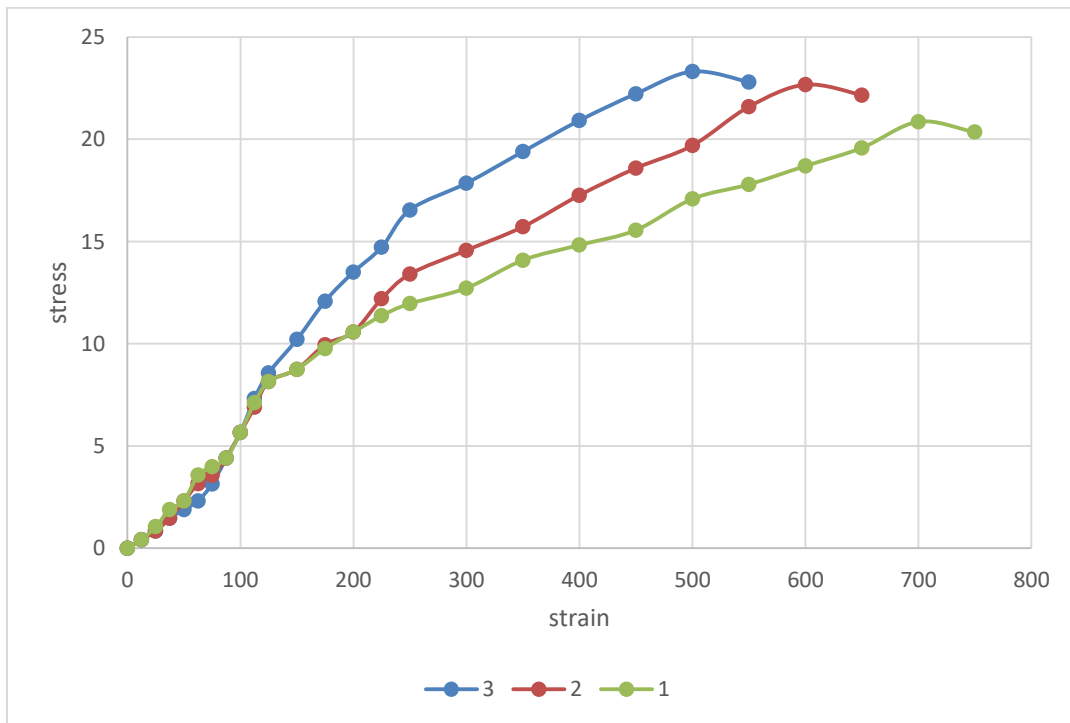
DIVISION	CHANGE IN LENGTH	AXIAL STRAIN	DIVISION(PR OVING RING READING)	APPLIED LOAD *PRC(2.54)	AREA	DEVIATOR STRESS
0	0	0	0	0	12.0073	0
10	0.1	12.5	2	5.08	12.0223	0.4225
20	0.2	25	4	10.16	12.0374	0.8440
30	0.3	37.5	11	17.78	12.0525	1.4752
40	0.4	50	13	27.94	12.0676	2.3153
50	0.5	62.5	15	38.1	12.0828	3.1532
60	0.6	75	17	43.18	12.0980	3.5692
70	0.7	87.5	21	53.34	12.1133	4.4034
80	0.8	100	27	68.58	12.1236	5.6567
90	0.9	112.5	33	83.82	12.1439	6.9022
100	1.0	125	39	99.06	12.1543	8.1502
120	1.2	150	42	106.68	12.1906	8.7510
140	1.4	175	48	121.92	12.2212	9.9565
160	1.6	200	51	129.54	12.2524	10.5726
180	1.8	225	59	149.86	12.2836	12.2000
200	2.0	250	65	165.1	12.3153	13.4061
240	2.4	300	71	180.34	12.3787	14.5686
280	2.8	350	77	195.58	12.4425	15.7187

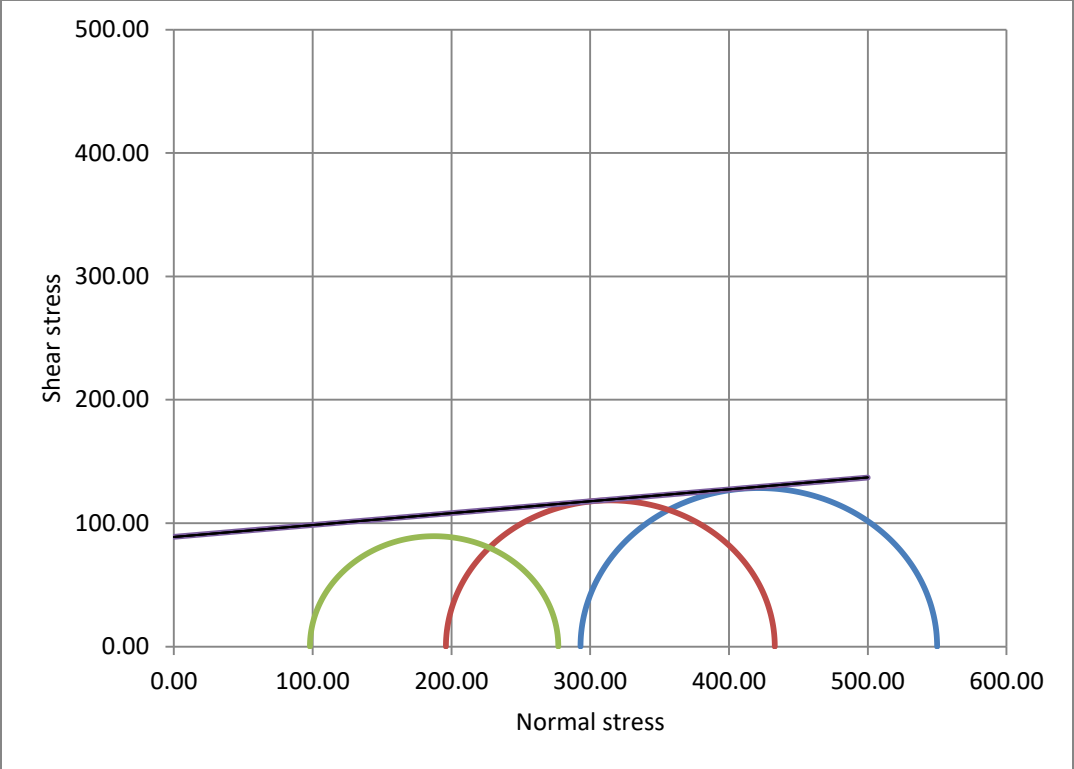
320	3.2	400	85	215.9	12.5076	17.2615
360	3.6	450	92	233.68	12.5731	18.5857
400	4.0	500	98	248.92	12.6395	19.6938
440	4.4	550	108	274.32	12.7061	21.5896
480	4.8	600	114	289.56	12.7737	22.6685
520	5.2	650	112	284.48	12.8430	22.1506

SAMPLE 1

DIVISION	CHANGE IN LENGTH	AXIAL STRAIN	DIVISION(PR OVING RING READING)	APPLIED LOAD *PRC(2.54)	AREA	DEVIATOR STRESS
0	0	0	0	0	12.0073	0
10	0.1	12.5	2	5.08	12.0223	0.4225
20	0.2	25	5	12.7	12.0374	1.0550
30	0.3	37.5	9	22.80	12.0525	1.8917
40	0.4	50	11	27.94	12.0676	2.3153
50	0.5	62.5	15	43.18	12.0828	3.5737
60	0.6	75	19	48.26	12.0980	3.9891
70	0.7	87.5	21	53.34	12.1133	4.4034
80	0.8	100	27	68.58	12.1236	5.6567
90	0.9	112.5	34	86.36	12.1439	7.1114
100	1.0	125	39	99.06	12.1543	8.1502
120	1.2	150	42	106.68	12.1906	8.7510
140	1.4	175	47	119.38	12.2212	9.7683
160	1.6	200	51	129.54	12.2524	10.5726

180	1.8	225	55	139.7	12.2836	11.3729
200	2.0	250	58	147.32	12.3153	11.9625
240	2.4	300	62	157.48	12.3787	12.7219
280	2.8	350	69	175.26	12.4425	14.0856
320	3.2	400	73	185.42	12.5076	14.8246
360	3.6	450	77	195.58	12.5731	15.5554
400	4.0	500	85	215.9	12.6395	17.0814
440	4.4	550	89	226.06	12.7061	17.7915
480	4.8	600	94	238.76	12.7737	18.6915
520	5.2	650	99	251.46	12.8430	19.5795
560	5.6	700	106	269.24	12.9111	20.8534
600	6.0	750	104	264.16	12.9801	20.3512





FLYASH 18% ESP 0%**SAMPLE 3**

DIVISION	CHANGE IN LENGTH	AXIAL STRAIN	DIVISION(PR OVING RING READING)	APPLIED LOAD *PRC(2.54)	AREA	DEVIATOR STRESS
0	0	0	0	0	12.0073	0
10	0.1	12.5	5	12.7	12.0223	1.0564
20	0.2	25	9	22.86	12.0374	1.8991
30	0.3	37.5	15	38.1	12.0525	3.1612
40	0.4	50	21	53.34	12.0676	4.4201
50	0.5	62.5	26	66.04	12.0828	5.4656
60	0.6	75	33	83.82	12.0980	6.9284
70	0.7	87.5	38	96.52	12.1133	7.9681
80	0.8	100	44	111.76	12.1236	9.2184
90	0.9	112.5	51	129.54	12.1439	10.6671
100	1.0	125	57	144.78	12.1543	11.9118
120	1.2	150	63	160.02	12.1906	13.1265
140	1.4	175	68	172.72	12.2212	14.1328
160	1.6	200	74	187.96	12.2524	15.3407
180	1.8	225	77	195.58	12.2836	15.9220
200	2.0	250	85	215.8	12.3153	17.5229
240	2.4	300	91	231.14	12.3787	18.6724
280	2.8	350	98	248.92	12.4425	20.0056
320	3.2	400	105	266.7	12.5076	21.3230
360	3.6	450	118	299.72	12.5731	23.8382

400	4.0	500	124	314.96	12.6395	24.9187
440	4.4	550	120	304.8	12.7061	23.9885

SAMPLE 2

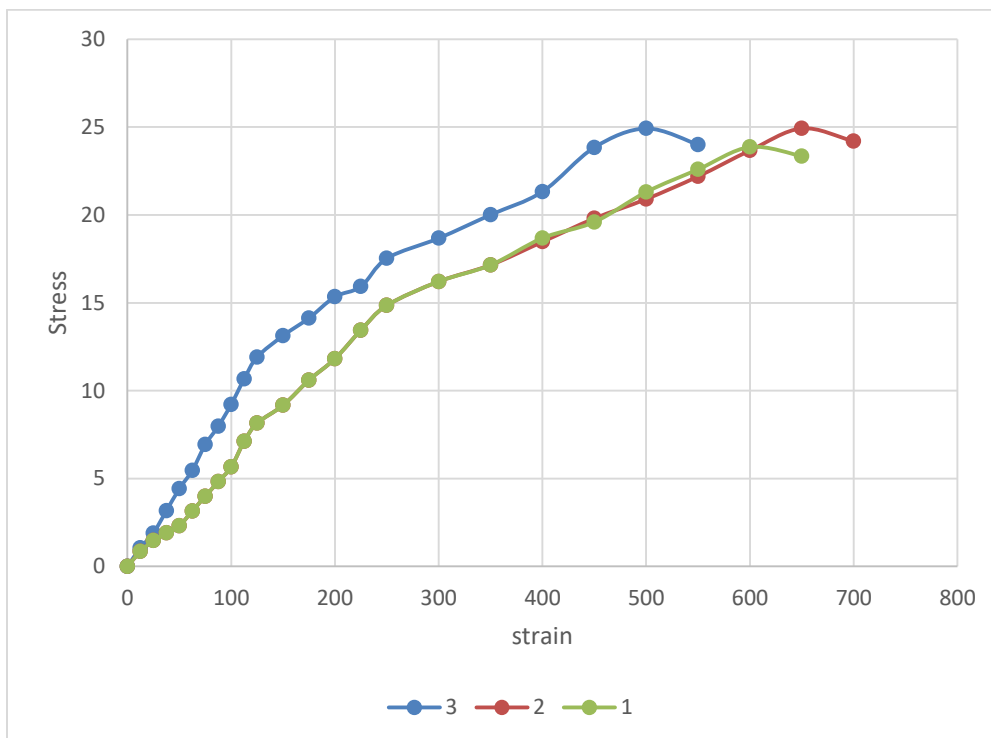
DIVISION	CHANGE IN LENGTH	AXIAL STRAIN	DIVISION(PR OVING RING READING)	APPLIED LOAD *PRC(2.54)	AREA	DEVIATOR STRESS
0	0	0	0	0	12.0073	0
10	0.1	12.5	4	10.16	12.0223	0.8451
20	0.2	25	7	17.78	12.0374	1.4771
30	0.3	37.5	9	22.86	12.0525	1.9010
40	0.4	50	11	27.94	12.0676	2.3153
50	0.5	62.5	15	38.1	12.0828	3.1532
60	0.6	75	19	48.26	12.0980	3.9891
70	0.7	87.5	23	58.42	12.1133	4.8228
80	0.8	100	27	68.58	12.1236	5.6567
90	0.9	112.5	34	86.36	12.1439	7.1114
100	1.0	125	39	99.06	12.1543	8.1502
120	1.2	150	44	111.76	12.1906	9.1677
140	1.4	175	51	129.54	12.2212	10.5996
160	1.6	200	57	144.78	12.2524	11.8165
180	1.8	225	65	165.1	12.2836	13.4407
200	2.0	250	72	182.88	12.3153	14.8498
240	2.4	300	79	200.66	12.3787	16.2101
280	2.8	350	84	213.36	12.4425	17.1477

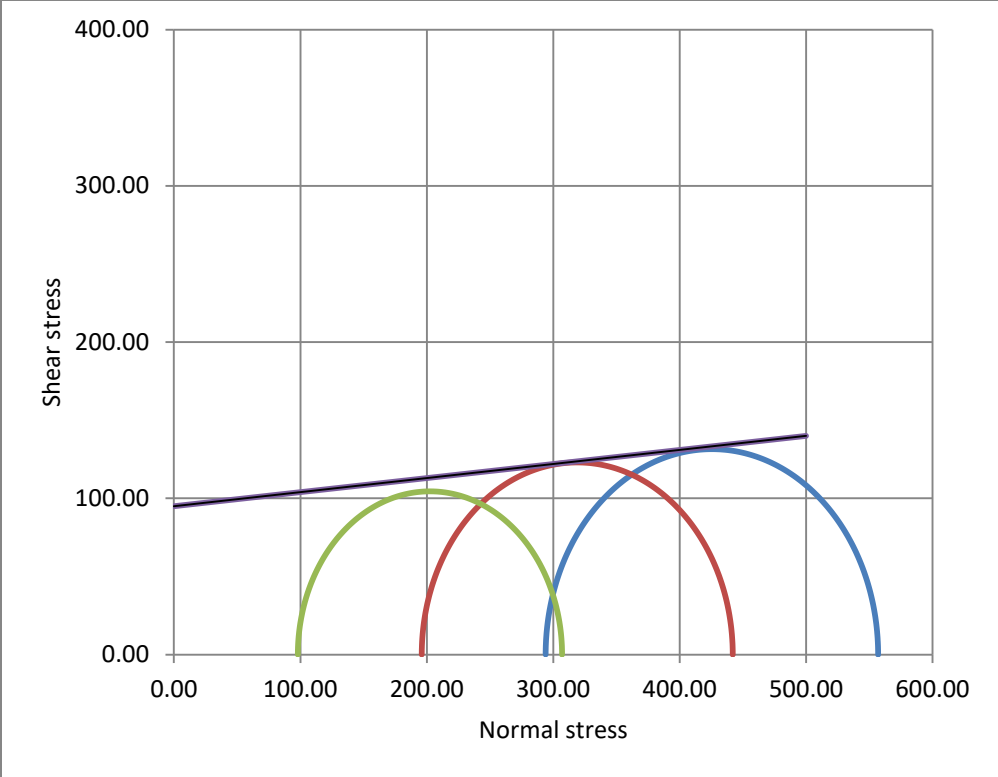
320	3.2	400	91	231.14	12.5076	18.4800
360	3.6	450	98	248.92	12.5731	19.7978
400	4.0	500	104	261.16	12.6395	20.8996
440	4.4	550	111	281.94	12.7061	22.1893
480	4.8	600	119	302.26	12.7737	23.6627
520	5.2	650	126	320.04	12.8430	24.9194
560	5.6	700	123	312.42	12.9111	24.1978

SAMPLE 1

DIVISION	CHANGE IN LENGTH	AXIAL STRAIN	DIVISION(PR OVING RING READING)	APPLIED LOAD *PRC(2.54)	AREA	DEVIATOR STRESS
0	0	0	0	0	12.0073	0
10	0.1	12.5	4	10.16	12.0223	0.8451
20	0.2	25	7	17.78	12.0374	1.4771
30	0.3	37.5	9	22.86	12.0525	1.9010
40	0.4	50	11	27.94	12.0676	2.3153
50	0.5	62.5	15	38.1	12.0828	3.1532
60	0.6	75	19	48.26	12.0980	3.9891
70	0.7	87.5	23	58.42	12.1133	4.8228
80	0.8	100	27	68.58	12.1236	5.6567
90	0.9	112.5	34	86.36	12.1439	7.1114
100	1.0	125	39	99.06	12.1543	8.1502
120	1.2	150	44	111.76	12.1906	9.1677
140	1.4	175	51	129.54	12.2212	10.5996

160	1.6	200	57	144.78	12.2524	11.8165
180	1.8	225	65	165.1	12.2836	13.4407
200	2.0	250	72	182.88	12.3153	14.8498
240	2.4	300	79	200.66	12.3787	16.2101
280	2.8	350	84	213.36	12.4425	17.1477
320	3.2	400	92	233.68	12.5076	18.6830
360	3.6	450	97	246.38	12.5731	19.5958
400	4.0	500	105	269.24	12.6395	21.3015
440	4.4	550	113	287.02	12.7061	22.5892
480	4.8	600	120	304.8	12.7737	23.8615
520	5.2	650	118	299.72	12.8430	23.3372





OPERATING THE TRIAXIAL MACHINE

